CERAMIC STATIONARY GAS TURBINE DEVELOPMENT

Technical Progress Report

Solar Turbines
A Caterpillar Company

DOE/CE/40960--T1

CERAMIC STATIONARY GAS TURBINE DEVELOPMENT

Technical Progress Report
April 1, 1993 through October 31, 1994

Prepared By:

Staff of
Solar Turbines Incorporated
P.O. Box 85376
San Diego, Ca. 92186-5376

For:

U.S. Department of Energy
Chicago Operations Office
Industrial Cogeneration Programs
Programs & Facilities
Management Division
9800 S. Cass Avenue
Argonne, Il. 60439
Under Contract DE-AC02-92CE40960

SR93-R-5921-29
December 1994

ACKNOWLEDGEMENTS

The inputs and comments from the subcontractors and consultants for the DOE Ceramic Stationary Gas Turbine Development program for the preparation of this Phase II Technical Progress Report are hereby gratefully acknowledged.

TABLE OF CONTENTS

TABLE OF CONTENTS (Cont'd)

LIST OF FIGURES

LIST OF FIGURES (Cont'd)

LIST OF FIGURES (Cont'd)

LIST OF TABLES

ACRONYMS AND ABBREVIATIONS

ABB	Asea Brown Boveri
aft	after
AGT	Automotive Gas Turbine
Al_2O_3	Alumina
Al_2O_3/Al_2O_3	Alumina Fiber-Reinforced Alumina Matrix Composite
ANL	Argonne National Laboratory
ANSYS	Computer Software Used for Finite Element Analysis
ARCO	Atlantic Richfield Company Oil & Gas
AS-800	Silicon Nitride Manufactured by CC
ASCC	AlliedSignal Ceramic Components
ASME	American Society of Mechanical Engineers
ATS	Advanced Turbine Systems, Advanced Test Systems
ATTAP	Advanced Turbine Technology Applications Project
B&W	Babcock and Wilcox
CARES	Ceramics Analysis and Reliability Evaluation of Structures
CARES/LIFE	Uprated Version of CARES
CAT TC	Caterpillar Technical Center
CC	Abbreviation for ASCC
CDP	Combustor Discharge Pressure
CED	Cold End Drive
CEM	Continuous Emissions Monitoring
CES	Controlled Engineering Specification
Centaur 'H'	Solar Centaur Model 'H' Gas Turbine
Centaur 50	Solar Centaur Model 50 Gas Turbine
Centaur 50S	Centaur 50 with SoLoNOx Combustor
CF	Centrifugal Force
CFCC	Continuous Fiber-Reinforced Ceramic Matrix Composite
CFD	Computational Fluid Dynamics
cm	centimeter
cm/s	centimeter per second
CO	Carbon Monoxide
CSGT	Ceramic Stationary Gas Turbine
CT	Computed Tomography
CTAHE	Ceramic Technology for Advanced Heat Engines
CVI	Chemical Vapor Infiltration
DLC	DuPont Lanxide Composites
DOE	Department of Energy
DS	Directionally Solified
D-5B	Low Expansion Alloy
EE	Energy Efficiency and Renewable Energy Resources
EDS	Energy Dispersive X-Ray Spectroscopy
EDX	Energy Dispersive X-Ray Analysis
Fe	Iron
FE	Finite Element or Fossil Energy
FEA	Finite Element Analysis
FPI	Fluorescent Penetrant Inspection

ACRONYMS AND ABBREVIATIONS

GN-10	Silicon Nitride Manufactured by CC
HIP	Hot Isostatic Pressing
Hexoloy®SA SiC	Alpha Sintered Silicon Carbide Manufactured by Carborundum
HP	Horsepower
hr	Hour
Hz	Hertz
in	Inch
in/min	Inch per Minute
INCONEL-718	Inconel Turbine Alloy
IN-738LC	Ni-Base Superalloy
ISO	International Standards Organization
KICC	Kyocera Industrial Ceramics Corporation
kg/s	Kilograms Per Second
kPa	Kilopascals
ksi	Thousands of Pounds Per Square Inch
kW	Kilowatt
LCF	Low-Cycle Fatigue
lb	Pounds
MAR-M47	Ni-base Turbine Alloy
Mars	Solar Mars Model Engine
MIL-SDTD	Military Standard
mm	Millimeter
MPa	Mega Pascal
MPS	Maximum Principal Stress
MRB	Materials Review Board
Msi	Millions of Psi
MW	Megawatts
NAC	Norton Advanced Ceramics
NASA	National Aeronautics and Space Administration
NCX 5102	Silicon Nitride Manufactured by NAC
NDE	Nondestructive Evaluation
NGK	NGK Insulators, Limited
NOx	Oxides of Nitrogen
NT154	Silicon Nitride Manufactured by NAC
NT164	Silicon Nitride Manufactured by NAC
NT230	Reaction Bonded Siliconized Silicon Carbide Manufactured by NAC
N-155	Turbine Alloy
OIT	Office of Industrial Technologies
ORNL	Oak Ridge National Laboratory
PI	Principal Investigator
PLC	Programmable Logic Controller
POS	Probability of Survival or Success

ACRONYMS AND ABBREVIATIONS

ppmv	Parts Per Million by Volume
psi	Pounds Per Square Inch
psia	psi atmospheric
PSIG	psi gauge
R&D	Research and Development
rev	Revolution
ROD	Report of Discrepancy
RPM	Revolutions per Minute
SCG	Slow Crack Growth
SDR	Supplier Disposition Request
SEM	Scanning Electron Microscope
SHP	Shaft Horsepower
SiC	Silicon Carbide
SiC/SiC	Silicon Carbide Fiber-Reinforced Silicon Carbide
Si_3N_4	Silicon Nitride
SN-88	Silicon Nitride manufactured by NGK
SN-253	Silicon Nitride manufactured by KICC
Solar	Solar Turbines Incorporated
SoLoNOx	Solar Low NOx Combustor
SOW	Statement of Work
SPS	Sundstrand Power Systems
SPSLIFE	Sundstrand Power Systems Life Assessment Computer Code
TBO	Time Between Overhaul
TEF	Solar Operations Practice Abbreviation
TIT	Turbine Inlet Temperature
TRIT	Turbine Rotor Inlet Temperature
UDRI	University of Dayton Research Institute
V-57	Disk Alloy
WBS	Work Breakdown Structure
2-D	2-Dimensional
3-D	3-Dimensional
ΔP	Differential (change in) Pressure
°C	Degrees Centigrade (Celsius)
°F	Degrees Fahrenheit

1.0

SUMMARY

This report summarizes the work performed by Solar Turbines Incorporated (Solar), a wholly owned subsidiary of Caterpillar Inc., and its subcontractors, during the period April 1, 1993 through October 31, 1994 under Phase II of the DOE Ceramic Stationary Gas Turbine (CSGT) Development program. The objective of the program is to improve the performance of stationary gas turbines in cogeneration through the implementation of selected ceramic components. The work was performed for the Department of Energy (DOE) Office of Industrial Technologies under Contract No. DE-AC02-92CE40960. The program is administered by the DOE Chicago Operations Office, Chicago, Illinois. Mr. Stephen Waslo of the DOE Chicago Operations Office is the Technical Manager for the DOE CSGT program.

Solar is leading a team consisting of major suppliers of monolithic and composite ceramic components: AlliedSignal Ceramic Components (CC), Norton Advanced Ceramics (NAC), Carborundum, Kyocera Industrial Ceramics Corporation (KICC), DuPont Lanxide Composites (DLC), Babcock & Wilcox (B&W), and NGK Insulators, Ltd (NGK). Also supporting the team efforts is Sundstrand Power Systems (SPS) in the areas of ceramic engine design, materials properties evaluation, and life prediction, Argonne National Laboratory (ANL) and the Caterpillar Technical Center (CAT TC) in the area of nondestructive evaluation, and the University of Dayton Research Institute (UDRI) with long term testing of ceramics. Key consultants provide support in design, fabrication and testing of ceramic materials. The team is completed with an end user of cogeneration gas turbine equipment, ARCO Oil & Gas (ARCO).

The global goals of the program are to achieve national energy savings and reduced emissions of environmental contaminants through improved gas turbine performance resulting from the incorporation of ceramics. It is also anticipated that the development of high performance ceramic stationary gas turbine technology will be incorporated into advanced gas turbine designs that will provide a quantum jump in performance improvement over existing state-of-the-art gas turbine designs.

The reporting period covers the first half of Phase II, Final Design, Material and Component Testing of the Statement of Work. Activities included detailed design of the test engine (Task 7), set up and modification of test facilities (Task 8), fabrication and evaluation of test specimens and simulated components (Task 9), low emission combustor work (Task 10), and program management and reporting (Task 16). Planning for a 4,000 hour performance test will be performed during the latter part of Phase II.

TASK 7 - TEST ENGINE (WBS 2.7.0)

The detailed design for the key ceramic components selected in Phase I (first stage blade and nozzle, combustor liner) was completed. Design of secondary components interfacing with the ceramic parts was also nearly completed. A test engine was procured to be modified for the testing of inserted ceramic components.

The program engine is the Solar Centaur 50 which currently operates at a turbine rotor inlet temperature (TRIT) of 1010°C (1850°F). This engine is being uprated to a TRIT of 1121°C (2050°F). The uprate is estimated to provide a 5.6% improvement in thermal efficiency and a 25.9%

increase in output power in simple cycle operation. The Centaur 50 engine with the components selected for ceramic replacement is shown in Figure 1-1.

The design strategy for all ceramic components was to minimize stresses. Table 1-1 shows the final design stresses in critical areas for the three program components.

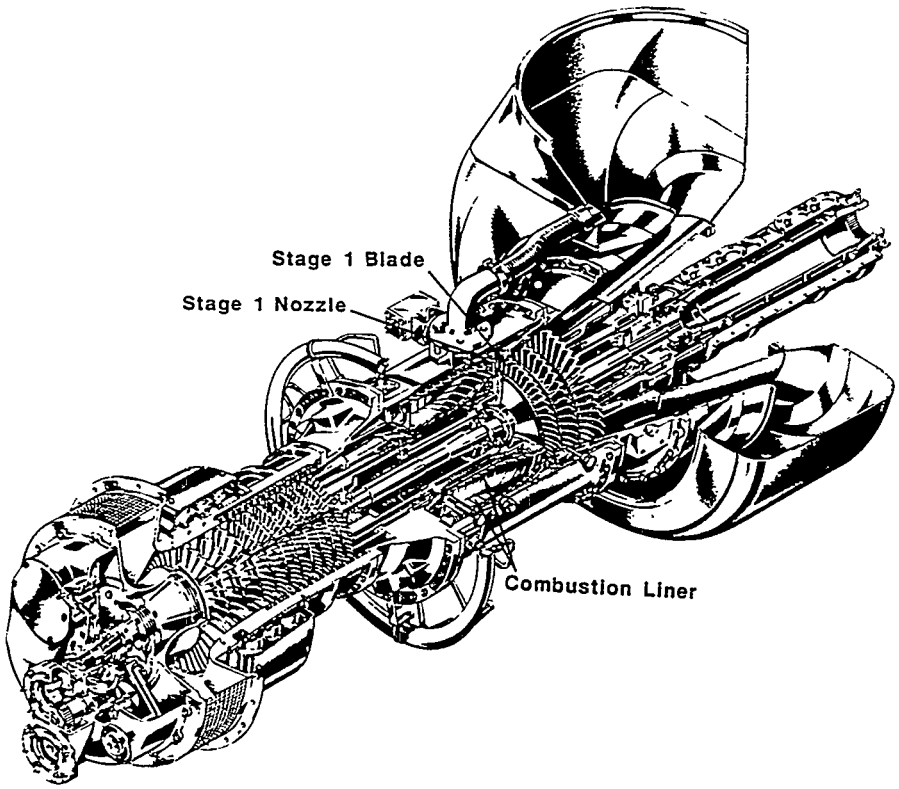

Figure 1-1. Centaur 50 Gas Turbine with Components Selected for Ceramic Insertion

Table 1-1. Critical Steady State Ceramic Component Temperatures and Stresses

Component	Material	Peak Temperature	Peak Stress
Blade	Si_3N_4	1116°C (2041°F)	165-214 MPa (≈24-31 ksi)
Nozzle	Si_3N_4	1297°C (2366°F)	179 MPa (≈26 ksi)
Combustor Tile	SiC	1204°C (2200°F)	190 MPa (≈28 ksi)
Combustor Ring	SiC	1204°C (2200°F)	75 MPa (≈11 ksi)
IntegralCombustor	CFCC*	1150°C (2100°F)	78-163 MPA (≈11-24 ksi)

* CFCC: Continuous Fiber-Reinforced Ceramic Matrix Composite

Blade

The blade design was derived from the current cooled first stage metal Centaur 50 blade. The airfoil configuration is very similar to that of the metal blade with a slight addition of cord towards the blade tip to eliminate a harmful vibrational interference. Two blade root configurations were conceived,

a conventional dovetail with a 55° angle to be used in conjunction with a compliant layer and a modified (two-tang, oval cavity) pinned root blade to be used in conjunction with an oval diameter shaped pin (and without a compliant layer). The maximum principal stress (MPS) in the blade airfoil is life limiting due to slow crack growth (see Table 1-1).

The two blade designs are shown in Figure 1-2.

Nozzle

The conceptual nozzle design was also derived from the current (cooled) first stage nozzle design of the Centaur 50 engine. For ease of fabrication the current metallic two-airfoil nozzle was replaced by two ceramic single-airfoil nozzles, and the current integral tipshoe was decoupled from the outer nozzle shroud in the metal nozzle.

The major challenge for the nozzle design was to minimize the stress at the critical hot spot locations in the airfoil which essentially results from the response to the combustor exit temperature profile and pattern factor. The worst case scenario corresponds to about a 537°C (966°F) maximum temperature difference. Several nozzle configurations were analyzed including a single shrouded vane configuration attached to the nozzle case via an intermediate ceramic ring attachment as well as several two-shroud nozzle (integral, one-piece) designs attached to the first stage diaphragm. All integral nozzle designs based on the current aerodynamics of the Centaur 50 first stage metallic nozzle have high stresses in the 393-483 MPa (57-70 ksi) range in the critical trailing edge region. These stresses are known to be unacceptable in view of the target component design life of 30,000 hrs, representing an average Time-Between- Overhaul (TBO) for a gas turbine in the field. Slow crack growth and creep are the limiting failure modes.

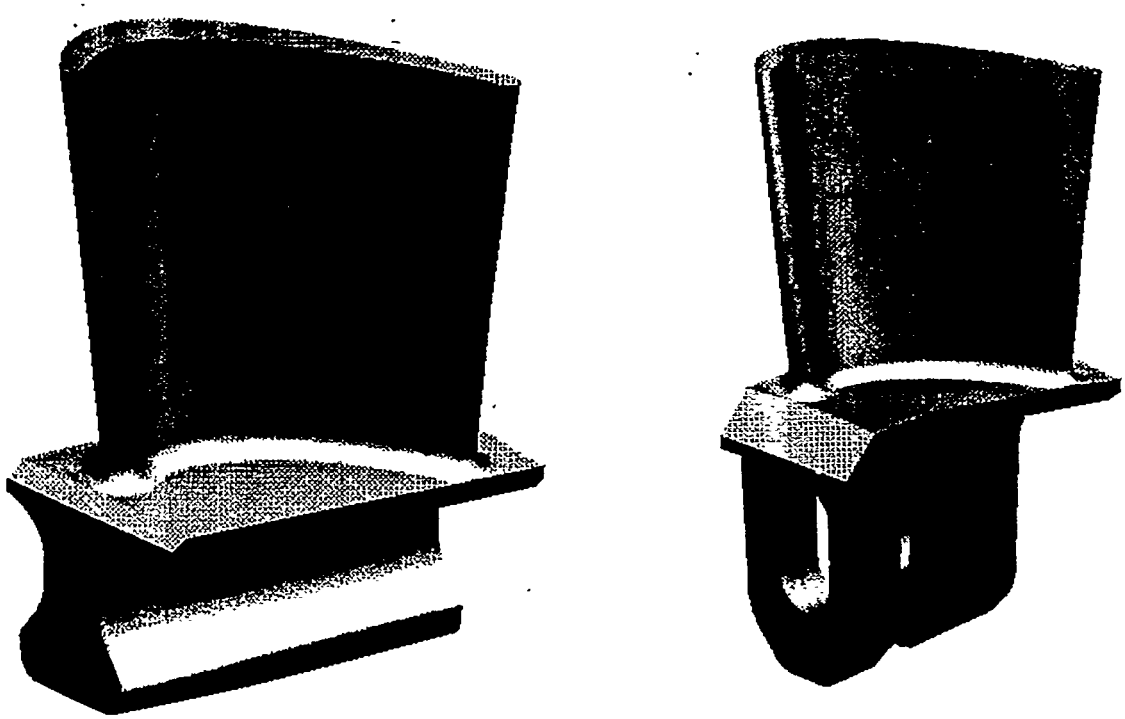

Figure 1-2. Two Ceramic Blade Designs. Dovetail Blade (Left). Pinned Blade (Right).

A number of potential design solutions were evaluated to lower the stress levels, including cooling of the airfoil and nozzle segmentation. These design solutions were assessed to be less optimal for the retrofit character of this program because they either required extensive component development, or were costly, or had known performance detriments. The design solution ultimately adopted was based on a strategy to lower the stresses in the critical airfoil trailing edge region through redesign. The elements of the redesign process included shortening of the airfoil chord, and introducing axial and tangential displacements. The redesign and optimization process was an iterative effort in which aerodynamic, mechanical design and analytical considerations were taken into account to provide an overall balance of properties. MPS levels in the airfoil are about 200 MPa (29 ksi). The selected nozzle design is identified as "bowed" because of airfoil shape bowing in the axial and tangential directions. The bowed nozzle is shown in Figure 1-3. Life prediction results indicated that this stress level on the nozzle airfoil provides acceptable service life at the prevailing nozzle (hot spot) temperature.

Combustor Liner

The combustor design work description has been integrated with the combustor test section under Task 10 (Low Emission Combustor).

Secondary Components

Significant effort was devoted to redesign of the components interfacing with the ceramics. This is required to ensure matching the thermal growth of adjacent ceramic and metal parts and to accommodate the heat management in view of the increase in TRIT from 1010°C (1850°F) to 1121°C (2050°F) and elimination of cooling in the first stage blade and nozzle. The primary design and/or materials changes involved the disks, diaphragms, higher stage blades, and the nozzle support housing. Rim seals were incorporated into the first stage to provide adequate stress rupture margin on the disk which will experience an increased heat flux because of the TRIT increase, the altered combustor radial profile, and the elimination of blade cooling.

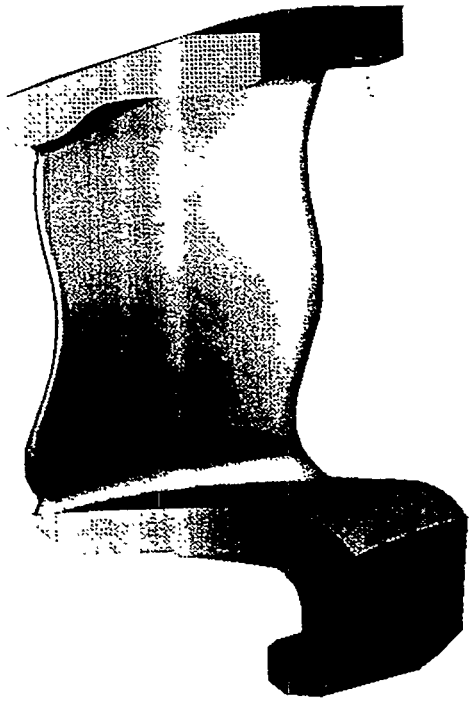

Figure 1-3. Bowed Nozzle Design

Another major activity has been the development of an FE model of the static structure of the engine. The model predicts the expansions of the hot section assembly and enables the prediction of thermal movement during start up, shut down, and trip conditions. It also predicts all clearances in the hot section. The latter information is important for it enables the designer to optimize efficiency and avoid undesirable component contact loads.

TASK 8 - TEST FACILITIES (WBS 2.8.0)

The work in this task involved providing the test facilities to evaluate the ceramic stationary gas turbine components for which the design was detailed under Task 7. The integrated design/test strategy for the program is to test the components as much as possible under the actual engine conditions. For this purpose a metallic Centaur 50 engine was procured and installed in a test area dedicated for this program. The engine is being modified to test the ceramic components and interfacing metal support structure. This test bed identified as the gasifier rig engine is being fully instrumented to enable comprehensive data gathering during the test sequence. The engine rig is set up in a dedicated test facility fully instrumented for the scheduled test plan.

The engine rig testing schedule includes 14 separate test runs in which the selected ceramic components are tested separately or in combination over a TRIT range from 1010°C (1850°F) to 1121°C (2050°F).

All individual ceramic components will be subjected to proof testing under conditions of stress and temperature typical of or more severe than in service. The proof testing is to ensure that the ceramics can survive the stress/temperature conditions imposed during engine operation. Simulated blades and prototype blades will be subjected to cold spin testing. For this purpose an existing spin rig was uprated to the safety level required when testing ceramic parts. A nozzle proof rig is being designed to screen prototype nozzles. Combustor liner designs will be tested initially as subscale components in a can type rig which was modified to enable more complete data gathering. The combustor can rig will provide realistic stress/temperature conditions simulating a full scale combustor. Two other rigs were included for testing of full scale combustor components, an atmospheric rig which will operate at ambient pressure, and a high pressure (loop) rig which will test the combustor liners at realistic conditions of temperature and pressure expected for the engine. All three types of combustor rigs were tested during the reporting period.

TASK 9 - CERAMIC COMPONENTS (WBS 2.9.0)

This task involves procurement, fabrication, and testing of ceramic test specimens and components. Excluded are subscale and full scale combustor testing which is being performed under Task 10. The results of the testing is incorporated in design iterations for Task 7. The work is being performed under three subtasks.

Task 9.1 - Component Design and Material Selection (WBS 2.9.1)

Most of the work under subtask 2.9.1 involved the procurement of test specimens and subscale components, including flexure bars, tensile bars, blade attachment specimens, and subscale combustor liners. The test bars will be used for short term and long term materials property testing under subtask 2.9.2, and for design configuration evaluation under subtask 2.9.2 and Task 2.10. The suppliers for monolithics and CFCC's contributed to this subtask. Included in the work were also specifications written for the program ceramic materials, and the inspection of all incoming ceramic hardware. Subtask 2.9.1 was nearly completed during the reporting period.

Task 9.2 - Component Fabrication Development and Testing (WBS 2.9.2)

This subtask involves the procurement of the first generation of prototype ceramic components which will be proof tested in the test rigs defined in Task 8. Of particular importance is the testing of prototype ceramic blades and nozzles in the engine simulating gasifier rig.

Dovetail blades are being procured from AlliedSignal Ceramic Components (CC) and Norton Advanced Ceramics (NAC). The silicon nitrides selected are GN-10 (CC) and NT164 (NAC). Pinned root blades are being procured from Kyocera Industrial Ceramics Corporation (KICC). The KICC silicon nitride is SN-253. Two suppliers, NGK Insulators Ltd. (NGK) and KICC were selected for nozzle fabrication. The nozzle materials are both silicon nitrides as well, SN-88 (NGK) and SN-253 (KICC). Co-processed flexure bars are being fabricated along side with the blades and nozzles.

Testing of test specimens and simulated components is an important element of subtask 2.9.2. Specimen testing during the reporting period included 4-point flexure testing under blade root and airfoil conditions, 4-point flexure and tensile testing under most severe nozzle airfoil conditions, and limited creep and oxidation testing. Dynamic fatigue testing of tensile bars (at Solar and at UDRI) and flexure bars (at Solar) in conjunction with life prediction proved to be effective tools to guide the selection of the nozzle materials/suppliers. Support for this work is also provided by long term testing under a broader range of conditions at ORNL and UDRI under a separate DOE Contract. Results to-date indicated that if fast fracture is considered alone the candidate materials have a sufficient margin of safety over the operating temperature/stress range. Considering time dependent strength in addition to fast fracture indicates that not all candidate materials have sufficient slow crack growth (SCG) resistance over the operating range of the engine. Extensive life prediction work at Solar and Sundstrand is being used to elucidate safe operating ranges and ranking of candidate ceramics for specific component applications.

Fast fracture tensile testing of attachment specimens of the two blade configurations was performed, mostly at room temperature. The results indicated that for all candidate blade materials there is about a 3-4x safety factor over the design stress of the dovetail blade root and about a 2x safety factor for the pinned blade root. The testing also indicated that various compliant layers perform well under room temperature conditions. Attachment testing at elevated temperature was started towards the end of the reporting period. The results of the latter testing will be used in the selection of the compliant layer material for the blade.

Dynamic fatigue testing of tensile bars and flexure bars in conjunction with life prediction was performed to guide the selection of the nozzle materials/suppliers.

The development of nondestructive evaluation (NDE) techniques is also an important element of this subtask. The basic techniques have been developed for the monolithic and CFCC components. For the monolithics these methodologies include microfocus X-ray, fluorescent dye penetrant inspection (FPI) and laser scattering. For the CFCC materials the most promising methods appear to be infrared imaging, and computed tomography (CT). Most success to-date has been achieved for CFCC's using infrared imaging and CT to areas of reduced bonding and possibly delamination. NDE data for CFCC's were found to correspond well with observed failures and lowering of strength upon exposure of CFCC's.

Task 9.3 - Component Manufacture and Testing (WBS 2.9.3)

The work planned for subtask 9.3 involves procurement and testing of the ceramic components for the 4000 hour Phase III field test. These are second generation ceramic components incorporating

design modifications from testing under subtasks 9.1 and 9.2. Work for this subtask was not initiated yet during the reporting period.

TASK 10 - LOW EMISSION COMBUSTOR (WBS 2.10.0)

This task involves the development of a hot-wall low emission combustor. This combustor is to achieve less than 25 ppmv of NOx in field testing. The Solar program has set a target of demonstrating 10 ppmv NOx for the combustor to be developed under this task. The task has two main elements. The first element focuses on an annular combustor with the same basic configuration as the SoLoNOx combustor of the current Centaur 50 engine. This combustor configuration is targeted to meet at least 25 ppmv NOx and possibly less. Since achieving a level of 10 ppmv NOx will be very difficult with an annular combustor a second element was incorporated that considers an off-line can type combustor.

Annular Combustor

The CSGT combustor, developed to fit the Centaur 50 gas turbine, incorporates a ceramic liner in the hot cylindrical wall surfaces of the metallic SoLoNOx combustor. The DOE program goal is to demonstrate NOx emissions levels of 25 ppmv or less. As for the nozzle, critical factors are minimizing stresses, and attaching the ceramic liner to the metallic support structure.

Three ceramic insert designs with a common envelope were developed for the CSGT combustor: integral continuous fiber-reinforced ceramic matrix composite (CFCC) cylindrical liners, concentric monolithic rings, and axial monolithic tiles. MPS levels for the monolithic designs range from 75-190 MPa (11-28 ksi) for the monolithic materials to 78-163 MPa (11-24 ksi) for the CFCC's. Figure 1-4 shows the two monolithic designs conceived in a subscale configuration.

The design work for the annular combustor design was essentially performed under Task 7. The SoLoNOx combustor design was modified by replacing the cylindrical sections of the primary zone with a ceramic hot wall. The hot wall is isolated from a metallic combustor casing via a fibrous insulating blanket. The first tests of the hot wall concepts were conducted under a Solar in-house effort using CFCC cans with a diameter of 20 cm (8 inch) and a length of 40 cm (16 inch). Those results were successful in that cans of several materials survived up to two hours of exposure at an average wall temperature of about 1204°C (2200°F). A B&W can fabricated from a filament wound alumina/alumina CFCC was tested at an average wall temperature of 1038°C (1900°F). While the B&W can did survive, significant delamination was detected. As a result of this preliminary evaluation B&W modified its fabrication process to a 3-D woven preform. Three of these 3-D alumina/alumina cans are scheduled to be tested. Other prototype tiles, rings and integral CFCC liners will be evaluated in can, and full scale combustor testing and in the engine rig.

Ultra-Low Emissions Combustor Design and Testing

A separate activity was included under Task 10 to evaluate alternative approaches to achieving the 10 ppmv level of NOx. Two approaches were considered, both based on an off-line can type combustor configuration. The first approach uses a lean-premix system and the second approach is based on a rich lean strategy. The lean -premix approach was found to be the more useful for this program since it naturally extends the capabilities of the annular SoLoNOx combustor which is the baseline for the primary combustor development strategy. The added advantage is that the lean-premix strategy uses simpler ceramic hardware than in the rich-lean approach and that the same test rigs can be used as for the primary combustor approach.

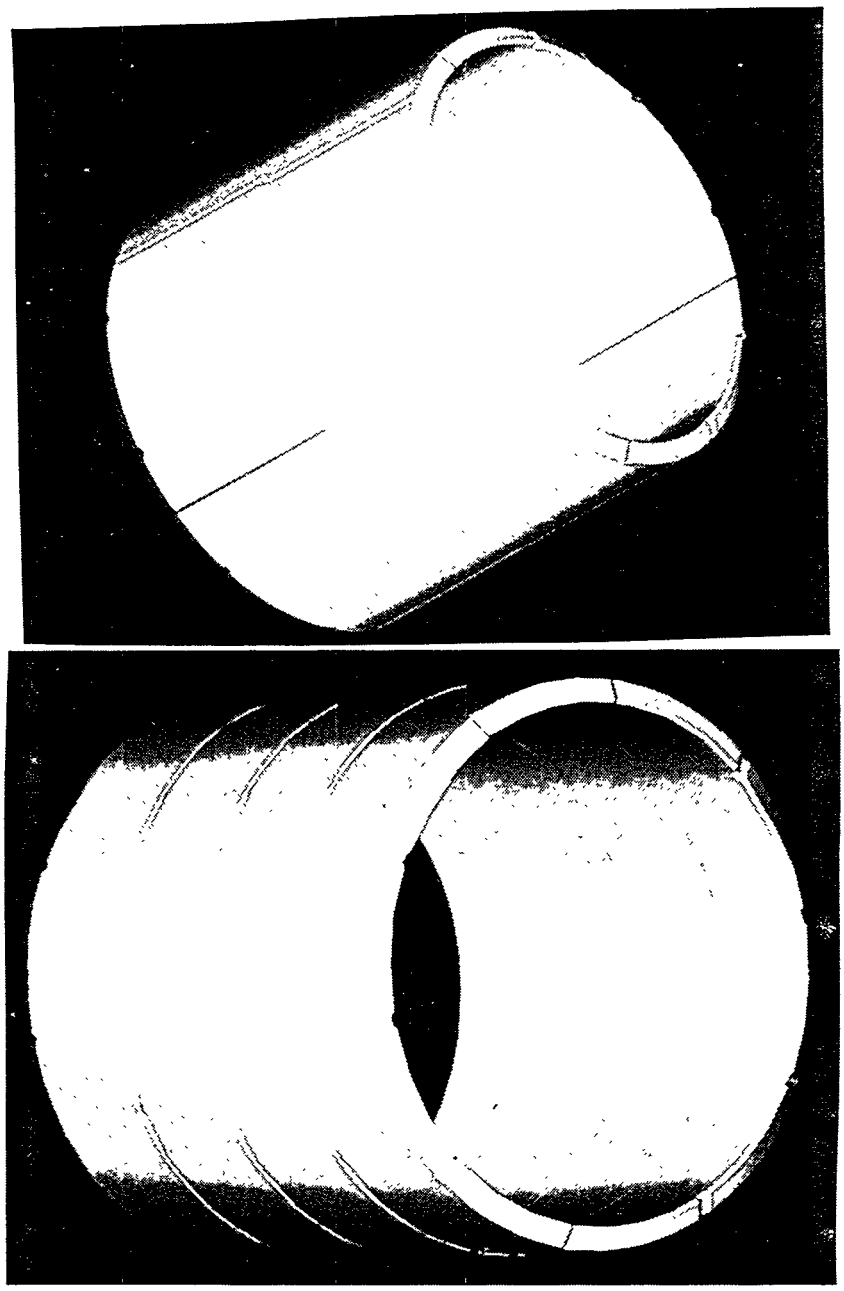

Figure 1-4. Monolithic Tile (Top) and Ring Design (Bottom)

TASK 11 - PLAN FOR 4000 HOUR PERFORMANCE TEST (WBS 2.11.0)

The plan for the 4000 hour performance test to be conducted under Phase III will be addressed in a later stage of the Phase II program.

TASK 16 - MANAGEMENT AND REPORTING (WBS 2.16.0)

The project management and reporting functions for Solar and the subcontractors on the program are included in this task, contract and subcontract administration, as well as design reviews, and conference presentations and publications for the program.

2.0

INTRODUCTION

This Technical Progress Report covers the period April 1, 1993, through October 31, 1994 of Phase II of the "Ceramic Stationary Gas Turbine (CSGT) Development Program" performed under DOE Contract No. DE-AC02-92CE40960. Phase II is scheduled to be completed by September 30, 1996. The project is sponsored by the DOE Office of Industrial Technologies and administered by the DOE Chicago Operations Office, Chicago, Illinois. Mr. Stephen Waslo of the DOE Chicago Operations Office is the Technical Manager for the DOE CSGT program. The objective of the program is to improve the performance of stationary gas turbines in cogeneration through the implementation of selected ceramic components.

The "Ceramic Stationary Gas Turbine Development" program is being performed by a team headed by Solar Turbines Incorporated (Solar), of San Diego, California, a wholly owned subsidiary of Caterpillar Inc. Solar is a U.S. manufacturer of industrial gas turbine equipment in the 500-25,000 HP range, with a strong position in the domestic and international markets in power generation and cogeneration, and mechanical drive applications. Supporting Solar on this program are the leading U.S. and offshore manufacturers of monolithic and composite ceramic components, AlliedSignal Ceramic Components, Norton Advanced Ceramics, Carborundum, Kyocera Industrial Ceramics Corporation, DuPont Lanxide Composites, Babcock & Wilcox, BF Goodrich, and NGK Insulators, Ltd. Also supporting the team efforts are Sundstrand Power Systems in the areas of ceramic engine design, materials properties evaluation and life prediction, Argonne National Laboratory, and the Caterpillar Technical Center in the area of nondestructive evaluation, and the University of Dayton Research Institute with long term testing of ceramics. Key consultants provide support in design, fabrication and testing of ceramic materials. The team is completed with an end user of cogeneration gas turbine equipment, ARCO Oil & Gas.

2.1 BACKGROUND

For the program contract a domestic natural gas fired turbine engine model is selected that falls within the following specifications:

- air flow of 10 - 40 kg/s
- rated for continuous duty
- capable of a turbine rotor inlet temperature over 1000°C when fitted with ceramic components
- pressure ratio that is less than 20:1
- an axial flow turbine geometry

The engine selected for the program is the Solar Centaur 50. Under the program design modifications will be undertaken in the engine:

1. To accept and fasten the ceramic parts to the interfacing metallic structures;

2. To ensure structural integrity, mechanical, and vibrational stability, and safety;

3. To endure a minimum of 25 start-ups without rebuild of parts other than maintenance or rebuild caused by ceramics;

4. To demonstrate a potential for performance improvements in a non-optimized engine configuration;

5. As a minimum to conform to the environmental and safety standards of the all-metal engine;

6. And to demonstrate reliability under conditions of enhanced performance.

The Centaur 50 model selected for the program, formerly known as the Centaur 'H', is nominally a 5880 HP engine, operating at a turbine rotor inlet temperature (TRIT) of 1010°C (1850°F), with a shaft thermal efficiency of 29.63%. The ceramic Centaur 50 engine to be developed under the program from the baseline engine has a shaft output target of about 7400 HP, a TRIT of 1121°C (2050°F), and a thermal efficiency goal of 31.29%. These goals are envisioned to be achieved by replacing key components, the first stage turbine rotor blade and nozzle, and critical segments of the combustor liner with ceramic parts. A further goal of the program is to demonstrate emissions of NOx of 25 ppmv, with a stretch goal to achieve NOx levels of 10 ppmv or better.

Ceramic turbine technology is a key factor in advancing turbine equipment capabilities, and development and implementation of this technology will be critical for ensuring a continued favorable share of domestic and international markets for the U.S. gas turbine industry. The program can achieve these goals if it accelerates the development of the ceramic turbine technology and demonstrate its effectiveness in improving engine performance in a manner that is convincing to the end user of turbomachinery equipment. A 4000 hour field test at an end user cogeneration site is planned to provide an opportunity to prove performance improvement potential under conditions that will be the ultimate test of ceramic hardware durability. It has been Solar's experience that a field test of this duration is a necessary first step to introduce a new product to the market place. The market study included in this report presents a clear time frame for commercialization of the new ceramic turbine technology.

The DOE Ceramic Stationary Gas Turbine Development Program is structured in three phases. Phase I which was performed from 25 September, 1992, through 30 April, 1993, involved turbine and component preliminary design, materials selection, ceramic component fabrication planning, technical and economic evaluation of the ceramic gas turbine technology, concept assessment and planning for Phases II and III. The results of the Phase 1 work have been compiled in a Final Report which was released for publication (1). Portions of the work have also been published separately (2-6).

Phase II, Final Design, Material and Component Testing, focuses on completing the detailed design of the ceramic gas turbine and its components, the procurement and testing of ceramic parts, and the gathering of long term test data to ensure the ceramics will provide adequate performance in an engine in service. The program plan for the field test will be refined. Phase III is directed to conducting a 4000 hour field test of the ceramic stationary gas turbine at a cogeneration test site. In preparation for the field test engine hardware is procured and pre-tested. A full evaluation of the engine and its components following the field testing will be conducted.

2.2 PHASE II STATEMENT OF WORK

This report focuses on the work conducted for the first half of Phase II of the program, between 1 April 1993 and 31 October, 1994, performed at Solar Turbines and its subcontractors. The Phase II work is structured in six tasks:

Task 7: Test Engine (WBS 2.7.0)

Task 8: Test Facilities (WBS 2.8.0)
Task 9: Ceramic Components (WBS 2.9.0)
Task 10: Low Emission Combustor (WBS 2.10.0)
Task 11: Plan for 4000 hr Performance Test (WBS 2.11.0)
Task 16: Management and Reporting (WBS 2.16.0)

Figure 2-1 gives the Timeline schedule for the six Major Tasks in Phase II. The Phase I Statement of Work has organized the work under these tasks according to the Work Breakdown Structure (WBS) shown in Figure 2-2. The work presented in this Phase II Technical Progress Report follows closely the logical sequence of the WBS. The overall work scope for the Major Tasks is summarized below.

PHASE II: FINAL DESIGN, MATERIAL AND COMPONENT TESTING (WBS 2.0)

The work for this phase focuses on material testing, component development, rig testing and final design of the engine.

TASK 7 - TEST ENGINE (WBS 2.7.0)

The detailed design is to be completed for the engine and key ceramic components selected in Phase I. A baseline engine will be procured and modified to accept the selected ceramic components. This engine will be used as a test bed to evaluate the ceramic components and interfacing metallic support structure.

TASK 8 - TEST FACILITIES (WBS 2.8.0)

The work in this task involves set up of the test facilities to evaluate the ceramic stationary gas turbine components. Existing test facilities for materials property testing, spin testing, and combustor liner testing are to be modified if needed for the testing envisioned. A standard Centaur 50 engine procured under Task 7 is to be modified to accept the ceramic hardware as detailed under Task 7.

TASK 9 - CERAMIC COMPONENTS (WBS 2.9.0)

This task involves procurement, fabrication, and testing of ceramic test specimens and components. Excluded are subscale and full scale combustor testing which is performed under Task 10. The results of the testing will be incorporated in design iterations for Task 7. The work is performed in three subtasks:

Task 9.1 - Component Design and Material Selection (WBS 2.9.1) - The detailed design of the key ceramic components defined in Task 7 is used to definitize manufacturing methodology, proof testing, and interfacing with the engine including seals and joining. Test specimens, subscale and simulated components, and full scale components are all being procured under this task including subscale combustor hardware for the annular combustor.

Task 9.2 - Component Fabrication Development and Testing (WBS 2.9.2) - This subtask involves the procurement of first generation of prototype ceramic components which will be proof tested in the test rigs defined in Task 8. Of particular importance is the testing of prototype ceramic blades and nozzles in the test engine rig. Long term testing of the ceramic materials for critical materials properties such as creep and oxidation is also included in this subtask. All findings will be correlated with life prediction and NDE data.

Task 9.3 - Component Manufacture and Testing (WBS 2.9.3) - Ceramic components for installation into the ceramic stationary gas turbine for the 4000 hour field test in Phase III will be procured and proof tested in this subtask. These are second generation ceramic components incorporating design modifications from testing under Tasks 9.1 and 9.2.

TASK 10 - LOW EMISSION COMBUSTOR (WBS 2.10.0)

This task involves the development, design, and fabrication of a hot-wall low emission combustor. This combustor is to achieve less than 25 ppmv of NOx in external testing. The Solar program has set a target of demonstrating 10 ppmv NOx for the combustor to be developed under this task. Prototype tiles, rings and integral CFCC liners are to be evaluated in can, and full scale combustor testing and in the engine rig. Alternative combustor designs which have a high likelihood of achieving ultra-low emissions levels of 10 ppmv NOx or better are being evaluated under a separate subtask.

TASK 11 - PLAN FOR 4000 HOUR PERFORMANCE TEST (WBS 2.11.0)

The plan for the 4000 hour performance test to be conducted under Phase III will be completed under this task.

TASK 16 - MANAGEMENT AND REPORTING

The project management and reporting functions for Solar and the subcontractors on the program contract and subcontract administration, as well as the travel to design reviews, and conferences for the program are included in this task.

The organization for the program is summarized in Figure 2-3. The program organization is structured following a team approach in which the Solar engineering, technical, and administrative staff conducts the work following a concurrent engineering strategy. The concurrent engineering approach is the official Solar strategy for new product development. This strategy integrates all aspects of the product development cycle including engine and component design, materials and testing support, manufacturing, customer services, purchasing, marketing, and finance from the conception of the design to the commercialization of the finished product. The subcontractors on the program are integrated to a high degree in the concurrent engineering approach. Work is conducted through teams with broad focus on design, materials, testing, new product development, and subcontract management and administration.

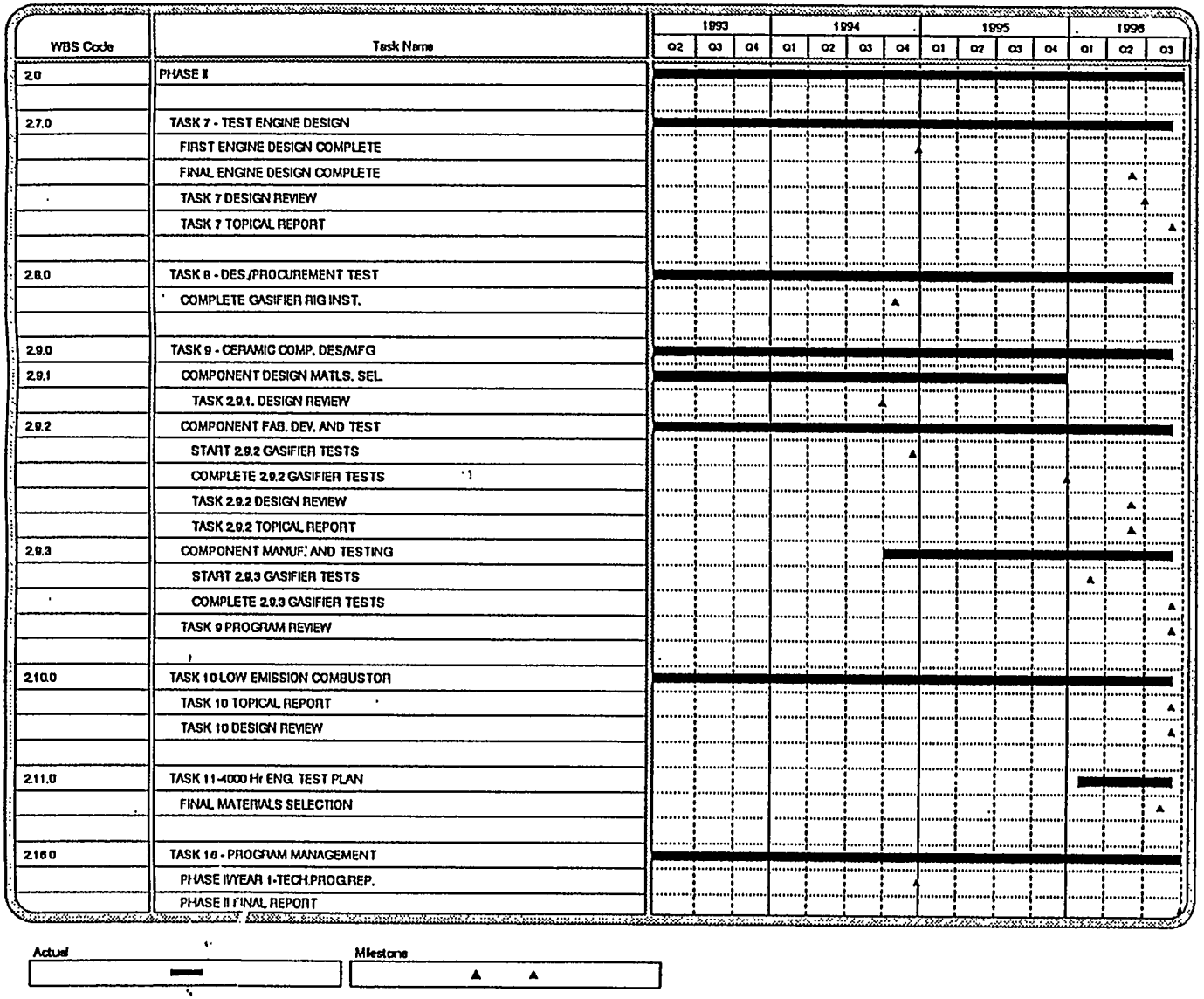

Figure 2-1. Timeline Schedule for Phase II

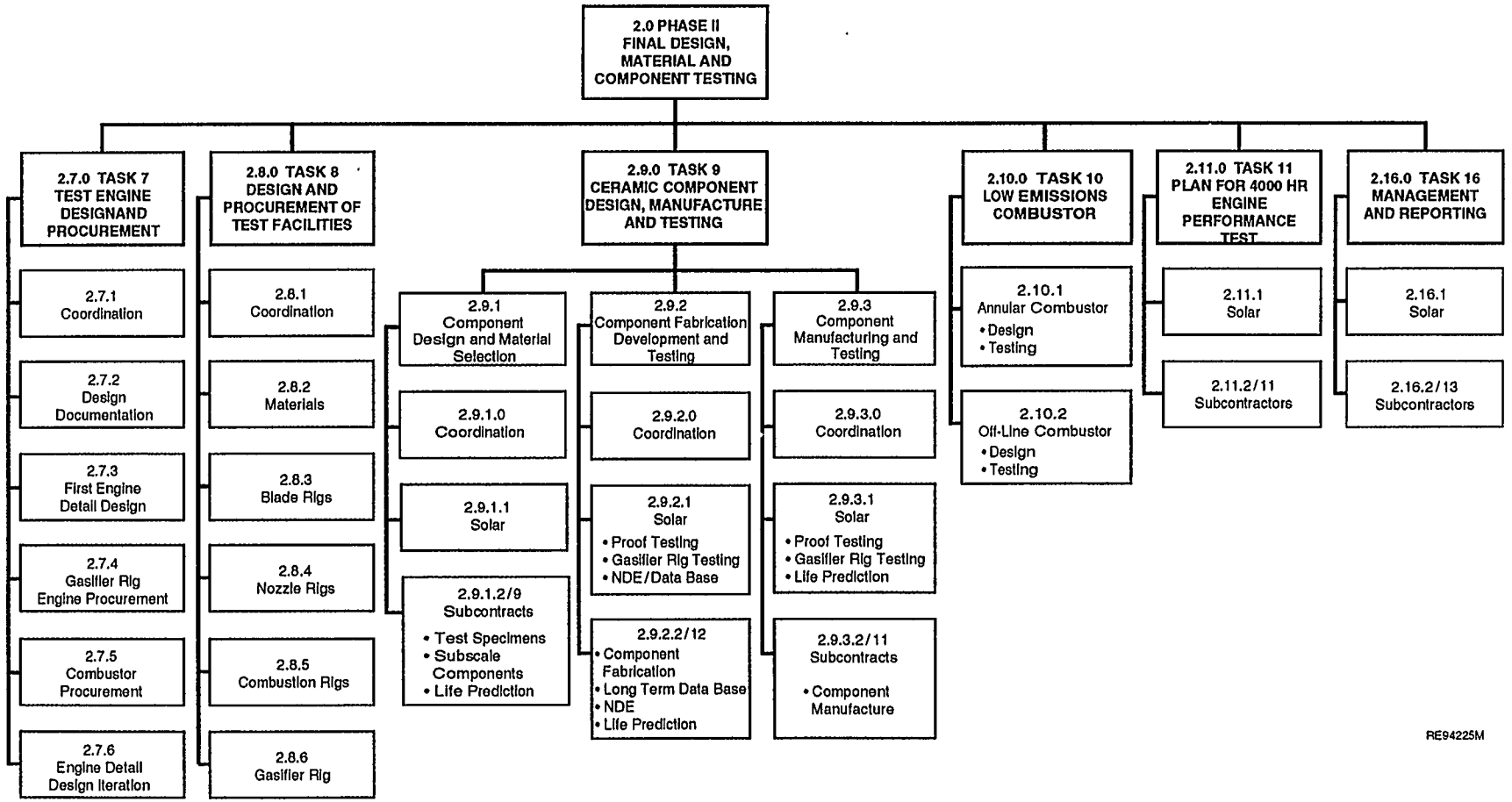

Figure 2-2. Major Tasks and Subtasks in the Work Breakdown Structure - Phase II

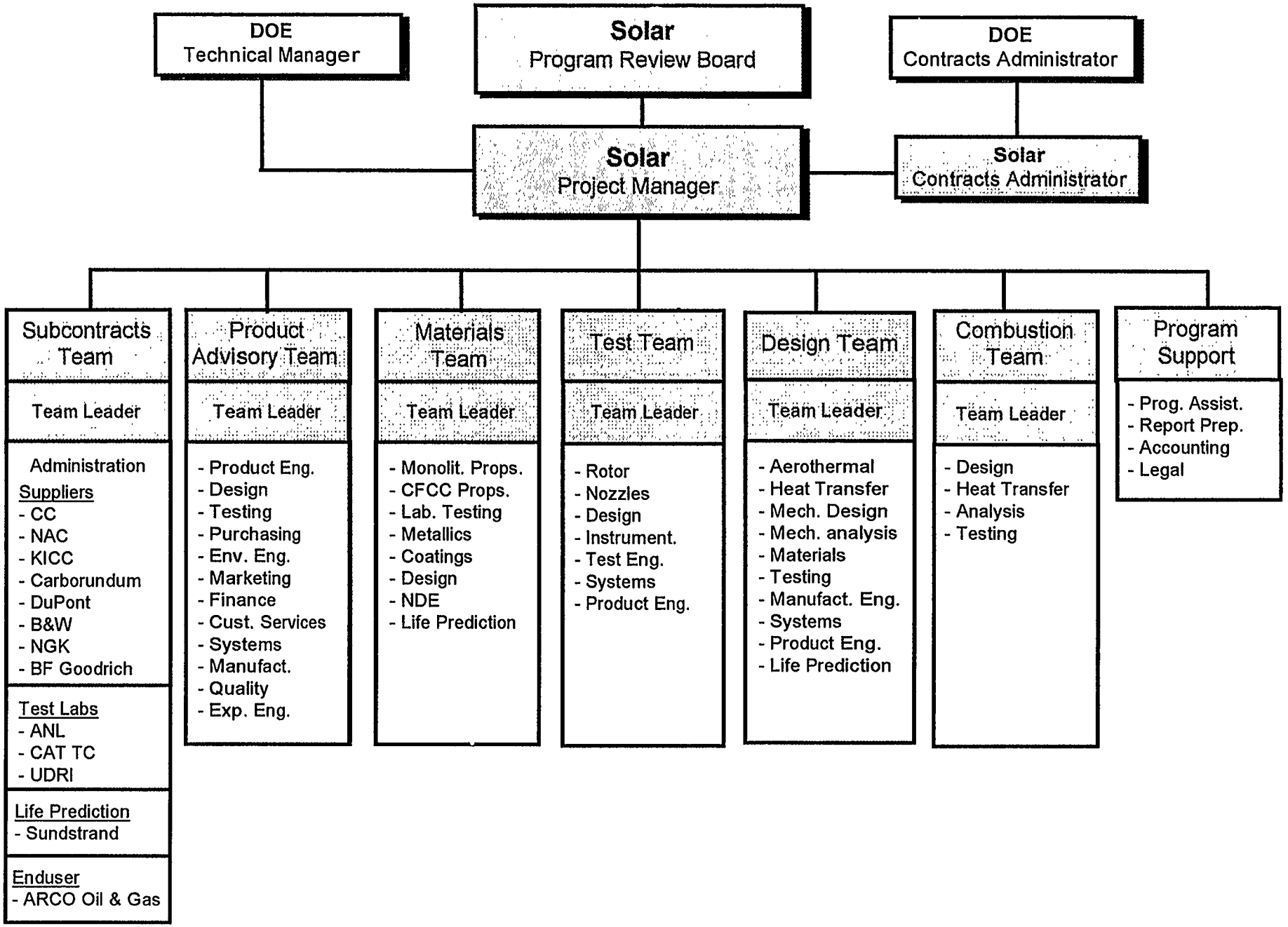

Figure 2-3. CSGT Program Organization

REFERENCES

1. "Ceramic Stationary Gas Turbine Development Program", 1993, Phase I Final Report, Solar Turbines Incorporated, DOE Contract Number DE-AC02-92CE40960. Under review.

2. "Ceramic Stationary Gas Turbine Development", M. van Roode, W.D. Brentnall, P.F. Norton, and G.P. Pytanowski, ASME Paper 93-GT-309, presented at the International Gas Turbine and Aeroengine Congress and Exposition, Cincinnati, Ohio, U.S.A., May 24-27, 1993.

3. "Application of SPSLIFE to Preliminary Design Evaluation and Life Assessment of CSGT Components", A. Saith, P.F. Norton, and V.M. Parthasarathy, ASME paper 94-GT-420, presented at the International Gas Turbine and Aeroengine Congress and Exposition, The Hague, The Netherlands, June 13-16, 1994.

4. "Ceramic Stationary Gas Turbine Development - First Annual Summary", M. van Roode, W.D. Brentnall, P.F. Norton, and G.L. Boyd, ASME Paper 94-GT-313, presented at the International Gas Turbine and Aeroengine Congress and Exposition, The Hague, The Netherlands, June 13-16, 1994.

5. "Ceramic Retrofit Program", M. van Roode, Paper presented at the Joint Contractors Meeting, FE/EE Advanced Turbine Systems Conference, FE Fuel Cells and Coal-Fired Heat Engines Conference, U.S. Department of Energy, Office of Fossil Energy, Morgantown Energy Technology Center, Morgantown, West-Virginia, U.S.A., August 3-5, 1993.

6. "Advanced Small Gas Turbines for Cogeneration", D. Anson, W.P. Parks, Jr., O. Evensen, and M. van Roode, Paper presented at the 7th Congress & Exposition Gas Turbines in Cogeneration & Utility, Industrial and Independent Power Generation, Bournemouth, England, U.K., September 21-23, 1993.

3.0

TASK 7 - ENGINE DESIGN

During the reporting period the detailed designs of the CSGT engine and key ceramic components selected in Phase I were completed. A Centaur 50 engine was procured for modification to accept the selected ceramic components. This engine will be used as a test bed to evaluate the ceramic components and interfacing metallic support structure.

3.1 BACKGROUND

Figure 3-1 shows the a schematic of the Centaur 50S engine. The S designation indicates that the conventional combustor has been replaced with a dry low-NOx SoLoNOx combustor. The lower portion of the schematic is the all-metal Centaur 50 configuration. The components targeted for ceramic substitution, the first stage blade, the first stage nozzle, and the combustor liner have been indicated. The engine has been modified with a Taurus power turbine to handle more effectively the increased volume flows of the Centaur 50S at the increased TRIT of 1121°C (2050°F). The top portion of the schematic incorporates the conceptual design of the ceramic hot section as of the end of Phase I.

Figure 3-2 shows the most recent layout of the engine hot section with the inserted ceramic first stage nozzle and first stage blade. The hot section layout represents the current status of the evolution of the ceramic component designs from conception through the preliminary and detail design phases. The design changes to the ancillary hardware, such as disks, rim seals, diaphragm, nozzle seals, tip shoe and nozzle case have also been indicated.

Designs have been detailed for the primary ceramic components, and fabrication is underway. Two blade designs with markedly different attachment systems conceived and taken through preliminary design in Phase I were detailed. The two designs share a common airfoil to facilitate tooling and fabrication in the event that program requirements dictate that blade suppliers change from one design to the other. One of these blade designs has a conventional dovetail root, the other design is of the pinned variety similar to that found in steam turbines (1).

The ceramic nozzle has a completely redesigned airfoil aimed at minimizing thermal stresses, and a novel mounting attachment which uses operational gas loading to improve seating loads.

Three combustor liner designs were detailed in subscale configuration. Two of the designs are monolithic, representing a tile and a ring configuration. The third design, represented by a simple cylindrical liner configuration was conceived for fiber-reinforced ceramic matrix composites (CFCC's) as a structural material. All three designs fit into a common envelope at the cylindrical sections of the primary combustor zone. The ceramic combustor liner designs have been described in detail with the Task 10 efforts in Section 6.0 (Low Emission Combustor).

Secondary components were modified to adapt to the interfacing ceramics and to enable operation at the TRIT of 1121°C (2050°C) increased from 1010°C (1850°F) of the baseline all-metal engine.

Designing for ceramics presents somewhat of a different challenge than designing for metal components. A few fundamental design guidelines had to be established at the onset, in order to create a framework within which designs could be evaluated on a consistent basis. The first and most important of these, was to establish by analysis of ceramic material data, acceptable stress

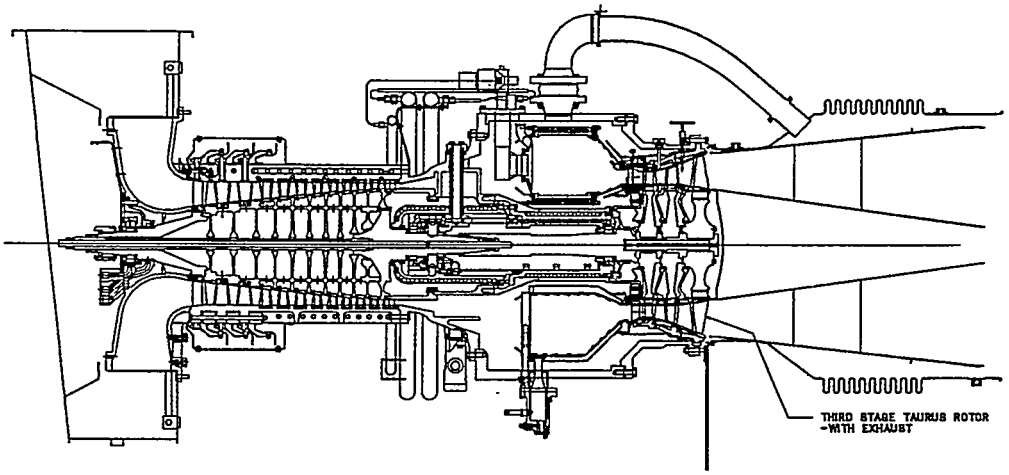

Figure 3-1. Schematic of Solar Centaur 50S. Lower Half: All-Metal Engine. Top Half: Engine with Ceramic Hot Section

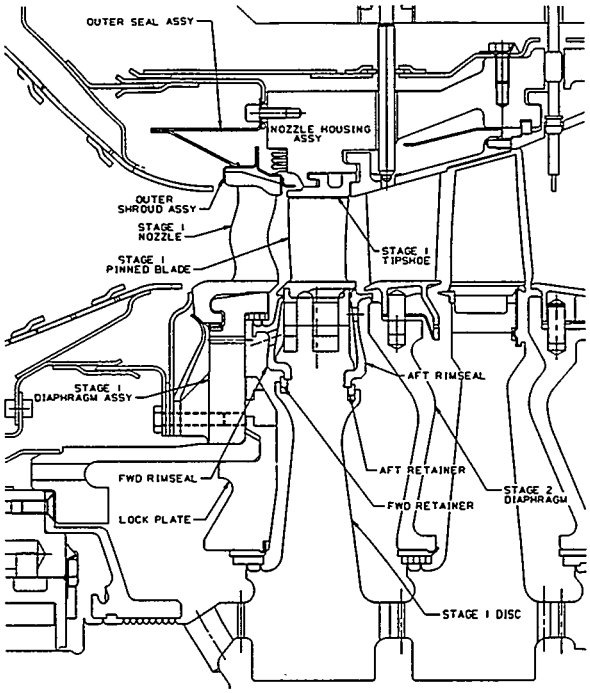

Figure 3-2. Schematic of Centaur 50S Hot Section with Inserted Ceramic Components

levels within each component consistent with a sufficiently high reliability for 10,000 hours continuous duty operation. The 10,000 hrs design life was selected since it affords an adequate margin over the 4,000 operating hrs scheduled for the Phase III field test. To design for the targeted life was not a simple task in many respects, in large part due to the fact that the material properties affecting component life differed considerably from one supplier to another. Moreover, the data base for ceramics for long term materials properties is very limited. A significant effort is underway in the program to provide long term materials properties to aid the component design an life prediction efforts.

Performance parameters based on product history for the baseline Centaur 50 engine and on aerothermal estimates for the Centaur 50 CSGT uprate are shown in Table 3-1.

The performance data show a modest increase in electrical thermal efficiency, in relative terms amounting to 5.6% in simple cycle and 5.3% in cogeneration (6.6% in cogeneration overall thermal efficiency). A substantial gain is observed in output power. Relative gains in electrical output power amount to 25.9% in simple cycle and 25.6% in cogeneration. The performance gains are mainly attributed to the increase in TRIT from 1010°C (1850°F) to 1121°C (2050°F), and to a minor extent to the reduction of parasitic cooling losses in the hot section. An additional performance goal of the program is to demonstrate emissions of NOx of 25 ppmv, with a stretch goal to achieve NOx levels of 10 ppmv or better.

Table 3-1. Centaur 50 Generator Set Compared with CSGT-Generator Set*

Engine Parameters	Centaur	CSGT
Airflow	18 kg/s	18 kg/s
Compressor Pressure Ratio	10:1	10:1
TRIT	1010°C (1850°F)	1121°C (2050°F)
Shaft Speed	14,950 rpm	14,950 rpm
Emissions: Uncontrolled Wet Dry (SoLoNOx®**)	106 ppmv 42 ppmv 42-25 ppmv	 25-10 ppmv***
In Simple Cycle Mode:		
TRIT	1850°F	2050°F
Shaft Output	5880 SHP	7402 HP
Shaft Thermal Efficiency	29.63%	31.29%
Electrical Output	4144 kW	5217 kW
Electrical Thermal Efficiency	28.01%	29.58%
In Cogeneration Mode:		
Electrical Output	4051 kW	5088 kW
Electrical Thermal Efficiency	27.38%	28.84%
Overall Thermal Efficiency	75.39%	80.33%

* Maximum Continuous Duty, ISO Conditions (Sea Level, 15°C Day)
** Solar Registered Trade Mark: Abbreviation of Solar Low NOx
*** 25 ppmv: DOE Program Demonstration Goal; 10 ppmv: Solar Goal

The work reported in this section focuses on the detail design efforts for the ceramic blade and nozzle and ancillary hardware.

3.2 CERAMIC BLADE DESIGN

Two different root attachment systems have been developed, a conventional dovetail, and a pin attached blade. This "two blade" philosophy was developed early in the program, as the ability of a compliant layer system to successfully withstand high loading conditions over many thousands of hours at engine operating conditions was not guaranteed. A pinned system which would not rely on a compliant layer was therefore viewed as a viable alternate design.

Another early goal of the program was to design ceramic blades which featured the same external airfoil profile as the current production cooled metallic blades. However, as the design analysis progressed, dynamic analysis showed that a second vibratory mode interference existed with the first stage nozzle passing frequency. To avoid this problem, the ceramic blade tip chord was increased slightly over that of its metal counterpart. Stress objectives for the blade airfoil were to achieve 138-172 MPa (20-25 ksi), with a higher allowance for the root due to the cooler temperatures.

The solid models in Figure 3-3 represent the preliminary designs of the two blade concepts taken into Phase II.

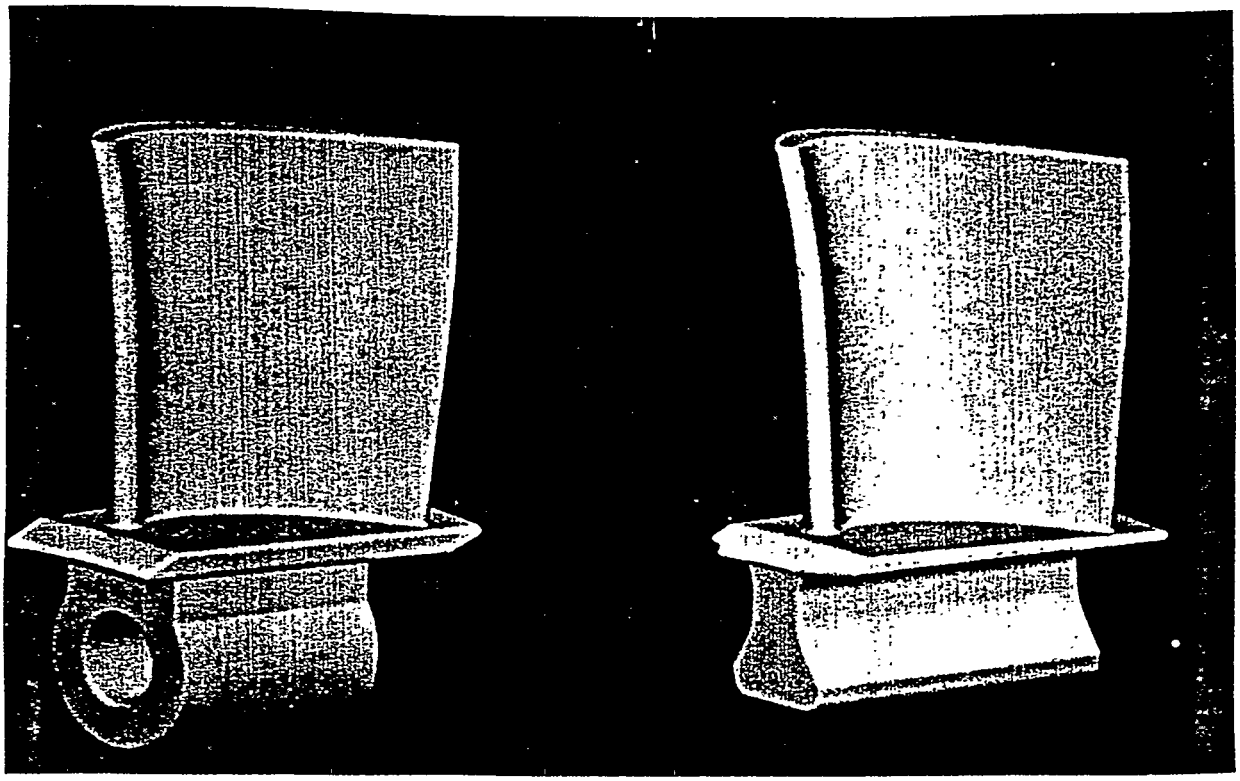

(A) Pinned Root Blade **(B) Dovetail Blade**

Figure 3-3. Solid Models of Two Ceramic Blade Designs

Sections 3.2.1 and 3.2.2 describe the detailing of the dovetail and pinned designs, respectively. Fabrication of both detailed designs is underway with first hardware delivery schedule for early 1995. Both ceramic blade designs represent detailed initial designs which may undergo modification based on the results of rig and engine testing scheduled to start in 1995 . The modifications represent design iterations scheduled as an integral part of the program statement of work.

3.2.1 Dovetail Blade

The dovetail blade may be considered a "conventional" ceramic design, it being very similar to other dovetail root ceramic blades developed on other programs (Figure 3-3B).

This design relies on a layer of relatively thin compliant material between the ceramic loading surface and the disk in order to equalize pressure face load distributions. The compliant layer also provides some level of protection from translation against the disk as hardware expands and contracts from thermal and mechanical loads. Furthermore, the compliant layer has also been designed to extend beyond the blade-blade gap to assist in sealing the inter-blade cavity from hot flowpath gas. More important is the benefit that comes from blade to blade frictional damping by the compliant layer scrubbing under the platforms.

The choice of compliant layer material is extremely important in this design, and one of the critical activities identified in Phase I was the selection and development of a compliant layer material that will meet the long life (30,000 hrs) service requirement of an industrial gas turbine. The material must be soft enough to smooth load distributions, but not so soft that it extrudes and permits direct blade/disk contact. It must also exhibit good wear characteristics as it will be exposed to relative motion between parts at high contact loads at the pressure faces. It also must resist wear from high frequency motion at light contact loads under the platforms. One of the advantages of ceramic blades is the ability to eliminate internal cooling air required for metal designs, but the metal disk posts still need some cooling air as the hot ceramic blades are in direct contact with the metal disk, providing a significant heat conduction path.

The dovetail angle has been set at 55 degrees. This was a design compromise between a smaller angle giving better anti - "stiction" characteristics (prevent sticking through frictional locking of the root in the disk on shutdown), and available space in the disk for generous fillet radii, given that the blade count remained unchanged from the metal firtree configuration.

The cooling air requirements for the dovetail (or pinned) blade/disk combination have been reduced by approximately 50% over the baseline Centaur 50 design at 1010°C (1850°F) TRIT. A solid model of the final dovetail blade design for component fabrication is shown in Figure 3-4.

<u>Dovetail Blade Transient Heat Transfer Analysis</u>

The determination of the thermal boundary conditions for the blade was relatively straight-forward as the external heat transfer environment is well defined and the blade itself is un-cooled. In this evaluation, the blade and disk post were analyzed with appropriate heat transfer boundary conditions input to simulate heat transfer from the blade to the disk. The steady state temperatures for the blade are shown in Figure 3-5.

A transient analysis was performed using measured flowpath temperatures from Centaur 50 combustor rig tests. Stress analysis was performed at numerous time points during the transient where radial and axial temperature gradients were maximum. The results of the analysis performed showed that peak stress occurred at steady state conditions. The final stress map for the blade is shown in Figure 3-6. The airfoil stresses are around 186 MPa (27 ksi), close to design objectives. A peak stress of 214 MPa (31 ksi) has been predicted in the cooler blade root region. It should be noted that the analysis performed assumed frictionless contact surfaces.

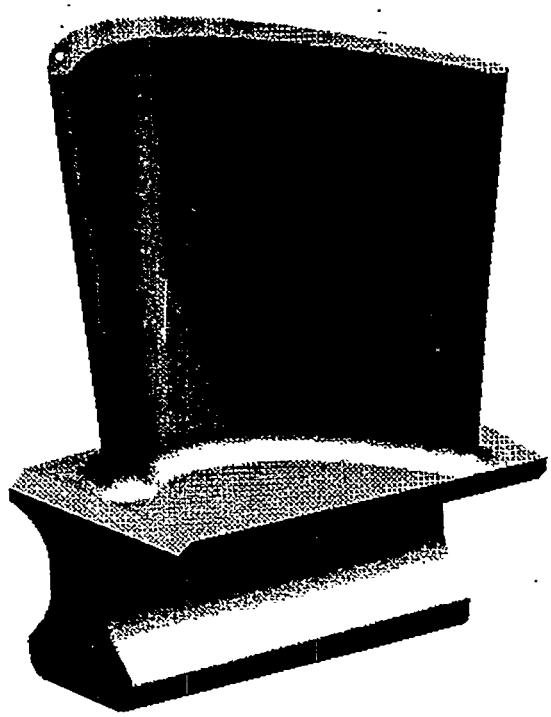

Figure 3-4. Solid Model of Final Dovetail Blade Design

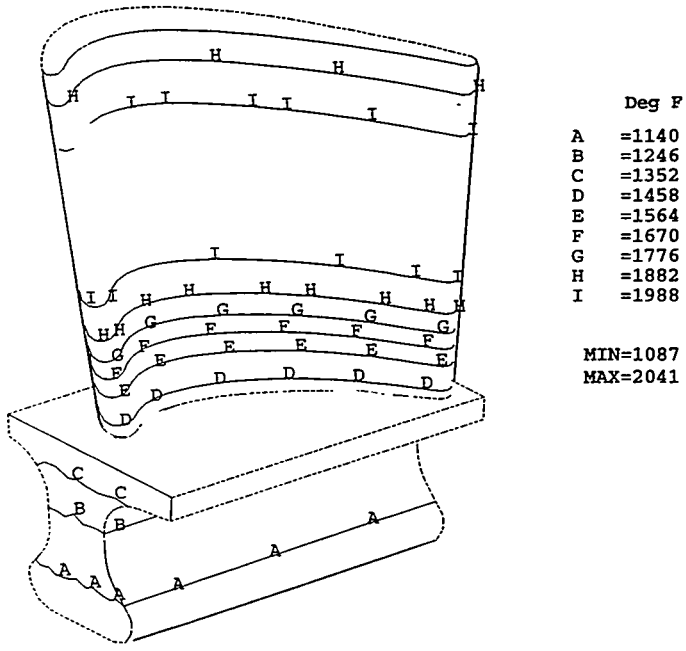

Figure 3-5. Predicted Steady State Dovetail Blade Temperatures at 1121°C (2050°F) TRIT

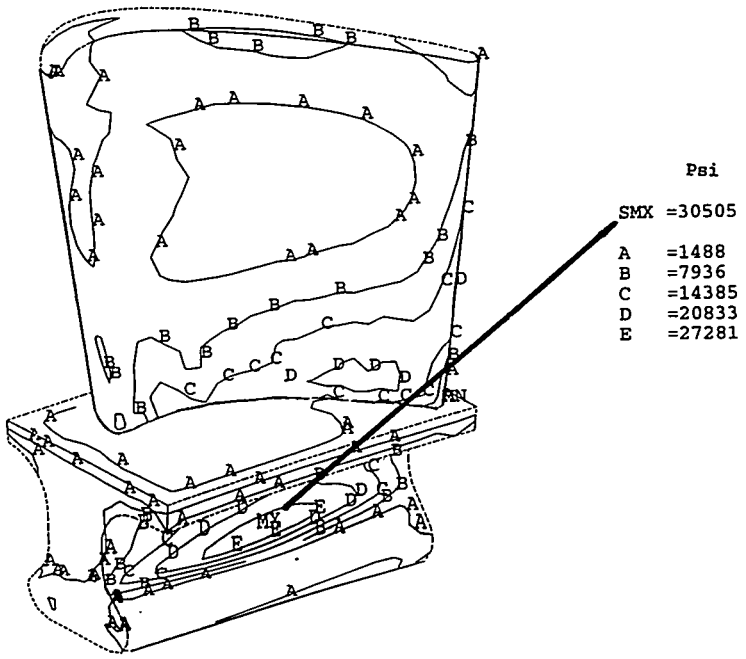

Figure 3-6. Predicted Steady State Dovetail Blade Stress Distribution (CF Load + Gas Load + Temperature Gradient)

Dovetail Blade Vibratory Frequency Prediction

Figure 3-7 shows the finite element model used for installed blade frequency prediction as well as a Campbell diagram illustrating crossings of concern. The data shown is for GN-10 silicon nitride material. Slightly higher frequencies have been predicted for NT164 silicon nitride blades. Major excitation sources include 12/rev which is the number of combustor fuel injectors, 30/rev which is the number of stage 1 metallic vanes upstream of the blades, and 42/rev which is the number of stage 1 ceramic vanes upstream and stage 2 metallic vanes downstream of the blades. To minimize fatigue damage the engine will be accelerated quickly through the crossings near 85% speed with GN-10 blades. The crossings for NT164 blades occur nearer to 90% speed due to the slightly higher modulus of elasticity for the latter material.

3.2.2 Pinned Blade

The first pinned root concept which was studied was a simple round hole with a close fitting ceramic pin (Figure 3-3A). This concept suffered from high local stresses in the pin and the blade root, and also presented a difficult cooling problem for the disk. As a result, a twin-lug, oval pinned blade evolved, the oval pin having a significantly higher bending stiffness in the radial direction than a circular geometry. A solid model of the final pinned blade design is shown in Figure 3-8.

With this design, the pin and blade stresses were reduced by over 55% from the preliminary single lug/round pin design. Moreover, the forward lug on the twin-lug blade isolates the disk from the hotter upstream gas path thereby ensuring a more efficient disk cooling system.

A two dimensional heat transfer analysis was used to derive root cooling flow and temperature distributions. Figure 3-9 shows the steady state temperature predictions for the root of the blade and the pin.

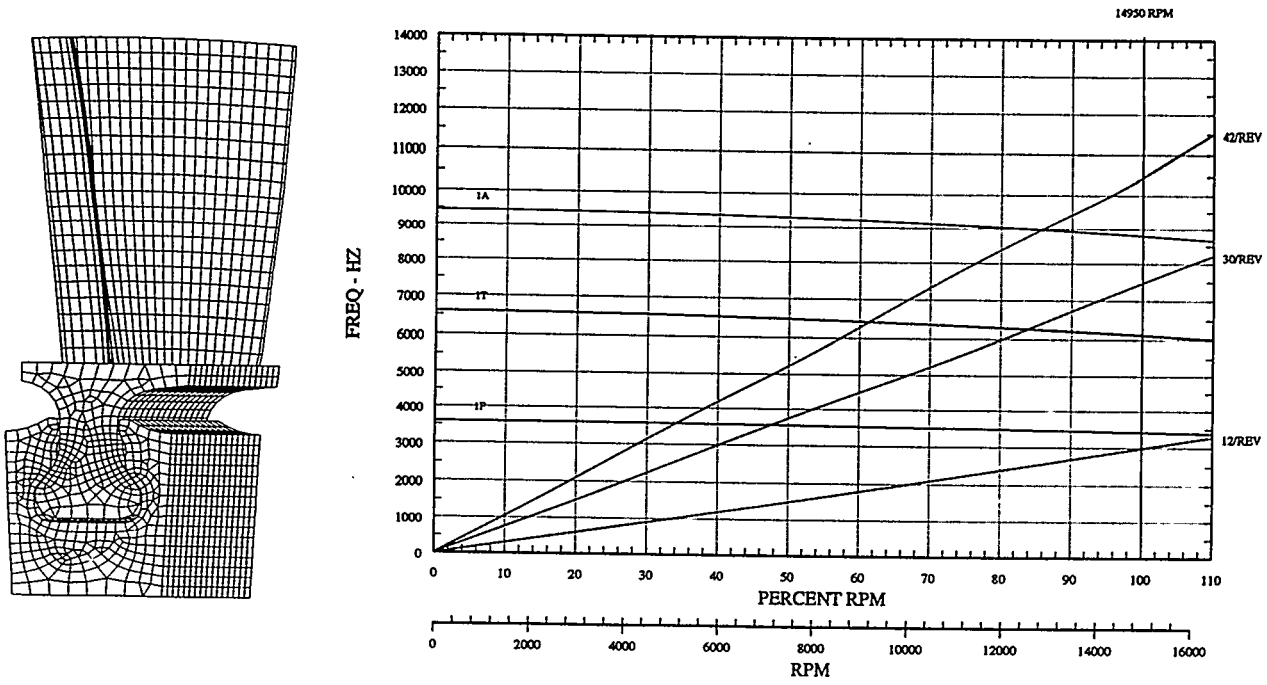

(A) Finite Element Model **(B) Campbell Diagram**

Figure 3-7. Dovetail Blade Vibratory Finite Element Model and Campbell Diagram

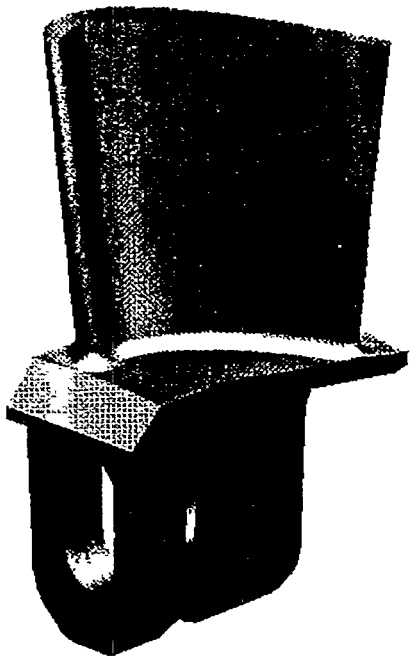

Figure 3-8. Solid Model of Pinned Blade Design

The above data, along with prior 3-D dovetail airfoil analysis enabled thermal boundary conditions to be mapped onto a 3-D pinned blade model. Resulting peak stress at steady state conditions for nominal hardware is presently at 277 MPa (~40 ksi), as shown in Figure 3-10. However, the critical hotter region airfoil stress is similar to that of the dovetail blade, and close to design objectives.

A major benefit of the pinned design over the dovetail design is lack of a compliant layer between the blade and the disk. Moreover, the relative displacement between the blade and the pin is an order of magnitude less than between the dovetail blade and the disk post. Very tight dimensional control of the fit between the pin and the blade has been found necessary to maintain reasonable blade root stresses.

Pinned Blade / Pin Tolerance Study

A two-dimensional non-linear contact analysis was performed to evaluate the sensitivity of blade root stress to tolerance variations between the pin and blade. Results of the analysis (Figure 3-11) show that tight dimensional control is required to maintain reasonable blade root stress. Surface profile tolerances of 0.005 mm (0.0002 inch) were specified on both the pin and blade drawings as a result of this study. This tight tolerance represents the blades most significant manufacturing challenge. Tolerance relief will be considered if successful tests are conducted using slightly out of tolerance hardware. Silicon nitride (SN-253, KICC) pin material was selected (the same material as for the pinned blade) due to the large blade root stress variations which would occur if materials with significantly different thermal expansion coefficients were used.

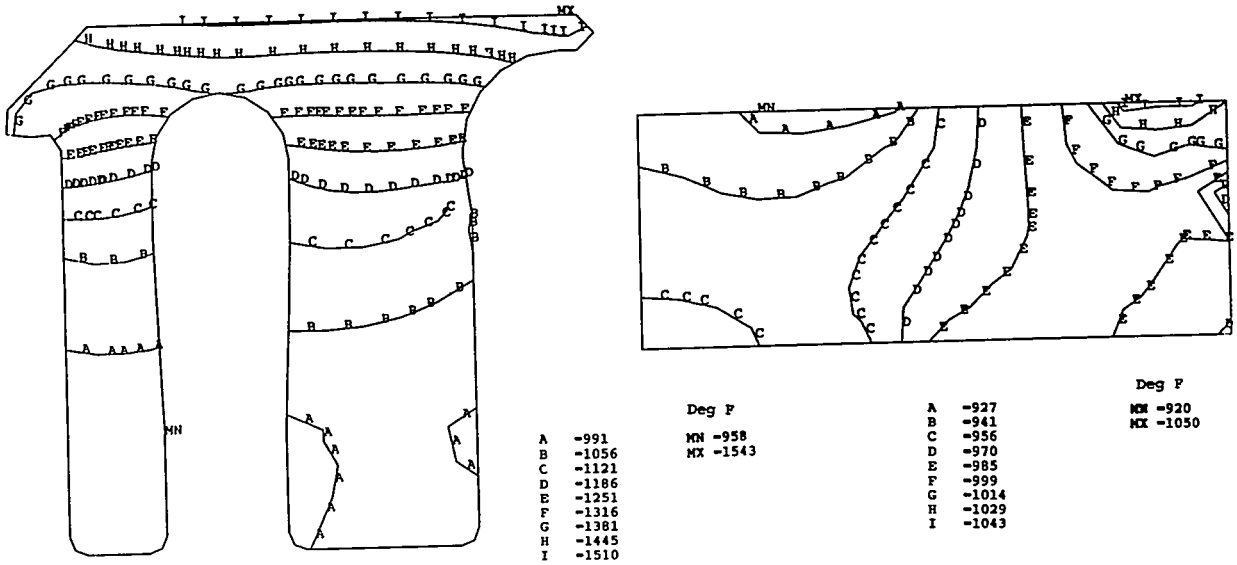

(A) Pinned Blade Root **(B) Blade Pin**

Figure 3-9. Steady State Temperature Predictions for Pinned Blade Root and Pin at a TRIT of 1121°C (2050°F)

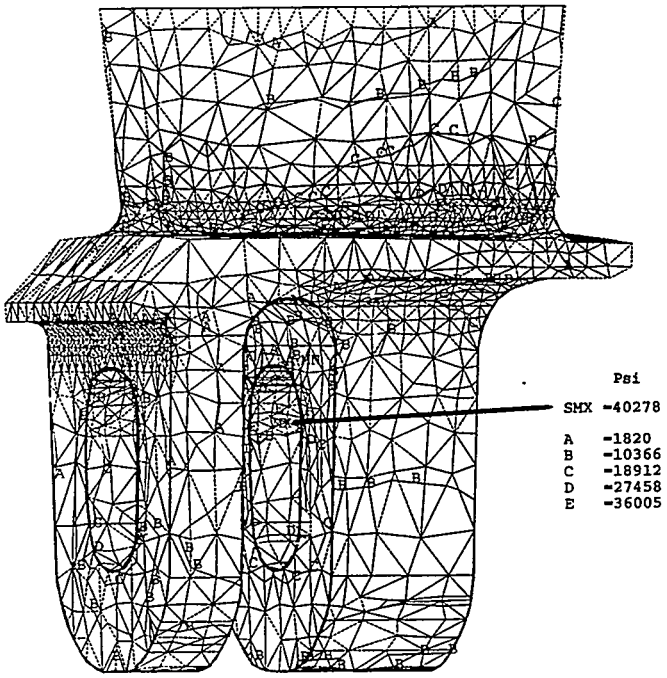

Figure 3-10. Predicted Stress in Pinned Blade (CF Load + Gas Load + Thermal Gradient)

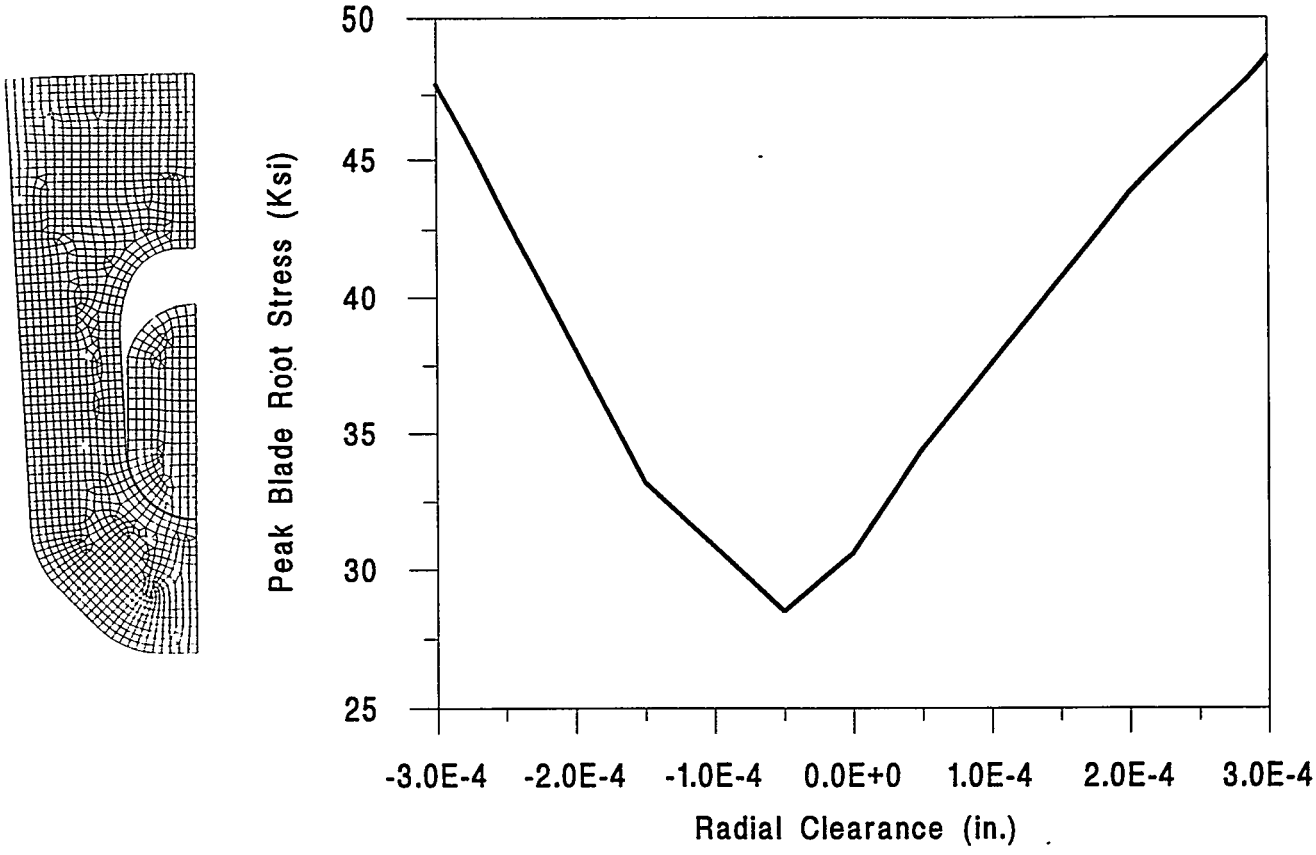

(A) Blade-Pin Finite Element Model (B) Peak Blade Root Stress vs. Radial Clearance

Figure 3-11. Effect of Fit between Pin and Blade

Pin/Blade Interaction Analysis

A three dimensional blade/pin interaction analysis was performed to predict pin stress and evaluate the impact of pin bending on blade root stress. Results of the speed-only analysis showed the maximum stress in the pin to be near that of the blade root at 290 MPa (42 ksi). Stress results in the blade root were very similar to those predicted assuming an infinitely rigid pin. While the disk flexibility was approximated in the analysis, consideration is being given to repeating the analysis with the actual disk rim modeled. Thermal stresses in the pin are expected to be very low based on the predicted pin temperature distribution. Figure 3-12 shows the model used for the analysis. Negative pressures were applied at the platform to simulate airfoil loading.

Pinned Blade Vibratory Frequency Prediction

A model of the blade, pin, and disk rim was constructed to predict installed blade natural frequencies. The model and results from the analysis are shown in Figure 3-13. The main crossing of concern is 12/rev at 90% speed where again, the engine will be accelerated quickly to minimize fatigue damage.

Pinned Blade Damping

One source of damping for the pinned blade is contact with the forward rim seal. Substantial effort was expended designing the forward rim seal to provide relatively light contact loads at the forward face of the blades. An additional damper is being developed which consists of a metallic "chicklet" that is installed above the forward disk lug between pin holes. Speed forces the chicklet to contact side by side blades above the lug providing blade to blade frictional damping. Both dampers discussed contact the blade in low stress areas.

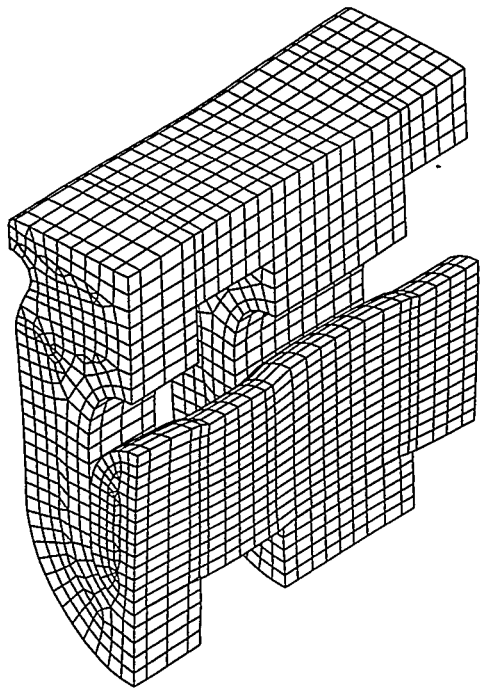

Figure 3-12. Blade-Pin Interaction Finite Element Model - Exaggerated Deflected Shape

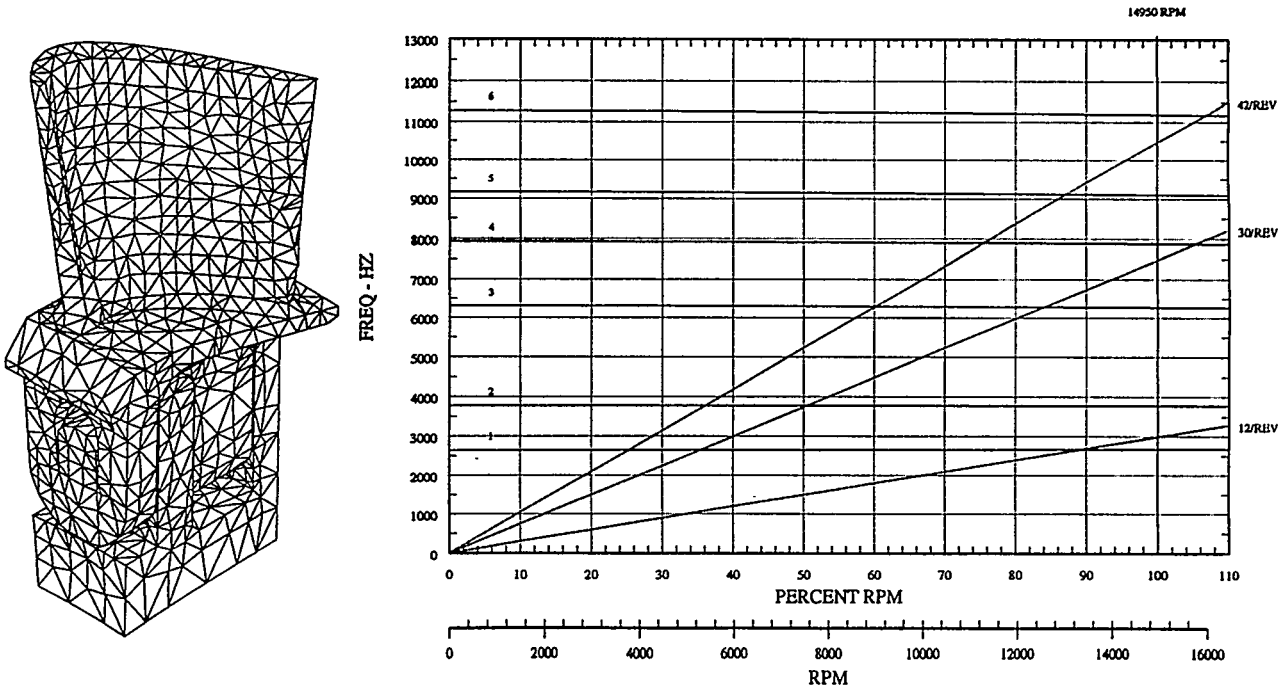

(A) Pinned Blade/Pin/Disk Rim Model **(B) Campbell Diagram**

Figure 3-13. Pinned Blade/Pin/Disk Rim Model and Resulting Campbell Diagram

Blade Life Prediction

Reliability analyses using NASA CARES/LIFE and SPSLIFE life assessment computer routines (2-4) have been performed during various stages of blade design.

Early analysis data on preliminary dovetail designs similar to the final design indicated about 98% probability of survival (POS) over 30,000 hrs of component life for a single as-processed blade with a machined root using NT154 silicon nitride (5). NT154 is a precursor material to NT164, one of the candidate materials for blade fabrication. This POS assumes the presence of a functional compliant layer between the dovetail root and disk. The current "dovetail" material has somewhat better properties in the slow crack growth regime and POS values are expected to be better. Slow crack growth was identified as the life limiting failure mode. The POS improved to 99.99% for a fully machined blade in which the reacted surface layer of NT154 which lowers as processed strength was effectively removed. This suggests that localized surface treatment through abrasive flow machining could be used to improve the POS for this blade design.

Life prediction work on the detailed designs reported here is in progress and results will be reported in the Phase II Final Report and other publications.

Ceramic Blade Manufacture

The selection of the ceramic materials and suppliers for blade fabrication was made early on in Phase II. The selection was based on materials property data, and supplier fabrication and commercialization plans, capabilities and experience. Two materials were selected for the dovetail design, GN-10 silicon nitride of AlliedSignal Ceramic Components (CC), and NT164 silicon nitride

of Norton Advanced Ceramics (NAC). The material selected for the pinned blade design was SN-253 of Kyocera Industrial Ceramics Corporation (KICC).

3.3 CERAMIC NOZZLE DESIGN

The initial strategy used in the hot section redesign was to maintain the aerodynamic shapes of the gas path currently used in the production metallic hardware, so as not to introduce a change which would impact the basic aerodynamic performance of the turbine. This goal was achieved to a large degree on the rotor blade, where only the tip section required modification to minimize vibratory response (see Section 3.2). However, the ceramic nozzle design represented an interesting retrofit design challenge for a number of reasons. Probably the major reason was that finite element thermal and stress analysis of preliminary designs using the existing nozzle airfoil revealed unacceptably high stresses in the airfoil trailing edge.

The design objective was to achieve stress levels in the 138-172 MPa (20-25 ksi) range, similar to the blade stress in the hotter airfoil region. The design of the interfaces between the ceramic nozzle and the metallic support structure represented another major design challenge. However, this is even more important for the nozzle as it runs significantly hotter than the blade.

Thermal boundary conditions applied to the nozzle finite element models were representative of a worst case combustor "hot spot" profile, a maximum combustor exit temperature of 1297°C (2366°F), having a probability of approximately 8% of occurring in any radial plane. Best statistical estimates from combustor injector data showed that approximately 28% of the nozzles in the stage would be directly affected by hot spot temperatures, (i.e. hot spot in the nozzle plane). Combining these two probabilities with the total number of nozzles in the stage gives an estimate of the total probability that any given nozzle will see the hot spot profile. The analysis showed that one (1) nozzle in the set may experience the worst case gradient, resulting in the combustor exit temperature distribution shown in Figure 3-14.

As a result of the high stress results, a number of alternatives were proposed focusing on reduction of the airfoil thermal stress. Proposals included airfoils detached from the shrouds, segmented/ slotted airfoils, and cooled/heated cored airfoils for thermal gradient reduction. A nozzle design proposed in Phase I in which the airfoil was detached from the inner shroud (1) failed to yield sufficient stress reduction at the design operating temperature and was abandoned from consideration early on in Phase II.

Multi-piece nozzles suffer from aerodynamic losses and potential sticking problems at cut interfaces. They also tend to be quite complex, requiring through holes and cooling air if metallic fasteners are used. The heating/cooling concept required holes in the airfoil which would cause stress risers and be difficult to produce. It became clear that none of the designs using the present airfoil would exhibit stress levels below 276 MPa (40 ksi) without introducing considerable complexity, aerodynamic losses, and risk.

The segmentation studies proved that for a given temperature gradient, stress levels can be reduced by using smaller components. The airfoil on the present metallic nozzle has a relatively long chord.

After unsuccessful attempts to retain the existing airfoil, a decision was made to redesign the vane, shortening the axial chord from 3.88 cm (1.53 inch) to 1.78 cm (0.7 inch). This required an increase in count over the present 30-vane metallic design. 42 Vanes were chosen for the new ceramic design for blade vibratory interference reasons.

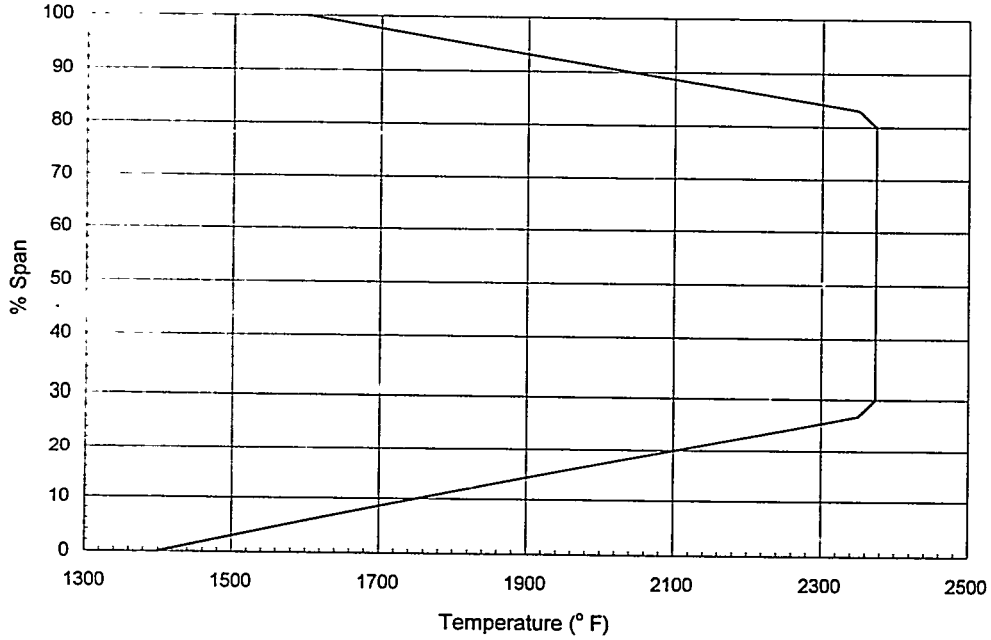

Figure 3-14. CSGT Worst Case Combustor Exit Temperature Profile at a TRIT of 1121°C (2050°F).

Stress analysis showed that shortening the chord alone did not reduce trailing edge stress to desired levels. A computerized airfoil stacking optimization routine was developed and applied to the new vane deriving combinations of axial and tangential curvature (bow) which resulted in significantly reduced stress. Several low stress shapes identified were provided to aerodynamicists for review/selection.

Aerodynamic and Mechanical Redesign of Existing Airfoil

Cycle matching studies of the existing Centaur 50 turbine operating at the increased firing temperature of 1121°C (2050°F) TRIT and reduced cooling flows showed that no changes were required to the turbine flow capacity (i.e. stage 1 nozzle area). Testing of the ceramic hardware is to be conducted in three phases: metallic nozzles/ceramic blades; ceramic nozzles/metallic blades; and ceramic nozzles/ceramic blades. These guidelines dictated that the ceramic hardware be aerodynamically matched to the existing metallic production airfoils.

Dawes 3-D viscous flow computational fluid dynamic (CFD) analysis of the most promising bow candidate showed acceptable aerodynamic loadings. Figure 3-15 shows the degree to which the airfoil sections were bowed relative to the initial straight stacked design.

Analysis indicated that reducing airfoil stiffness was a determining factor in minimizing thermally induced stresses. For this reason camber and maximum thickness were minimized for the new design.

The axial chord reduction caused the Zweifel loading coefficient to increase from 0.7 to 1.05, which is considered acceptable with respect to current design practice.

The ceramic nozzle is uncooled, which eliminated the need or desirability to maintain a constant section for simplifying cooling passages. The final airfoil was designed with five sections to optimize the spanwise aerodynamic loading. The root section trailing edge thickness and chord were increased over the other four sections to provide increased stiffness to better counter gas loads.

Throat openings were determined which, when integrated, would provide the same area as the existing hardware. The radial distribution of throat opening is the same as would be obtained with a constant section airfoil. The exit metal angle was fixed at 74 degrees for all sections. Normally, this type of design would produce a constant exit gas angle distribution, but due to the lean angles imposed by the airfoil bowing, CFD analysis was required to determine flow angles and establish bowed airfoil acceptability.

Whereas the original nozzle shape was nearly uniformly loaded radially, the CFD code predicted the highest aerodynamic loading from 0 - 50 % span for the ceramic nozzle as a result of bowing the airfoil (Figure 3-16). The loading distribution along the outer shroud contour has been improved over the current nozzle, (Figure 3-17), which was originally designed without the benefit of three dimensional CFD analysis.

The increased Zweifel loading coefficient of the new design raised some concern about a potential loss in airfoil efficiency, but average airfoil loading diffusion factors calculated from the CFD analysis were actually slightly better than those of the original metal design.

Results of the studies performed predict that the shortened chord bowed nozzle aerodynamic performance should be equivalent to, if not better than the existing metallic vane. A solid model of the final ceramic nozzle design is shown in Figure 3-18.

The ceramic nozzle shown has nearly 50% lower stress than if it had a straight stack similar to the current engine. Studies showed that stress magnitude could be correlated to bow magnitude (more curvature yielded lower stress). The amount of curvature selected was found to be acceptable both structurally and aerodynamically as the peak stress in the part (at steady state conditions) is now at 179 MPa (26 ksi), (Figure 3-19).

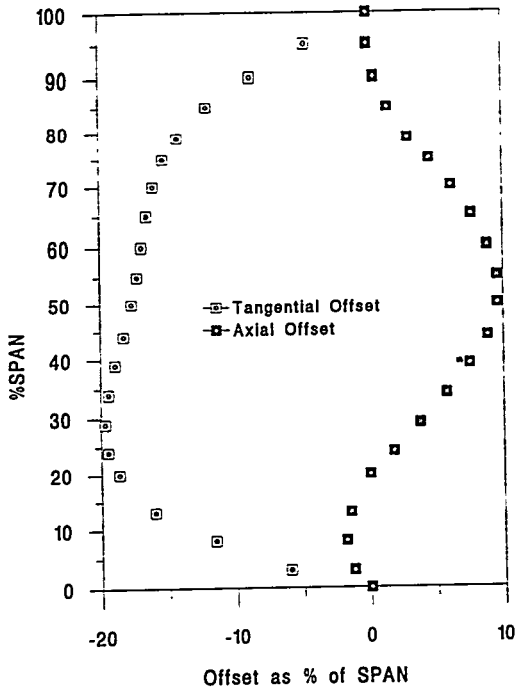

Figure 3-15. Nozzle Airfoil Stacking Offsets ("Bow")

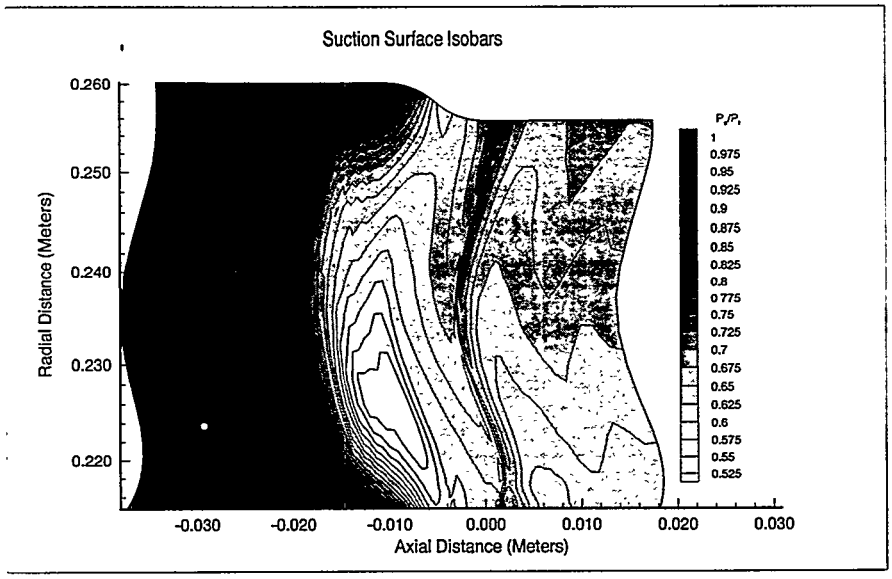

Figure 3-16. Dawes CFD Analysis - Suction Surface Isobars

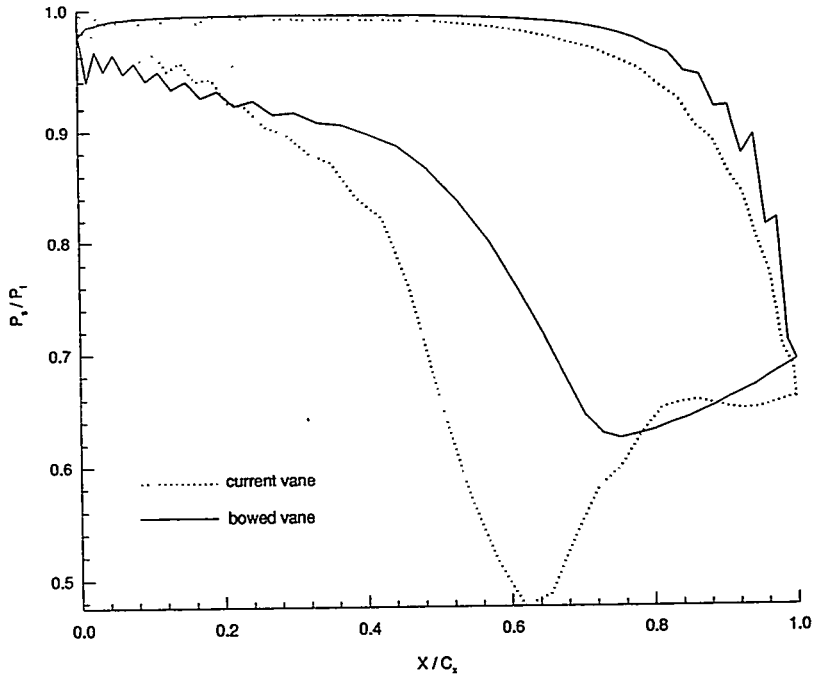

Figure 3-17. Nozzle Tip Section Loading Comparison

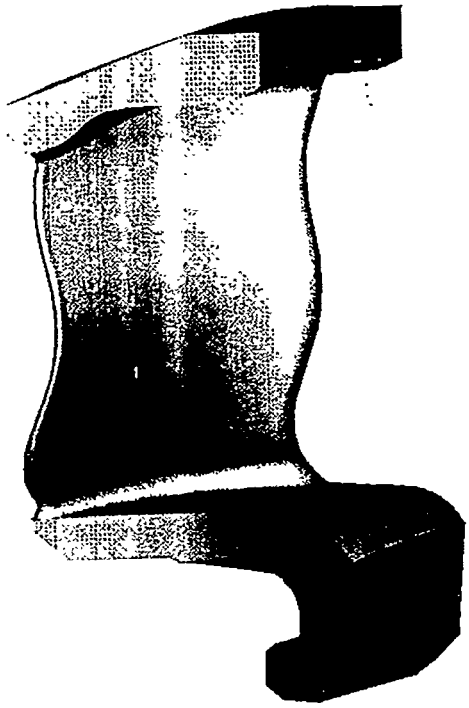

Figure 3-18. Solid Model of New Ceramic Nozzle

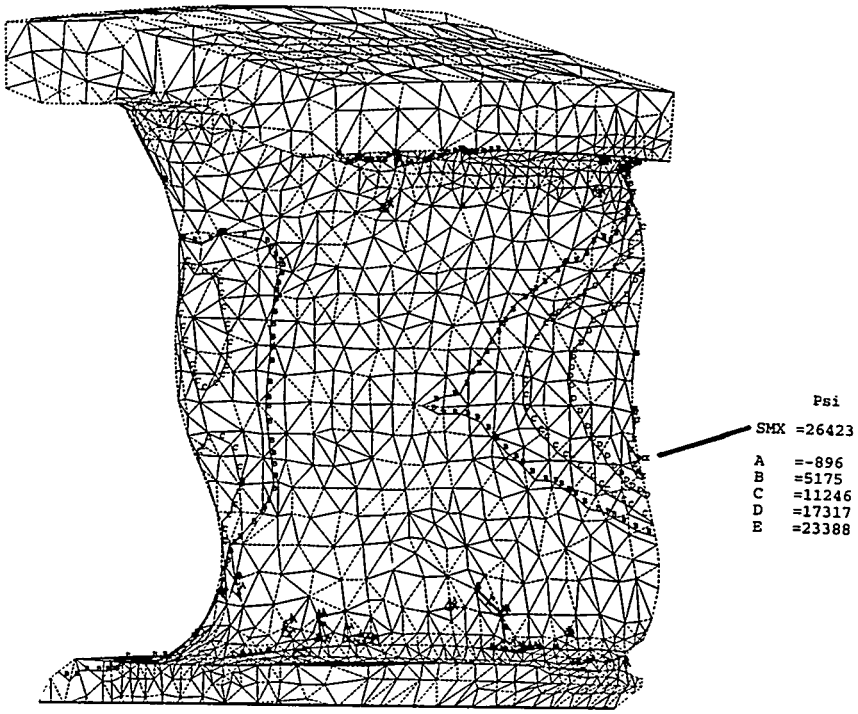

Figure 3-19. Predicted Stress Map for Stage 1 Ceramic Nozzle (Gas Load + Temperature Gradient)

Bowed Nozzle Transient Thermal/Stress Analysis

A transient (start/stop) thermal and structural analysis was performed on the bowed nozzle. The worst case flowpath temperature distribution shown in Figure 3-14 was assumed for the analysis. The external heat transfer coefficients were calculated using standard correlations. The nozzle steady state temperatures closely followed the combustor exit temperature distribution. Stresses 15% higher than for steady state were predicted shortly after shutdown. To counter this, the ceramic nozzle engine will be equipped with additional shutdown bleed valves to slow the transient helping to avoid the somewhat higher predicted stress.

Bowed Nozzle Frequency Prediction

Natural frequencies were predicted for the bowed nozzle mounted on the stage 1 diaphragm. The first mode has been predicted to cross 4/rev at 108% speed. The outer shroud sealing system is expected to provide a significant amount of damping for this mode as the vibratory displacement is predominantly axial. A trailing edge flap mode was predicted to cross 62/rev (# of 1st stage blades) at 90% speed. The engine will be accelerated quickly through this speed regime to minimize fatigue damage.

Airfoil Profile Tolerance Considerations

Manufacturing tolerances could impact the required throat area by approximately ±8%. Falling on the low end of this range could potentially cause surge problems, while falling on the upper end of this range will reduce thermal efficiency. It has been communicated with suppliers that the first product of the tooling be machined and inspected to determine actual throat openings, and adjustments made, if necessary, to the platform machining angles to obtain the desired throat opening.

Blade Use with Bowed Nozzle

While the aerodynamic performance of the bowed nozzle is expected to be similar to, if not better than for the existing metallic blade/vane combination, the current blade design could be improved upon in the second blade design iteration. Improvement can be realized by maintaining continuous channel flow acceleration as well as tailoring the blading to the flow angle distribution imposed by the new nozzle.

Nozzle Mounting Background - Metal Nozzle

Figure 3-20 shows the attachment method for the current metal nozzle. The metal nozzle is supported from the outside diameter of the diaphragm. No support of the nozzle outer shroud from the nozzle case is provided. However, this area of the nozzle is subjected to loads from the various seal components. The primary clamping function is performed by the clamp ring located on the front side of the nozzle. This clamp acts to load the nozzle rearward, with the clamping force being reacted at the diaphragm rear rail. The clamp also prevents the nozzle from lifting off the diaphragm when gas loads are applied. Also, each metallic nozzle segment (2 vanes per segment) engages into a dowel pin located on the aft rail. Its primary purpose is to provide precise circumferential positioning for each segment.

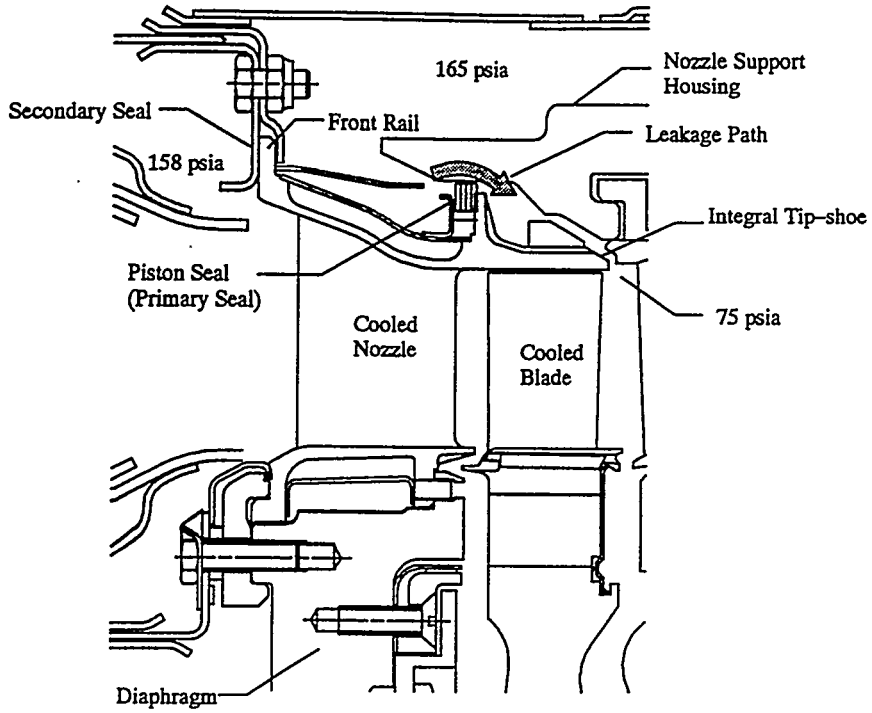

Figure 3-20. Present Centaur 50 Cooled Metallic Nozzle Mounting Arrangement

Ceramic Nozzle Mounting

For various reasons, it is not practical to apply the metal nozzle mounting scheme directly to the ceramic nozzle. The present production clamp is not compliant enough to avoid over-stressing the ceramic nozzle when part tolerances and differences in thermal expansion coefficients are considered. Also, the outer portion of the diaphragm for the cooled metallic nozzle is at a much lower temperature than predicted for the ceramic nozzle. The higher temperatures in the region would not likely permit the use of bolted fasteners.

Considering these and other shortcomings, a clean sheet conceptual design was initiated for the ceramic nozzle mounting scheme. The primary objectives of this concept phase were:

1. Provide a reliable, simple and compliant nozzle mounting design
2. Accurately position the nozzles to minimize nozzle to nozzle gaps/leakage
3. Minimize stress resulting from differences in ceramic/metal thermal expansion

The conceptual phase of developing a nozzle mounting design began by brainstorming possible design alternatives. Through this phase dozens of different mounting designs were considered.

After further analysis and review of all of the nozzle clamping systems, a "moment clamp" was chosen for more detailed analysis. In order to better understand the clamping loads required, a free body diagram was created and generalized force and moment balance equations were written. With these equations in a spreadsheet format it was possible to investigate the sensitivity to changing clamp angles, friction coefficients, gas forces, etc.

In summary, the analysis showed that a minimum clamping load of 181 kg (400 lbs) was required to ensure that the nozzle would not lift off the diaphragm when gas loads were applied. Each of the 42 nozzles will be subjected to an axial gas load of approximately 57 kg (125 lbs).

A desirable characteristic is to use a minimum amount of force to achieve adequate clamping. Due to concerns about the magnitude of the clamping load, a modification was made to the "moment clamp" design to incorporate a hook. When gas loads are applied, the loads are reacted directly onto the diaphragm rather than against the clamp. Required clamp loads are much less. Essentially they must satisfy positioning requirements at assembly and react outer seal frictional loads. Figure 3-21 shows the hook design and two dimensional reactions on the assembly assuming a 45 kg (100 lb) clamp load is used. Some of the features of the hook design are:

- Small clamp load required
- Self-clamping effect from gas load
- Clamp is farther removed from gas path
- Failure of clamp should not result in loss of nozzle
- Hot gas leakage under shroud will be small
- Straight ground hook is easy to machine
- Turned diaphragm provides precise positioning and is easy to machine

The nozzle hook geometry was designed to react the gas load moment at three radial contact positions on the diaphragm, two surfaces near the edges on the forward area of the hook, and one point on the aft underside of the inner shroud. The slash angles of the inner shroud are curved to better balance reactions at the three radial contact locations. The axial component of gas load is reacted along arc contact at the forward face of the diaphragm. The tangential component of gas load (23 kg/50 lbs) is reacted by dowel pins placed between slots in the diaphragm and simple to machine chamfers under the hooks of each nozzle segment. The dowel pins also provide precise tangential positioning for the segments.

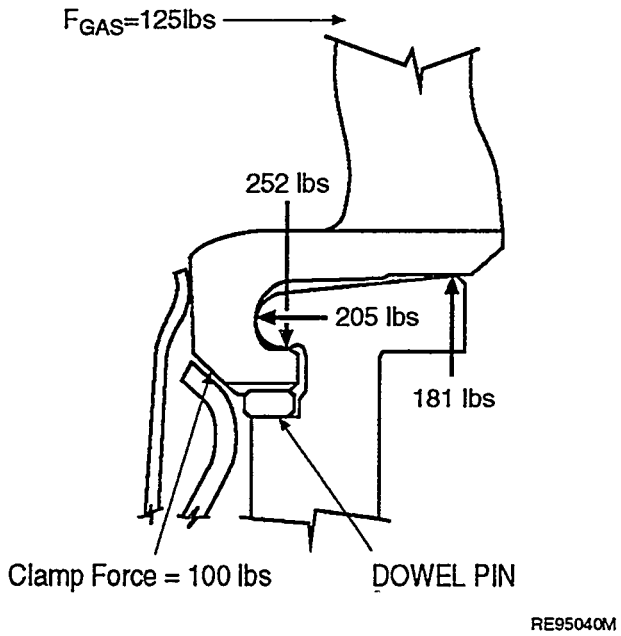

Figure 3-21. Hook Design and 2-Dimensional Reactions

The underside primary clamp has slots such that individual fingers contact each nozzle segment. This will insure that each segment is loaded uniformly. The clamp fingers have been designed flexible enough such that large variations in clamp loads will not be experienced due to manufacturing tolerances. The secondary clamp or seal loading the hook nearly axially is a continuous ring, but has been designed flexible enough such that it imparts minimal loads to the nozzle segments. Also, the stresses induced in the hook due to secondary clamp loads are very low.

Bowed Nozzle Life prediction

Results from one of the most detailed finite element models ever run at Solar (28000 elements) were fed into the NASA CARES/LIFE program. The most up to date materials data, some of which were reported in Section 5.0 were used. The predicted combined fast fracture and slow crack growth reliability for an engine set of nozzles for 30,000 hours of engine operation are 0.9995 and 0.9934 for SN-253 and SN-88, respectively. These values were substantially better than those for other nozzle materials investigated and contributed to the selection of these materials for fabrication of the first generation of prototype nozzles.

Nozzle Manufacture

An extensive comparison of material properties, component life assessment, component fabrication and commercialization plans, and suppliers experience and capabilities were used in the selection of the materials and suppliers for nozzle fabrication. This comparative evaluation resulted in the selection of two materials and suppliers for nozzle fabrication. The ceramic nozzles will be manufactured using SN-88 (NGK Insulators, Ltd.) and SN-253 (KICC) silicon nitrides. Initial nozzle deliveries fabricated from SN-88 are expected in the spring of 1995 permitting early simulated gas load/hook assurance testing. Engine testing is planned to be initiated in late 1995.

3.4 SECONDARY COMPONENTS

Substantial efforts in the detailed design were directed towards redesign of secondary components interfacing with the ceramic parts. Also, material changes were necessary to accommodate higher operating temperatures resulting from the increase in TRIT and/or altered component cooling. Some of these changes have been described in the Phase I Final Report (1). A summary of the recent and materials changes proposed is presented in Table 3-2.

Table 3-2. Materials Changes in Secondary Components

Component	Current Material	New Material
Stage 1 disk	V-57	Waspaloy
Front and Aft Rim Seals	Not in Current Centaur 50	Waspaloy
Stage 2 disk	V-57	Waspaloy
Stage 2 blade	IN-738LC	DS MAR M-247
Stage 2 diaphragm	N-155	Incoloy 903/909
Nozzle Support Housing	D-5B	Incoloy 909

Stage 1 Diaphragm Steady State Heat Transfer Analysis

The analysis was performed in order to ensure that the diaphragm temperature does not exceed 649°C (1200°F) in the load bearing structural portion supporting the hooked nozzles. Air being passed through holes in the diaphragm to supply disk rim cooling was found to be sufficient in maintaining the area of concern at 614°C (1137°F). The hot spot flowpath temperature was used at the inner shroud in order that circumferential maximum diaphragm temperatures would result. The steady state temperature distribution is shown in Figure 3-22 with the critical area and predicted temperature identified.

Nozzle Outer Shroud Sealing

To best understand the sealing requirement for the ceramic nozzle, a review of the metal nozzle sealing system is appropriate. This will also enable us to identify the changes that are necessary to accommodate the ceramic nozzle.

The metal nozzle with integral tip-shoe is supported by the first stage diaphragm at the nozzle inner shroud location as shown in Figure 3-23. The thermal response of the diaphragm closely matches the first stage disk, and therefore operating blade tip clearances are minimized.

The fundamental sealing requirement for the nozzle outer shroud is to prevent air which is at compressor discharge pressure (CDP) from leaking across the shroud and entering the gas path downstream of the first stage blade trailing edge. The CDP air is at a pressure of 1.14 MPa (165 psia), while the pressure downstream of the stage 1 blade is 0.52 MPa (75 psia), resulting in a net differential pressure of 0.62 MPa (90 psi). In addition to handling the pressure differential, the seal must also be able to accommodate the relative thermal growth between the nozzle outer shroud and the second stage nozzle support housing. For the metal or ceramic nozzle, this relative growth is such that the nozzle support housing moves 1.27 mm (0.05 inches) aft relative to the nozzle outer shroud.

The type of seal used for the metal nozzle is a piston seal design. It functions similarly to a piston ring seal in reciprocating engines. In addition to the piston ring seal, or primary seal, a secondary seal is located on the front rail of the nozzle. This seal keeps air at CDP pressure from entering the combustor exit area, since the combustor exit pressure is at a somewhat lower pressure of 1.09 MPa (158 psia). The seal also protects metal components including the nozzle support housing from exposure to hot combustion gases.

There are some important requirements of the ceramic nozzle design that require a different sealing philosophy than for the metal design. A critical requirement is to minimize mechanical loads that are imposed on the ceramic nozzle, and since experience with engines with metal nozzles has shown that large uneven loads are exerted by the piston seal onto the nozzle assembly, the piston seal design will not be used for the ceramic design. The primary seal that has been selected for the ceramic nozzle design is a triple convolution E-Seal made from IN-718 shown in Figure 3-24.

This type of seal has the advantage of small size, low leakage, low stiffness, and it easily conforms to sealing surfaces. Most applications for these seals have the convolutions aligned parallel to the engine axis. However, this seal has a radial orientation. The primary reason that a radial seal was chosen over an axial seal is that the radial seal accommodates the relative axial growths between the nozzle and nozzle support housing while applying only minimal additional mechanical loads to the nozzle. The E-Seal will also have one or more overlapped axial cuts. The cuts are necessary to eliminate excessive stiffness in the hoop direction if a continuous ring were used. The seal is positioned as radially inward as possible so as to minimize differential pressure loads that are exerted on the nozzle.

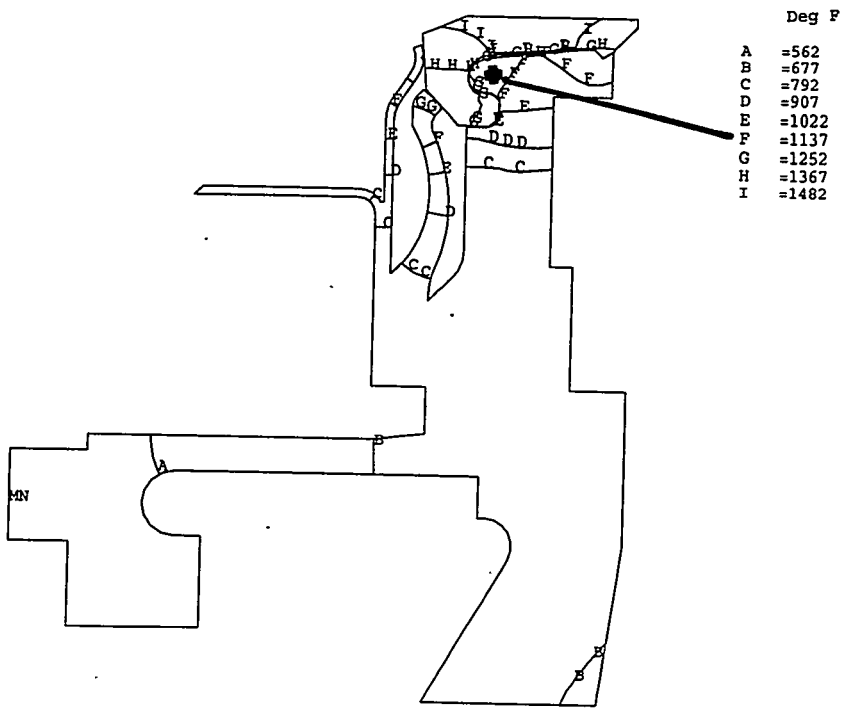

Figure 3-22. Stage 1 Diaphragm Predicted Steady State Temperatures at a TRIT of 1121°C (2050°F)

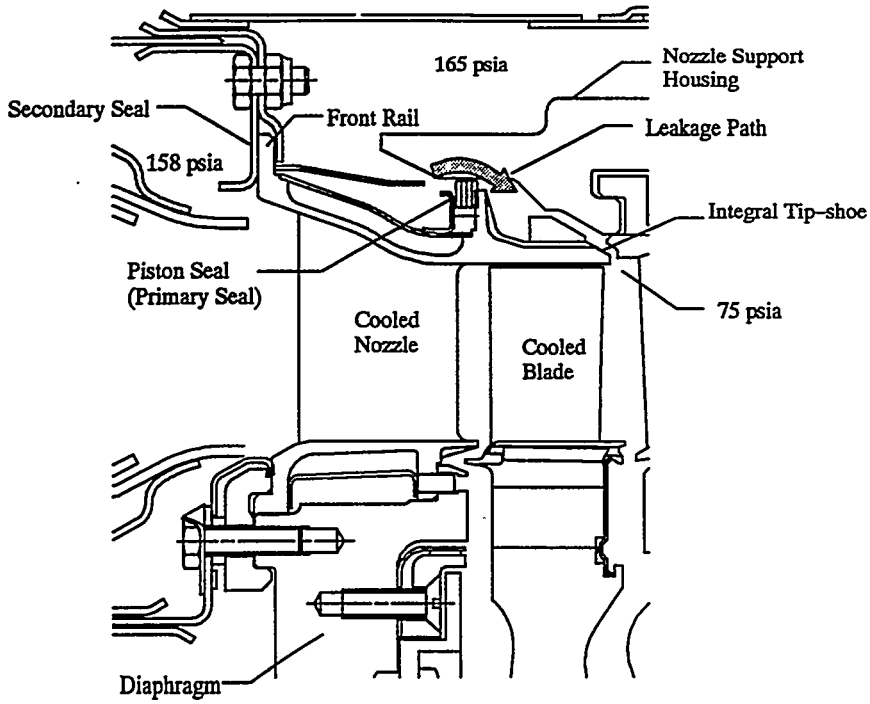

Figure 3-23. Stage 1 Metal Nozzle Sealing System

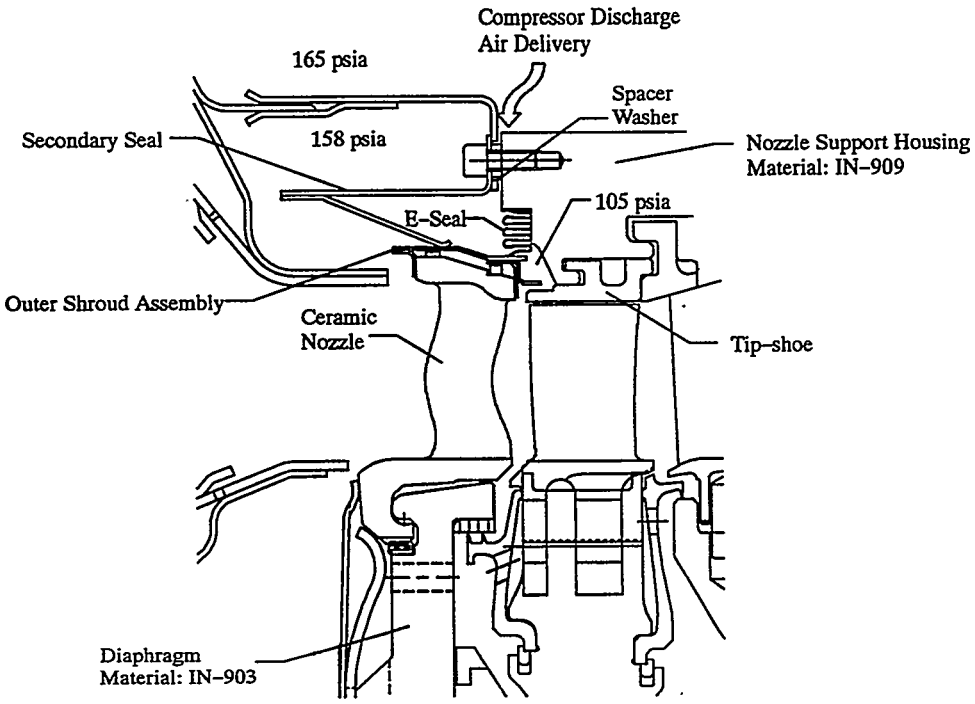

Figure 3-24. Ceramic Nozzle -Outer Shroud Sealing Scheme

In addition to the E-Seal which will be subjected to a pressure drop of 365 kPa (53 psi), there is also a low pressure seal or secondary seal (noted in Figure 3-24). This seal is subjected to the combustor pressure drop of approximately 48 kPa (7 psi). As proposed, this seal would be of sheet metal fabrication. Narrow axial slots will be required to reduce stiffness creating a "fingerlike" geometry. Spacer washers will be used at the location where the low pressure seal mounts to the nozzle support housing. This will allow CDP air to enter the sealing cavity, this cool CDP air protects the metallic components, housing, seals etc. from hot combustion gases.

The sheet metal nozzle outer shroud assembly is a key component for the ceramic nozzle design. This assembly serves a number of functions, though the primary purpose of the seal is to protect the ceramic nozzle from direct contact with relatively cool CDP air. CDP air is at approximately 399°C (750°F), while the ceramic nozzle outer shroud temperature is approximately at 871°C (1600°F). Without the seal, direct impingement of CDP air onto the nozzle outer shroud would result in increased thermal stresses in the ceramic nozzle. The assembly provides an intermediate temperature sealing surface easing seal wear concerns. The shroud assembly also protects the nozzle support housing from radiant heating. The assembly should also be effective in dampening nozzle vibration.

Candidate materials for the metal shroud assembly are Haynes A-230 and Hastelloy X. Protective coatings to further resist oxidation will be applied to the highest temperature regions of the sheet metal assembly.

At present the shroud assembly will have seven segments, rather than a single piece. One of the main advantages of a multiple segment design is that it will limit the radial growth that the E-Seal will have to withstand. A single piece/continuous shroud assembly would grow as much as 2.5 mm (0.1

inch) radially into the seal under a cold start condition. A segmented seal would reduce the radial compression of the E-Seal to approximately 0.25 mm (.010 inch).

Another key advantage of the segmented shroud design is that it eases assembly onto the ceramic nozzle. Each segment can be slid onto a group of nozzles, with metal overlapping both ends of the nozzle outer shroud, this would be difficult to achieve with a single piece design.

Finally, with a segmented design, compression of the seals will induce an inward reaction onto the nozzle assembly easing concerns over aft hook support liftoff during shutdown.

First Stage Tip-shoe

The metal nozzle has an integral tip-shoe. However , such a design was considered to be too ambitious for the first prototype ceramic nozzle design. Separate metallic tip-shoe segments will be supported from a low expansion alloy (Inconel 909) second stage nozzle support housing. The aft rail of the tip-shoe has been designed so that no changes will be required to the second stage nozzle.

Rim Seals

In order to reduce the cooling air requirements, forward and aft boltless rim seals have been designed for the stage 1 disk to assist in buffering the metallic hardware from the hot gas stream. This task represented a significant design challenge in that space was extremely limited in the disk rim area, as can be seen in Figure 3-2. The current all-metal Centaur 50 engine design has no rim seals.

Two forward rim seal labyrinth teeth were proposed to protect the forward stage 1 disk cavity from 871°C (1600°F) hot flowpath gas ingress. The aft rim seal required only one labyrinth tooth acting as a discourager because the temperature of the hot gas ingressing at the aft stage 1 disk cavity is 111°C (200°F) less than the temperature at the forward cavity.

As mentioned above, the incorporation of rimseals along with the uncooled ceramic blade, assisted in reducing the cooling requirements for the disk by 50% over current (lower TRIT) Centaur 50 requirements.

Disk/Rimseal Heat Transfer Analysis

Goals for the rimseals and disk were to maintain steady state maximum temperatures of 691°C (1275°F) and 649°C (1200°F), respectively. The tip of the forward rimseal requires cooling air to be passed through radial slots in order to maintain the tip below the 691°C (1275°F) allowable value.

The dovetail and pinned root disks use common rimseals except that the forward rimseal for the pinned blade has fewer scallops in the tip. As a result 0.2% less flow passes than for the dovetail rimseal. Less flow is required using pinned blades because they feature an overhang shielding the tip from the flowpath.

The aft rimseal which is exposed to cooler disk cavity temperatures still requires some cooling. This was accomplished by dumping spent air exiting from the blade/disk interface cooling channels. Figure 3-25 shows the cooling channels for both designs, and predicted (total stage) percent flows.

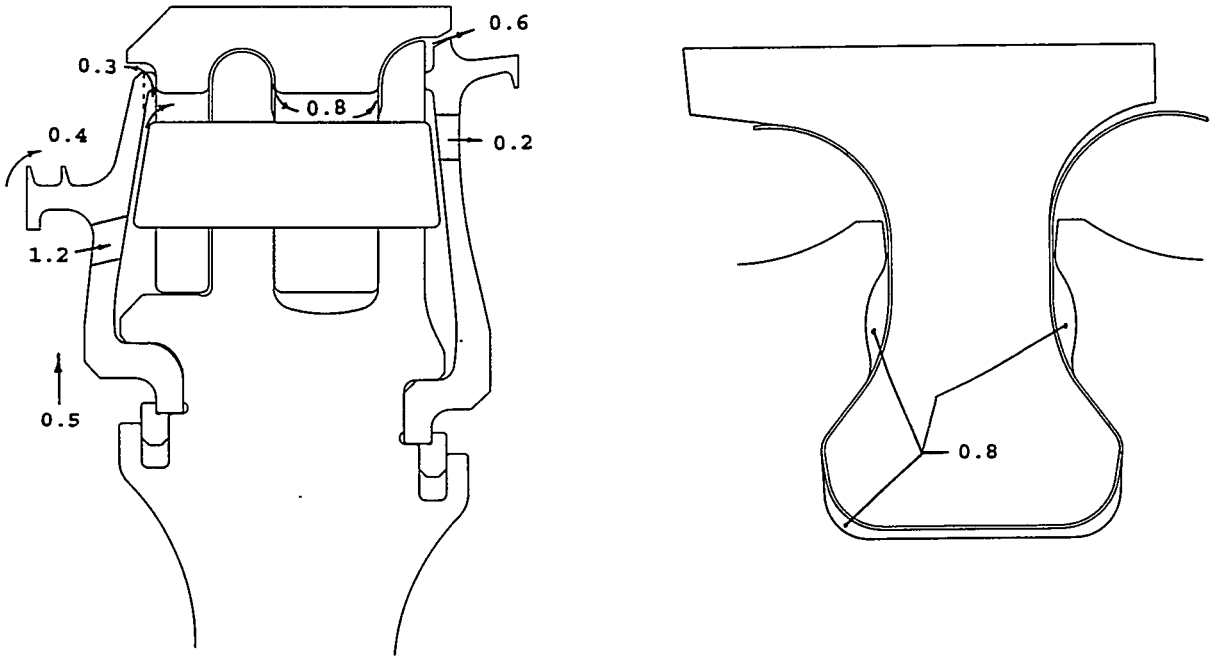

Figure 3-25. Flow Channels and Cooling Flow Percentages

The model used for the dovetail disk assembly analysis is shown in Figure 3-26. Resulting steady state temperatures of the rimseals and disk rims are shown in Figures 3-27 through 3-29. Peak rimseal temperatures are close to established limits. Dovetail disk post min-neck section steady state temperatures are at 622°C (1152°F) (somewhat below the 649°C (1200°F) limit). The pinned blade disk finger predicted peak temperature is 596°C (1105°F), again somewhat below the 649°C (1200°F) limit. A decision was made not to reduce cooling flows until test data becomes available confirming temperature predictions.

Rim Seal Stress Analysis

A transient startup/shutdown stress analysis was performed using a combined 2-D finite element model with non-linear gap elements at the interfaces of the disk, retainers, blade, and rim seals. Using a very thorough iterative process of modeling and analyzing, many different rim seal designs were evaluated before settling on the configuration shown. Several sensitivity studies were done on the interfaces in order to reduce stresses and interface loads.

The time points used for analysis were chosen by searching for the largest predicted temperature difference between the disk bore and the tips of the rim seals. Air hole concentrated stress predictions were obtained using detailed three dimensional sector models. Calculated hoop stress concentration factors were 2.5 and 2.8 for the forward and aft rim seal holes respectively.

The maximum stress range in the rim seals occurred in the aft seal cooling hole with a predicted low cycle fatigue life of 4400 starts/stops using minimum material properties. Shaped holes could be used to lower the stress concentration factor to increase the LCF life, but program requirements do not dictate excessive cyclic operation. For this reason, more expensive shaped holes were not judged necessary for the CSGT program, but could be introduced before commercialization.

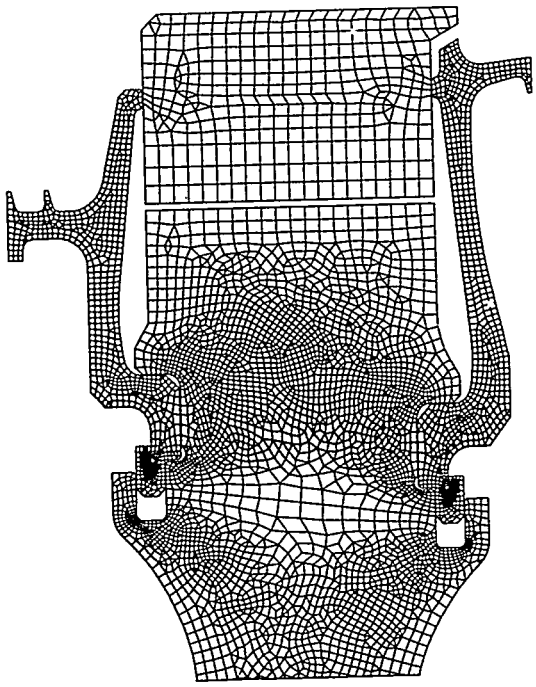

Figure 3-26. Rim Seal Finite Element Model for Dovetail Blades

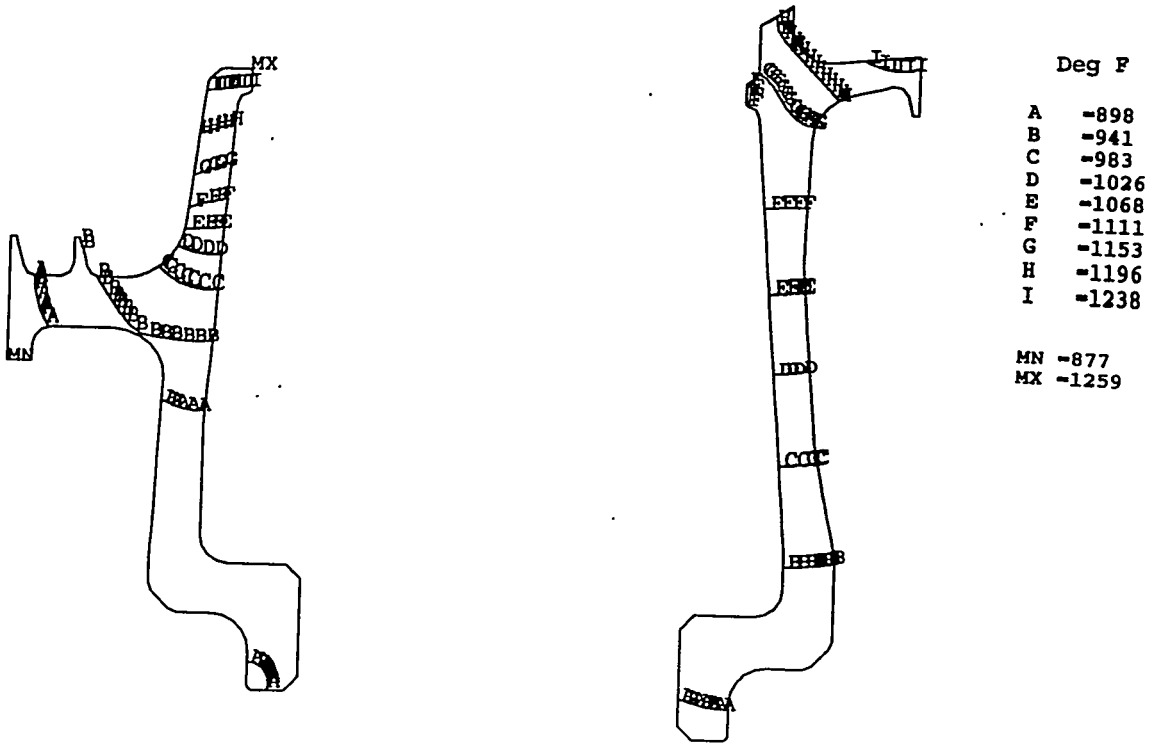

Figure 3-27. Steady State Rim Seal Temperature Predictions at a TRIT of 1121°C (2050°F)

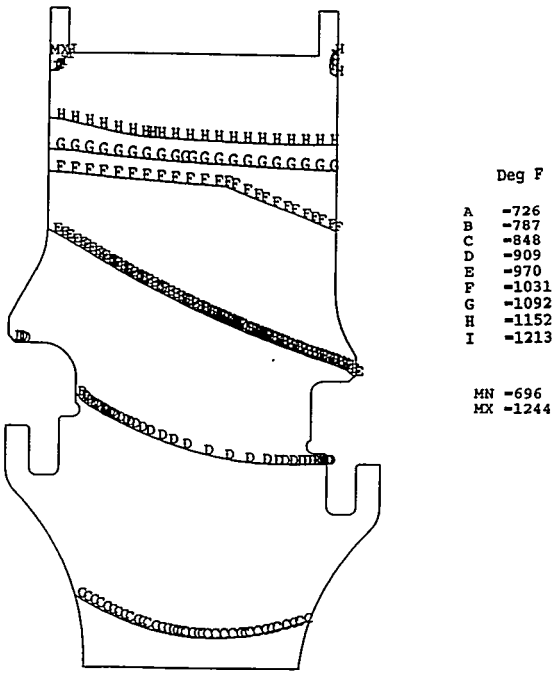

Figure 3-28. Steady State Dovetail Disk Temperature Predictions at a TRIT of 1121°C (2050°F)

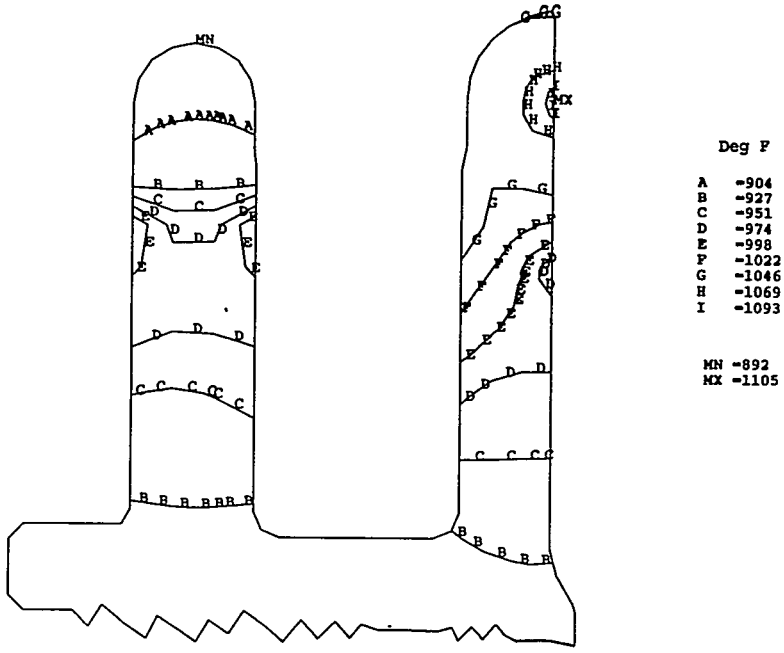

Figure 3-29. Steady State Pinned Blade Disk Temperature Predictions at a TRIT of 1121°C (2050°F)

Stage 2 Diaphragm Redesign

The stage 2 diaphragm was redesigned to provide clearance for the aft rimseal attachment. Back to back thermal/pressure finite element analysis substantiated the new design, as shown in Figure 3-30.

Clearance Analysis

Because ceramics are characterized by their low fracture toughness and low impact resistance, a basic design philosophy in this program has been to avoid a blade rub at all times under all engine operating conditions. Therefore, it is important to accurately predict the turbine blade axial and radial clearances for the whole operating cycle. As a result, a good deal of effort has been expended in developing a design tool to predict temperatures and displacements of ceramic and interfacing metal engine components during steady state and transient engine operation. The results of these analyses will be used to aid setting assembly clearances and estimate hardware relative displacements.

A detailed 2-Dimensional finite element model of the engine hot section was prepared for an early engine build targeted to operate at 1010°C (1850°F) TRIT. The build uses the current metal stage 1 nozzle with integral tipshoe, and a ceramic stage 1 blade. The model included all the components aft of the thrust bearing as shown in Figure 3-31 which illustrates the finite element model used for these analyses.

The transient start-up and shut-down conditions from a single shaft Centaur 50 were obtained from an engine test and were applied to the model for transient analysis. Thermal boundary conditions were either calculated, obtained from existing test data, or extracted from open literature empirical data.

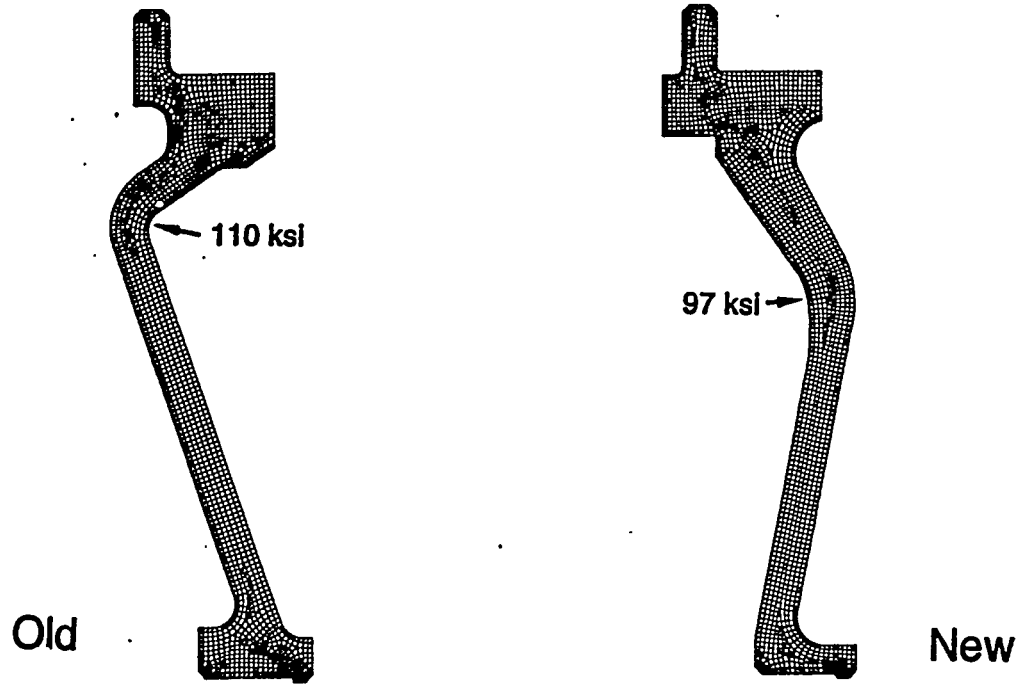

Figure 3-30. Present Engine and New Design Diaphragm Estimated Steady State Stresses

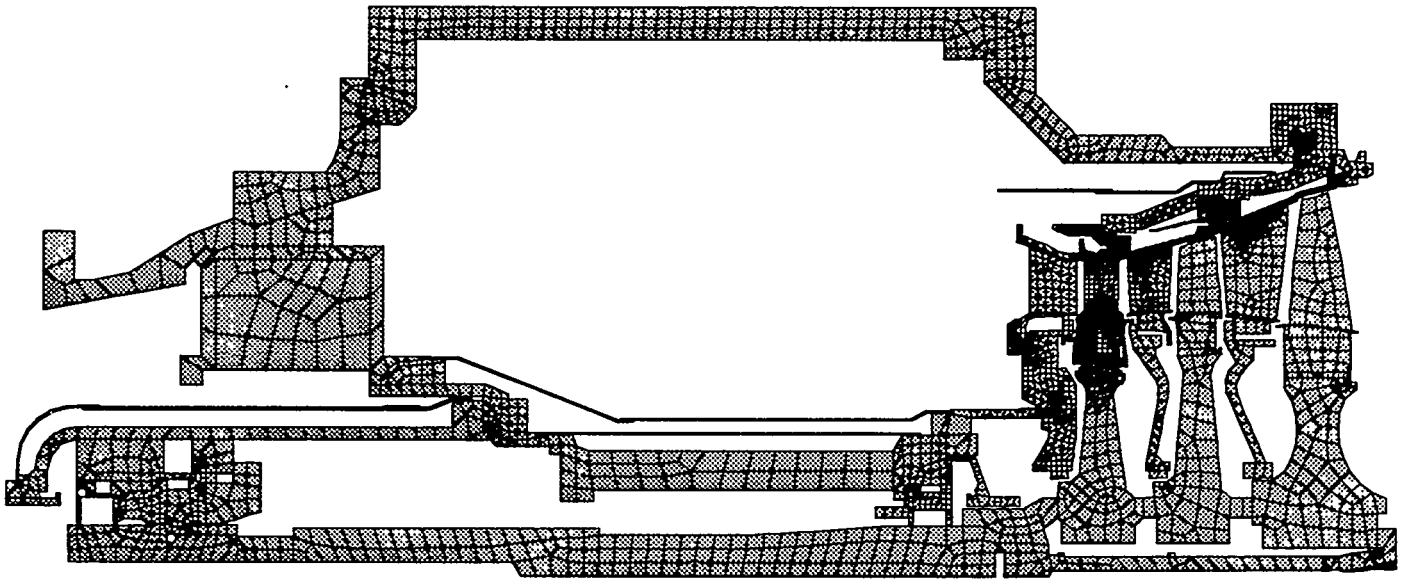

Figure 3-31. Finite Element Model of Static/Rotating Structure for Clearance Analysis

Figure 3-32 shows the steady state temperatures predicted in the turbine section of the engine. The hot gas components (i.e., nozzles and blades) are at total and total relative temperatures respectively, except the stage 1 nozzle which is cooled.

Figure 3-33 illustrates the thermal response of the blades, nozzle airfoils, and disk bores during a cold start. The hot gas components reach their steady state temperatures quickly due to very high heat transfer coefficients and their relatively small mass. The larger components have a much slower thermal response. For example, the disks and the turbine housing take as long as an hour for a complete thermal soak.

The resulting temperatures along with mechanical constraints (i.e., turbine bolt stretch) were applied to a stress/displacement model and evaluated for steady state and transient conditions. Pressures were applied to the nozzle vanes and the diaphragms. Gap elements were used where the displacement of adjacent components was difficult to predict, and components were coupled where possible to help convergence and reduce computation time.

The stress/displacement analyses of the rotating and stationary components were run separately. The thrust bearing was used as a reference datum for both the stationary and rotating models, so the displacements predicted from the two models could be compared directly.

Results of these analyses showed initial rotor compression due to bolt stretch, and then aft growth due to the thermal expansion. The stage 1 nozzle assembly grows aft since it is supported from the bearing housing and inner diaphragm. The stage 2 and 3 nozzles and tip shoes grow forward at start up, then grow aft when the combustor housing and turbine casing heat up. The axial movement of the rotor and stator does not affect the axial stage 1 blade clearances. The stage 2 and 3 radial tip clearances are affected by axial displacement since the gas path is conical aft of the stage 1 turbine.

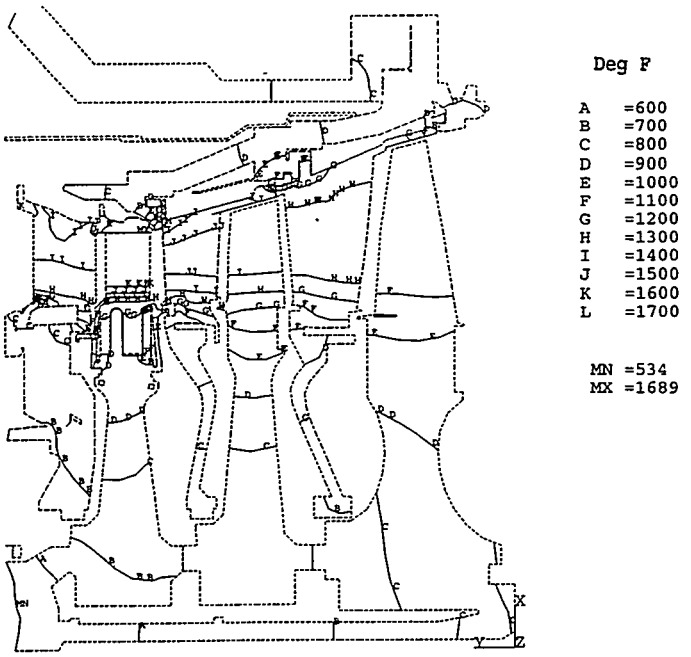

Figure 3-32. Predicted Steady State Temperatures for a 1010°C (1850°F) TRIT Build with Ceramic Stage 1 Blades and Metallic Stage 1 Nozzles

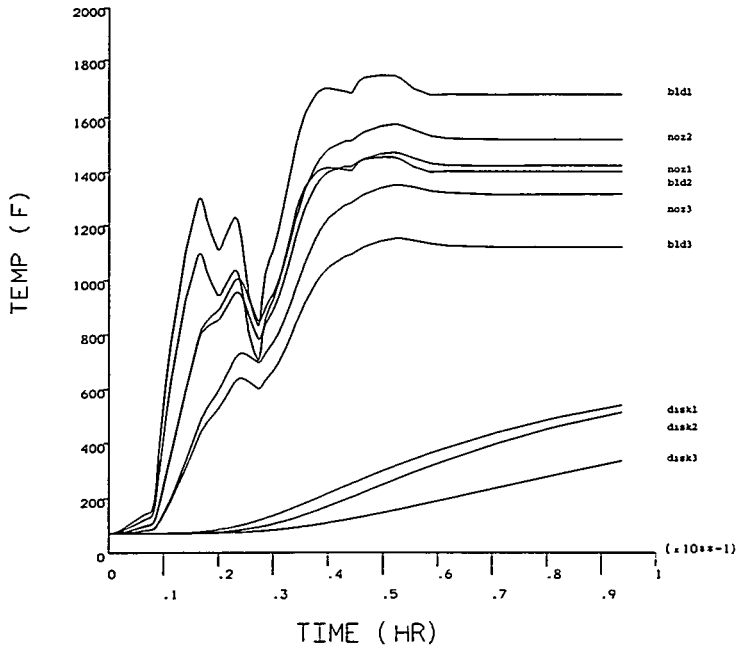

Figure 3-33. Temperature Response of Selected Components During a Cold Start

Figure 3-34 shows the predicted tip clearances for the stage 1, 2, and 3 blades during the steady state and transient cycle for a one hour engine run. The results were obtained by taking the difference in deflections of the blade tips and tip shoes. It can be seen that the tightest tip clearance for the stage 1 blade occurs at assembly. The tightest tip clearance for stages 2 and 3 occur at approximately 3 and 10 minutes after start up respectively.

Figure 3-35 shows the predicted axial displacement of the blade tip relative to the tip shoe for the stage 1, 2 and 3 blades. This figure indicates that all three blade tips move aft relative to the tip shoes at start up. Stage 1 tip clearance nearly returns to its start-up position at steady state. Stages 2 and 3 continue moving aft even after an hour of steady state engine operation. This is primarily due to slow thermal response of large components.

Stackups and existing engine experience will be factored into setting clearances as the above data was established without including the effects of the following:

- Mechanical tolerances
- Bearing clearances
- Warpage of the turbine casing and nozzle casing due to circumferential hot spots
- Vibration of the rotor and static components

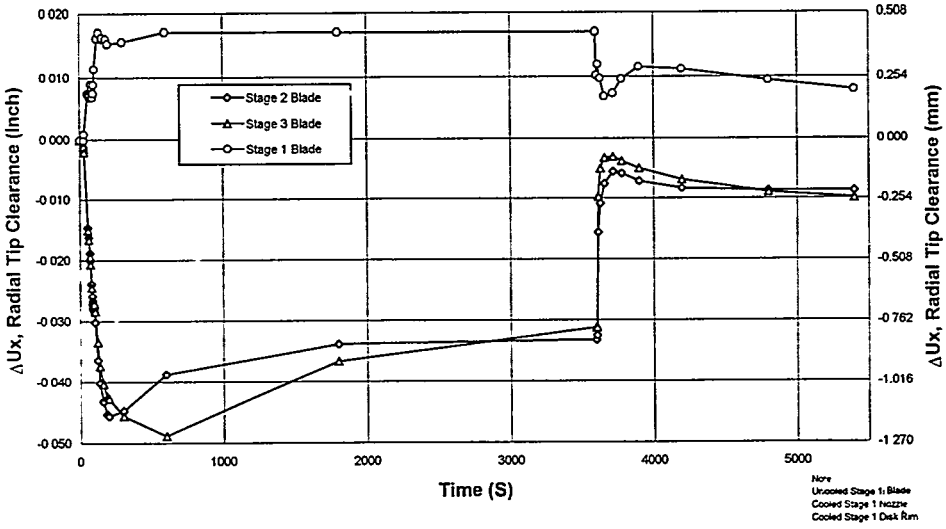

Figure 3-34. Turbine Blade Tip Clearance Predictions

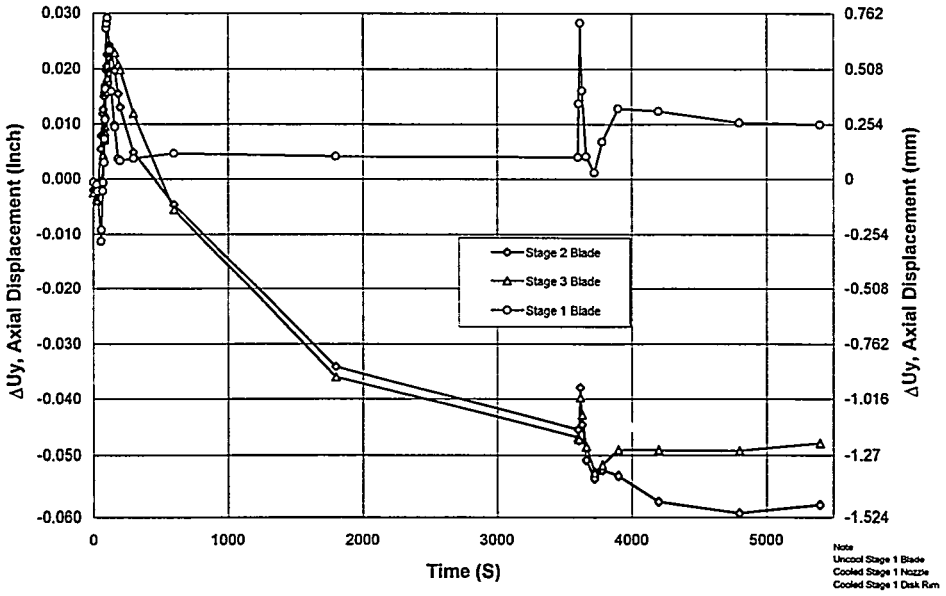

Figure 3-35. Turbine Blade/Tip Shoe Relative Axial Displacements

REFERENCES

1. "Ceramic Stationary Gas Turbine Development Program", 1993, Phase I Final Report, Solar Turbines Incorporated, DOE Contract Number DE-AC02-92CE40960. Under review.

2. "Ceramics Analysis and Reliability Evaluation of Structures (CARES)", N.N. Nemeth, J.M. Mandersheid, and J.P. Geykenyesi. NASA Technical Paper 2916, 1989.

3. "Time-Dependent Reliability Analysis of Monolithic Ceramic Components Using the CARES/LIFE Integrated Design Program," ASTM Symposium on Life Prediction Methodologies for Ceramic Materials in Advanced Applications - A Basis for Standards, Cocoa Beach, Florida, 1993.

4. "SPSLIFE: A User-friendly Approach to the Structural Design and Life Assessment of Ceramic Components", T. Bornemisza, and A. Saith. ASME paper 94-GT- 486, presented at the International Gas Turbine and Aeroengine Congress and Exposition, The Hague, The Netherlands, June 13-16, 1994.

5. "Application of SPSLIFE to Preliminary Design Evaluation and Life Assessment of CSGT Components", A. Saith, P.F. Norton, and V.M. Parthasarathy. ASME paper 94-GT-420, presented at the International Gas Turbine and Aeroengine Congress and Exposition, The Hague, The Netherlands, June 13-16, 1994.

4.0

TASK 8 - TEST FACILITIES

The work in this task involves set up of the test facilities to evaluate the ceramic stationary gas turbine components. Existing test facilities for materials property testing, spin testing, and combustor liner testing are to be modified if needed for the testing envisioned. A standard Centaur 50 engine procured under Task 7 is to be modified to accept the ceramic hardware as detailed under Task 7.

Figure 4-1 illustrates the integrated design and test philosophy of the CSGT program. In this approach mechanical design and design analysis are iterated with life prediction, fabrication, testing, and post-testing component characterization. Initially, simulated and subscale components will be tested in test rigs to prove key design concepts such as blade root configuration, compliant layers for the blade, attachments and cooling schemes for the nozzle, and fixturing to the metallic support structure for the combustor liner. Various rigs will be used, including an attachment tensile rig, a blade spin rig, a nozzle proof test rig, and subscale and full scale combustor rigs. Subsequently, the findings from these tests will be fed back into the design of the first component prototypes which will be tested in a Centaur 50 engine rig modified to accept ceramic parts. The results of the first generation prototype testing will be used to modify the component designs. In the final stage of the Phase II work second generation parts will be manufactured, which will also be tested in the engine rig. Second generation parts with superior performance will be used for the 4000 hour engine field test in Phase III of the program. Figure 4-2 summarizes the sequential testing of the simulated, subscale, and first and second generation prototype components.

Table 4-1 lists the requirements for rigs for the CSGT program. Indicated are whether existing rigs can be used without modification or whether changes need to be made to enable the testing of ceramic components.

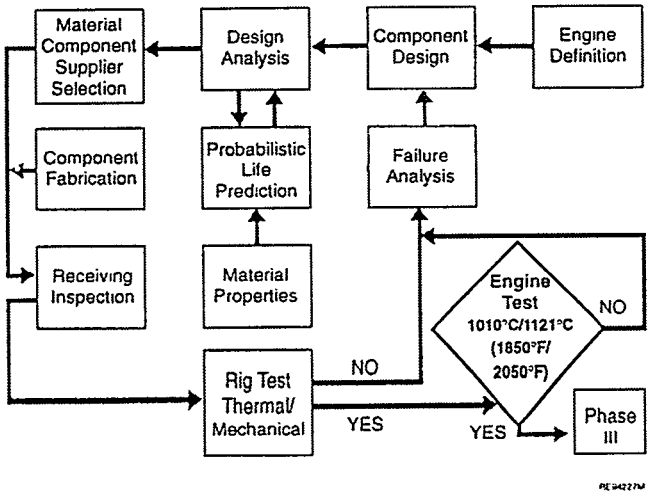

Figure 4-1. CSGT Integrated Design and Test Philosophy

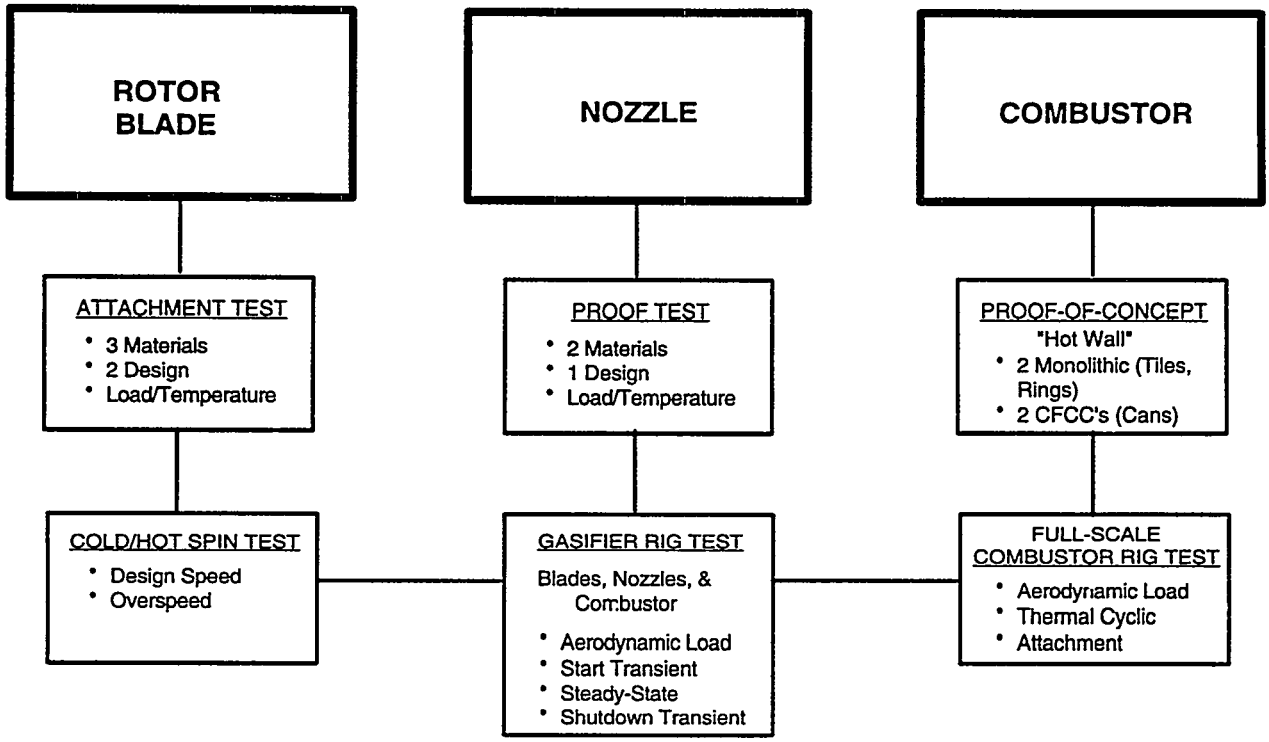

Figure 4-2. Flowpath of the Sequential Testing of the Three Program Components

Table 4-1. Rig Test Requirements for Phase II

Rig	Purpose	Existing/New	Modification
Cold	Cold spin testing of rotor blades	Existing cold spin rig was modified	Adapted to test ceramic blades; new safety features
Hot Spin Rig	Hot spin testing of rotor blades	Testing by outside source	Adapt to test ceramic blades at target operating temperatures; will be modified if needed
Attachment Test Rig	Test blade attachment configurations	Existing Instron tensile test equipment was modified	Adapted to accept various blade root designs
Nozzle Rigs	Test nozzle attachment Proof test nozzles	Fabricate two new rigs	Two new rigs
Small Scale Combustor Rig	Test combustor cans	Uprate of existing rig	
Full Scale Atmospheric Combustor Rig	Test full scale monolithic and CFCC liners	Use existing rig	Modify rig to accept ceramic liners
Full Scale High Pressure Combustor Rig	Test full scale monolithic and CFCC liners	Use existing rig	Modify rig to accept ceramic liners
Engine Rig	Test ceramic components in engine environment	Procure and modify Centaur 50 engine	Modify Centaur 50 engine with non-standard hardware to accept ceramics

4.1 RIGS FOR CERAMIC MATERIALS TESTING

Solar has extensive test equipment for materials property characterization including metallographic equipment, SEM/EDX, and various test equipment for flexure, tensile, creep and fatigue testing. Flexure, tensile and creep testing can be performed up to 1700°C (3092°F).

Figure 4-3 shows the ATS creep testing equipment at Solar. The modified tensile tester for blade attachment testing is shown in Figure 5-12 in Section 5.0.

Special Waspalloy grips were fabricated for the test for various root configurations. Waspalloy was selected since it is the first stage disk design material.

4.2 SPIN TEST RIG

4.2.1 Background

The CSGT program requires the use of a vacuum spin pit to test and evaluate various candidate monolithic ceramic inserted turbine blade attachment geometries along with candidate compliant layer materials (as required) deemed necessary to redistribute interfacial contact loads. The rig must be capable of providing a centrifugal load on either dummy mass blades or full size blades to at least 150% of the engine design load without introducing any loading conditions or forcing functions on the blades that would not be experienced in the actual engine environment. Prior spin pit experience has shown that the required spin pit partial pressure must be controlled in the range of 200 - 300 milli-torr to ensure stable test rotor operation. In addition to the speed and stability requirements (absolute vacuum level) of the CSGT spin pit design the rig may also include features which would allow metallic spin disk operation at elevated temperatures in the 649°C (1200°F) to 832°C (1500°F) range if testing under such conditions would be required.

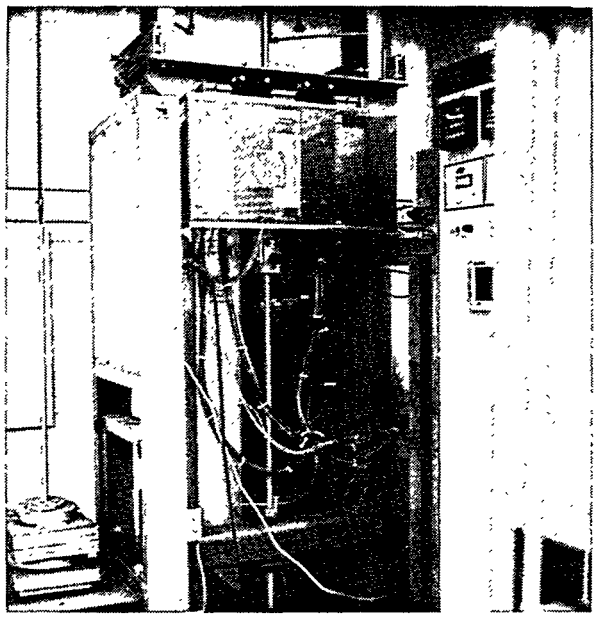

Figure 4-3. ATS Creep Testing Equipment

The existing Solar spin rig was designed before several important operating hazards had been identified in the industry. Further, when testing ceramic components, the ability to brake the spin driver rapidly after a blade failure is essential to limiting the secondary damage to the fracture origin of the test blade(s). Figure 4-4 shows the spin pit prior to the upgrade.

The spin pit operating hazards were identified (with focus on the revised CSGT test requirements for a heated spin pit capability) which would expose the operator and observers to possible dangers when operating with ceramic rotating components. Test Devices, Inc. of Hudson, MA, was consulted in this regard due to their experience in both supplying and testing of spin testing "systems" to worldwide manufacturers of turbomachinery. The spin pit uprate did not include refurbishment for "hot spin" testing, but the desired features can be incorporated if needed.

4.2.2 Review of Existing Equipment Safety

The existing spin test system lacked several important safety features which must be added before it is operated for the CSGT testing of ceramic blades.

Cover Bolts - The bolts which held the cover to the chamber were inadequate to contain the pressure expected from an oil mist deflagration (explosion). Additional high strength bolts needed to be added, designed to retain the cover at 1.38 MPa (200 psi) internal pressure. Additional lugs had to be welded to the side of the tank to receive them.

Lid Retention Dogs - Four sliding steel bars, air actuated, had to be added on the top of the cover lid to lock it in place. These had to be sufficiently strong to prevent cover ejection with a 1.38 MPa (200 psi) deflagration pressure. The lid dogs include limit switches to prevent drive operation until they are closed. They need to be controlled so that they cannot be opened until the chamber has been vented safely.

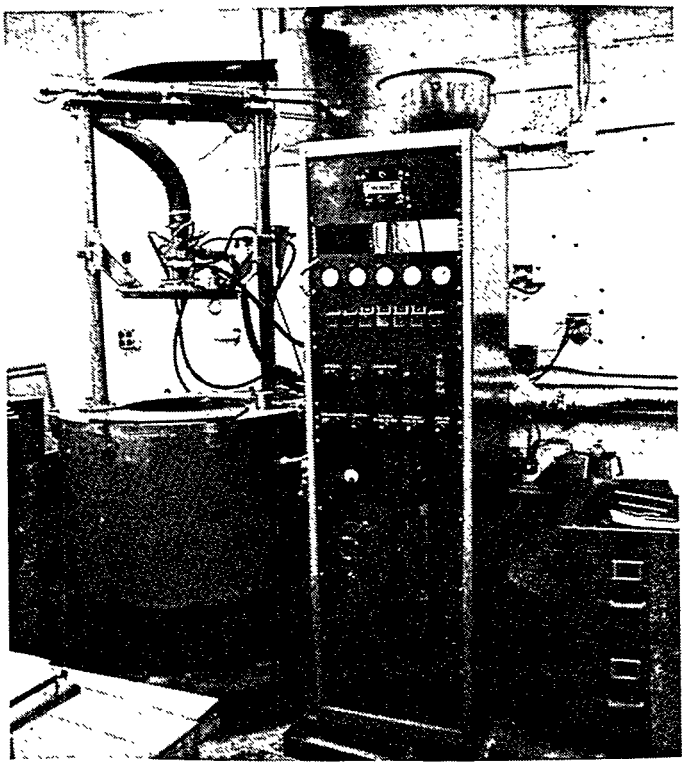

Figure 4-4. Spin Pit Prior to Upgrade

Sight Ports - The existing observation ports in the lid need to be closed off with flanged steel plugs inserted up from the bottom of the lid so that internal pressure would hold them in place. Complete lid replacement without the sight port holes would provide another option since the lid is relatively small in size.

Vacuum Integrity - Optimal protection against oil mist deflagration is to exclude oxygen in the chamber. Revisions to the vacuum piping and chamber vent system will help maintain vacuum and therefore prevent deflagration. Test Devices, Inc. recommended the installation of an automatic valve between the vacuum pump and the chamber to prevent back-venting of air if the vacuum pump should be shut off for any reason. Also, an automatic vent control system was to be installed to prevent the operator from manually venting the chamber at an inappropriate time.

Inert Gas Vent System - Upon completion of a heated test, it is important to vent the chamber with an inert gas (nitrogen or argon), again to prevent ignition of lubricating oil which may have leaked into the chamber. The vent control system needs to be interlocked with the temperature measuring equipment so that the chamber can only be vented with inert gas and the air venting valve cannot be opened after a heated test.

Operator Protection - In addition to the above upgrades, it is important to protect the spin test operator from an unexpected equipment failure. Spin testing presents a variety of hazards which are difficult to quantify, and spin operators need protection from known and unknown hazards. Test Devices, Inc. urged an upgrade of the test room by the addition of 13 mm (0.5 inch) steel plates or 20 cm (8 inch) thick solid concrete block laid up on the inside of the existing hollow black walls. The operator control station had to be moved outside of the test room.

4.2.3 Recommended Control System Upgrades to Reduce the Risk of Damage to the Test Article or the Drive System

Spindle Vibration Monitor - Test Devices, Inc. recommended the installation of a non-contact vibration monitor system to measure the vibration of the spindle and shut down the drive if vibration exceeds a preset threshold. The monitor needed to include a set of isolated contacts which transfer when composite vibration levels exceed a preset (adjustable) level. An additional set of contacts which transfer when failure of the vibration probe occurs had to be included as well. These contacts are used as an indication to the control system that the test article has burst or failed in some other way, and cause the damper oil valve to close as soon as rotation of the drive stops, avoiding large oil spills in the chamber after burst.

Lubrication Equipment Upgrade - One important hazard to the test article is the failure of the drive lubrication leading to turbine bearing failure and consequent spindle failure and test article loss. The following interlocks were recommended:

1) oil pressure switch
2) oil mist tank level switch
3) oil mist pressure switch
4) oil tank level switch
5) oil flow switch
6) oil filter contamination switch

After a test article failure (whether or not the spindle breaks), the spindle seal usually fails, allowing damper oil to flow into the chamber. The installation of a solenoid valve was recommended in the damper oil line to allow the control system to shut off the oil to stop the flow into the chamber.

Vacuum System Upgrade - The existing vacuum pump has adequate flow capacity to accomplish the desired testing, but the pipeline connecting the pump to the chamber is much smaller than needed to accommodate the flow rate of the pump. The line had to be replaced, and a new attachment flange welded to the side of the chamber.

Electronic Control System - A further recommendation was the installation of an automatic control system to coordinate all the functions necessary to operate the system safely and successfully. This can best be accomplished with an industrial programmable logic controller (PLC). All interlock contacts are connected as inputs to the controller and all solenoids and motor contactors are connected as outputs. Controller software routines are written to provide the necessary actions in response to various operating situations. The programmability of the PLC is an important feature because it allows easy and rapid revisions to the control strategies as testing needs change. The control system needs to include a programmable operator interface display system to eliminate hard-wired push buttons and pilot lights. The operator display presents messages to the operator at the time when they are most helpful, and in a format which is easiest to understand.

There are many control features which can be implemented with the PLC which are important to operator safety. For example, it is important to be sure that the chamber has been vented before the lid locks are opened, so that if oil deflagration occurs the locks are in place to hold the lid down. Without the automatic control system, it is common for the operator to open the lid dogs first, then vent the pit, completely defeating the primary purpose of the lid dogs. This is an example of the many different control situations which can be anticipated and are programmed to protect the equipment and the operator.

4.2.4 Blade Spin Rig Summary

An existing Solar spin dog and pit was modified such that the CSGT ceramic inserted blade testing can be accomplished without risk to the operator, and without undue risk of causing secondary damage to the ceramic test pieces. The pit will have the capability of operating at both ambient and elevated temperatures to 815°C (1500°F), at sustained vacuum levels of 200 to 250 milli-torr, with a programmable system controller designed to prevent oil mist deflagration in the event of a test article failure. The system modifications were recommended by Test Devices, Inc. to provide a safe and stable test rig apparatus for ceramic blade spin testing. Figure 4-5 shows the spin pit during the upgrade process. Modifications are to be completed by early 1995. Figure 4-6 shows the disk to be used for the testing of the dovetail blades. As can be seen blades can be tested two at a time during the spin test.

4.3 NOZZLE RIGS

Several nozzle rigs were contemplated during the Phase II work. One design was intended to evaluate the load distribution for an early preliminary nozzle design in which the component was suspended from a nozzle ring interfacing with the nozzle case. This rig was abandoned following the selection of a nozzle design attached to the first stage diaphragm.

Mechanical Nozzle Test Rig - Following the detailing of the "bowed" nozzle design (see Section 3.0) a need for a mechanical nozzle test rig was identified. The intent of the ceramic nozzle test rig is to cull out the components that were analytically predicted to have high stress locations. The aerodynamic load of the airfoil produces analytically predicted stresses in the ceramic to metallic attachment region (surface contact) and in the trailing edge inner airfoil root fillet. A thorough assessment of the design contact loads and resulting stresses will be evaluated in a mechanical attachment test rig. The rig will impose the aerodynamic loads analytically predicted for the nozzle segment on the attachment region through the use of a mechanical loading device (air cylinder). This device will be controlled by a pressure regulator which will provide accurate and repeatable load

conditions. The load (87 lbs. design load) will be applied to the predicted vector coordinates to a load arm position (outer nozzle shroud) that will apply the appropriate load couple ratio. The load will be reacted through exactly the same interface geometry (a segment of each component) present in the engine, and the materials will also be duplicated for both the nozzle and the inner metallic support diaphragm. This load is also expected to create the desired root stress condition in the airfoil trailing edge inner root. The applied test loads will include "failure" loads to determine the margin in the failure to design load ratio. Loads will be applied to a statistically significant number of test specimens from each of the nozzle suppliers to a determined greater design load. This rig will also be designed with the option of mounting to a shaker table for vibratory testing.

Thermal Nozzle Test Rig - A CSGT ceramic thermal nozzle test rig will be designed to produce a thermal gradient in excess of that caused by typical turbine operation. Application of the temperature gradient in effect produces stresses that proof test the nozzle durability prior to installation in an engine. The expected result is to eliminate nozzles that exhibit unacceptable material flaws.

The objective is to create a gradient of 607°C (1125°F) from the nozzle mid-span to the outer shrouds. This distribution corresponds to 125% of the maximum expected gradient in the engine. Predicted stress levels under these conditions will reach about 248 MPa (36 ksi), up from the baseline of 200 MPa (~29 ksi). Construction of the rig will involve electric resistance heaters focused at the nozzle mid-span along with impingement cooling at the outer shrouds. A thermal control system will regulate the heat input as well as the heat extraction. Using this approach, the intended thermal gradient, stress and component durability will be assured.

4.4 COMBUSTOR RIGS

Three rigs will be used for hardware testing.

Can Combustor Rigs - The subscale test facility that will be used has the capacity of achieving engine rated temperatures and pressures while maintaining a single injector's mass air flow into the rig. All subscale testing of the monolithic and CFCC combustor liners will be done with a production Centaur 50 SoLoNOx fuel injector. The facility is instrumented for temperature, pressure and flow measurements. Exhaust emissions will be done by a state-of-the-art Rosemount Analytical continuous emission monitoring system (CEMS). A newly acquired data acquisition system will capture all the data and provide data files in a customized report print out. To prevent the ceramic combustor liners from exceeding a wall temperature of 1204°C (2200°F) for monolithics and 1177°C (2150°F) for CFCC's, a fuel shutoff system has also been installed. The system is integrated with the 15 type K thermocouples that are instrumented on the liner wall. The fuel will shut off when the thermocouple exceeds the target temperature limitation. The subscale rig is shown in Figure 6-15 in Section 6.0.

Subscale combustor tests will typically be for durations between 1-100hrs. Following the results of short term testing, a decision will be made whether longer term testing (up to 1000 hours) will be necessary.

Full Scale Combustor Liner Test Rigs - Full scale combustor liners will be tested in an atmospheric combustor facility (Figure 4-7) and in a high pressure combustor test rig (Figure 4-8). The Atmospheric test rig will provide a preliminary indication of the performance of the full scale combustor hardware. The facility provides hot air at atmospheric pressure to the rig. A complete set of 12 Centaur 50 SoLoNOx fuel injectors is used to run the rig and the flow function is matched to the engine design point. A thermocouple rake system provides temperature data for pattern factor calculations and radial profiles. Exhaust emissions are measured by a CEMS and data is captured by a Daytronics and VAX RETS data acquisition system.

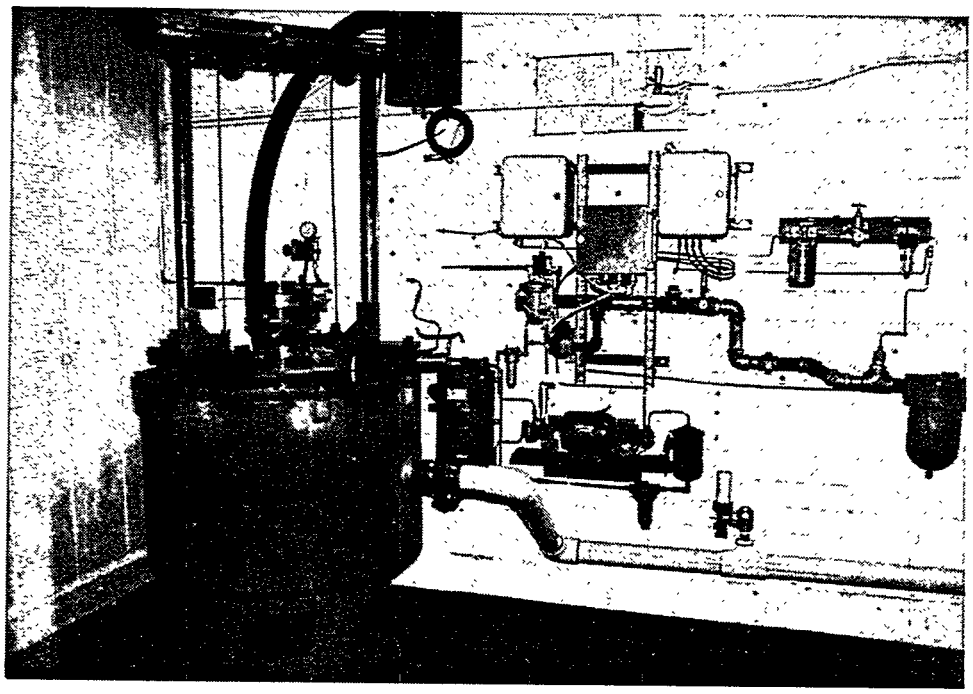

Figure 4-5. Spin Pit During the Upgrade Process

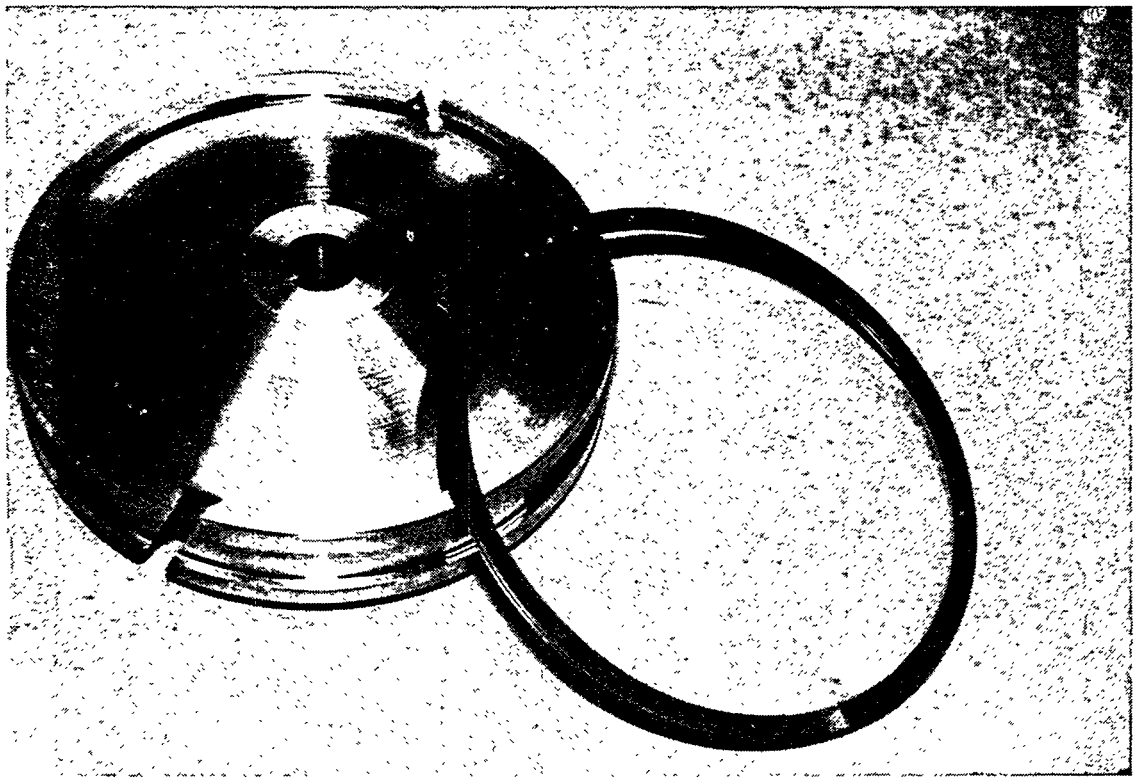

Figure 4-6. Dovetail Spin Test Disk

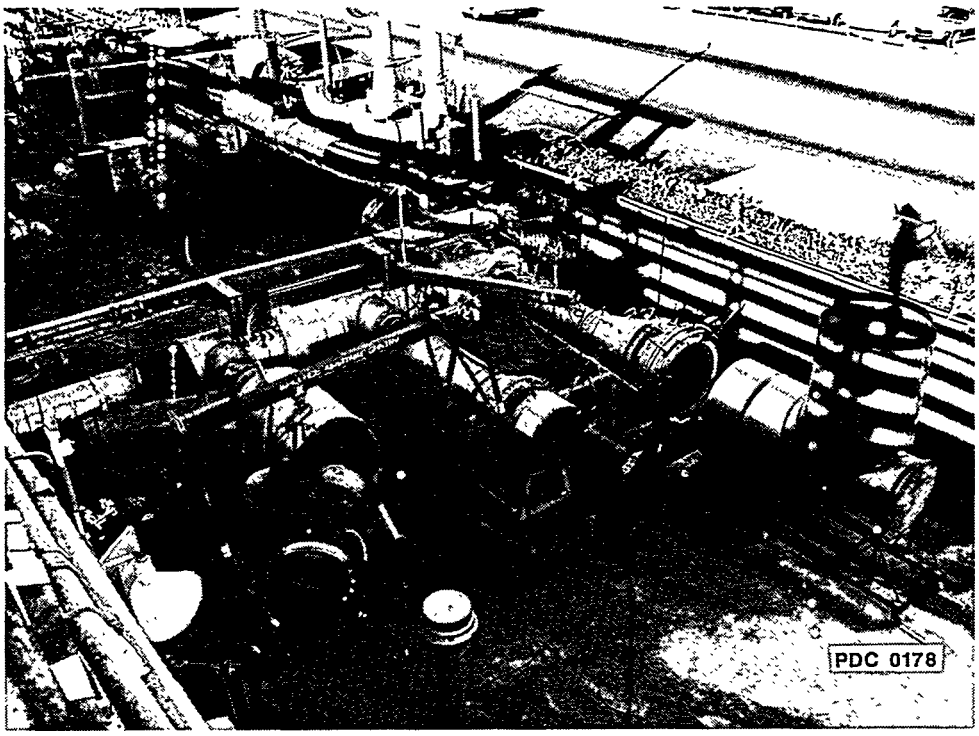

Figure 4-7. Atmospheric Combustor Test Facility

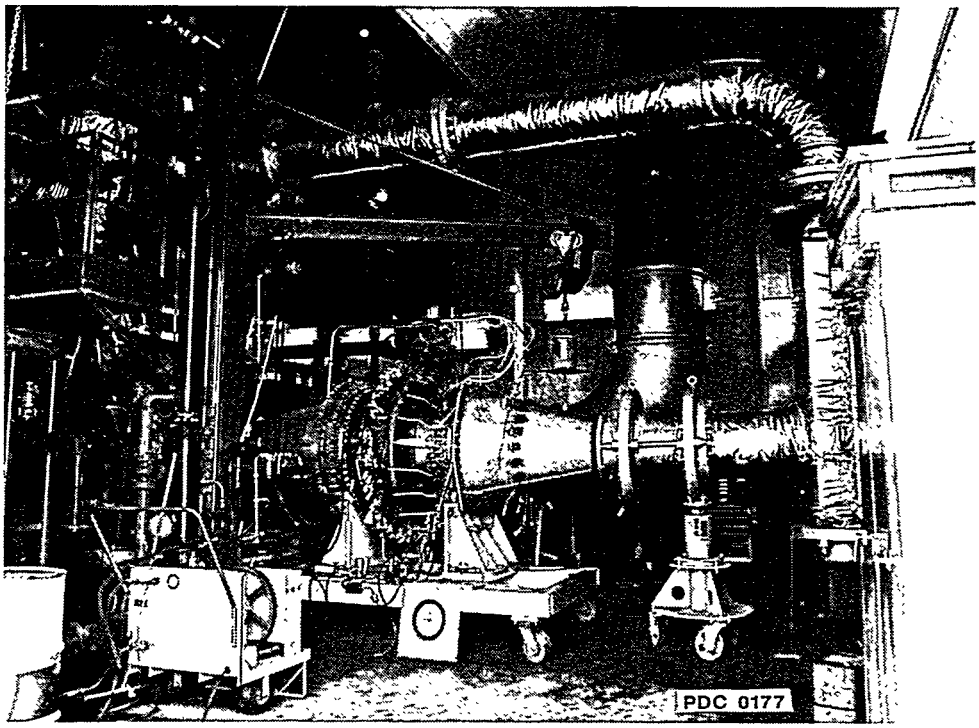

Figure 4-8. High-Pressure Combustor Test Facility

The High Pressure test facility (Loop rig) is a recuperated Centaur T4000 (early version of the Solar Centaur 40) engine which provides an appropriate test vehicle for the full scale ceramic combustor liner hardware. Full air flow (approximately 16 kg/s, 36 lbs/s) and combustor inlet temperature (332°C, 630°F) can be obtained with a maximum pressure of approximately 724 kPa (105 psig). The engine is fully instrumented with an Allen-Bradley controls system and has a complete data acquisition system, including Kessler type pressure oscillation sensors for monitoring the combustor harmonic frequencies. Pattern factor and radial profiles are measured with type K thermocouple rake assembly. There are 6 thermocouples per rake and a total of 4 rakes (90° apart) on one assembly. The rake traverses a span of 90° and collects 1152 temperatures. Emissions can be taken at the exit of the combustor plane or at the exhaust stack by a CEMS. Load transients and fast shutdowns can be performed on this engine. These will provide data for the heat transfer and stress models.

4.5 ENGINE RIG

4.5.1 Background

The Engine Test Rig is the test bed apparatus to be used in the Ceramic Stationary Gas Turbine Engine (CSGT) program to demonstrate the use of advanced ceramic components for the first stage rotor blade, first stage nozzle, and the combustor liner for an existing industrial turbine engine. The rig consists of a production Centaur 50 turbine engine, standard cold end drive gearbox, standard engine/generator mounting skid, and a (non-standard) 7000 hp Hoffman water-brake dynamometer. The engine rig will be operated to a maximum TRIT of 1121°C (2050°F) at 100% (14,950 RPM) engine speed which equates to a tip speed of approximately 442m/s (1450 ft/s). The engine rig will evaluate ceramic hot section components in a typical Solar Turbines generator-set operating environment.

Prior DOE sponsored ceramic engine programs have shown that ceramic components are evaluated most accurately in the actual engine environment for which the components have been designed. Smaller sub-assembly test rigs can typically only partially reproduce the engine operating environment, and therefore cannot completely be relied upon to expose ceramic components to all engine induced stress conditions prior to actual engine testing. The engine test bed engine thus serves the CSGT program as the final qualification test for all ceramic components before they are installed in the 4000 hour field test engine.

4.5.2 Engine Test Strategy

The test schedule is designed to fully evaluate each individual ceramic component by initially testing with the remaining flowpath components fabricated from metallics. This methodology will help prevent secondary damage to downstream ceramic components prior to those components having been tested individually.

The engine rig must test the ceramic components to the exact conditions these components will experience in the 4000 hour field test engine. The rig provides an engine test bed in which there is duplication of ceramic to metallic interface loading, engine vibration signature aerodynamic loading, and component temperature and stress distribution. The engine rig therefore provides accurate relatively short duration test results (up to 500 hours) on the ceramic components and the adjacent metallic components that will enable the designer to project wear rate in critical attachment areas. A "robust" component design can then be determined with a higher probability of survival for the 4000 hour field test.

The test philosophy for testing ceramic components in the engine rig is focused on the lowest risk assessment to both the ceramic components and the metallic flowpath components. Testing therefore will use an incremental approach to ceramic component evaluation. One ceramic component system at a time is to be tested with all other hot gas flowpath components fabricated from standard metallic materials.

The engine is to be tested at the standard operating TRIT of 1010°C (1850°F) for each component system until all three component systems have been individually tested. In subsequent testing, other ceramic components and ancillary hardware will be installed in the same build and the engine will again be operated at the standard TRIT. An increase in TRIT to 1121°C (2050°F) will then be incrementally imposed until a steady state operating condition in this temperature regime is achieved. This engine rig test schedule was determined to be the lowest risk approach to evaluating the ceramic components in an engine test bed and was used as the basis for all subsequent planning decisions on the location for the scheduled tests. The test plan to be implemented under subtasks 9.2 and 9.3 is summarized in Table 4-2.

Table 4-2. Engine Rig Test Schedule

Build No.	Temperature °C (°F)	Description
1	1010 (1850)	NT164 Dovetail blades/Metal Nozzle
2	1010 (1850)	Combustor Testing - SiC/SiC CFCC Liner - Combustion Team to Set Test Conditions
3	1010 (1850)	GN-10 Dovetail Blades/Metal Nozzle
4	1010 (1850)	SN-253 Pinned Blades/Metal Nozzle
5	1010 (1850)	Instrumented Engine - All metal parts, blade and nozzle uncooled - Generate boundary conditions
6	1010 (1850)	SiC/SiC CFCC Combustor + Ceramic Blade
7	1010 (1850)	SN-88 Nozzle/Metal Blades
8	1010 (1850)	SN-253 Nozzle/Metal Blades
9	1010 (1850)	SiC/SiC CFCC Combustor + Ceramic Blade + Ceramic Nozzle
10	1066 -> 1121 (1950 -> 2050)	SiC/SiC CFCC Combustor + Ceramic Blade + Ceramic Nozzle
11	1121 (2050)	SiC/SiC CFCC Combustor + Ceramic Blade + Ceramic Nozzle: 10 Hours/Emissions
12	1010 (1850)	2nd Gen. Ceramic Blade + Combustor
13	1010 -> 1121 (1850 -> 2050)	2nd Gen. Ceramic Blade + 2nd. Gen. Ceamic Nozzle + Combustor
14	1121 (2050)	2nd Gen. Ceramic Blade + 2nd Gen. Ceramic Nozzle + Combustor: 50 Hours

First Generation Ceramic Components Engine Testing - Builds Nos. 1-11 involve first generation ceramic components fabricated under subtask 9.2, i.e. dovetail blades (GN-10, NT164), pinned blades (SN-253), bowed nozzles (SN-88, SN-253). The full scale SiC/SiC combustor liners are supplied by BF Goodrich under a parts supply subcontract under Task 7.0. The latter are not fully optimized liners, but rather initial prototypes fabricated to provide a generic ceramic surface to enable approaching as closely as possible the materials conditions for the low emissions combustor to be further developed and optimized using the primary materials of the program.

Initial testing will be short term, 1-2 hours. Its purpose is to demonstrate the operation of individual ceramic components and their adjacent metallic hardware under actual engine conditions but at the current TRIT of the Centaur 50, i.e. 1010°C (1850°F). These tests are primarily intended to prove the designs and not performance. The ceramic blade and metallic nozzle and tipshoe, and the ceramic blade, nozzle and metallic tipshoe will operate with wide open clearances to avoid a rub and consequent possible catastrophic failure. An instrumented engine test, included as Build No. 5, is intended to provide the boundary conditions for subsequent design and iterative testing.

Builds Nos. 9-11 include all three ceramic components. Initial testing will be again at 1010°C (1850°F). The TRIT will be incrementally increased, first to 1066°C (1950°F), next to the design TRIT of 1121°C (2050°F). The testing for the final build will be extended to 10 hours, and an effort will be made to optimize emissions of NOx and CO.

The selection of the ceramic component designs, materials and suppliers to be evaluated in Builds Nos. 6 and 9-11, will be selected based on performance in prior testing.

Second Generation Ceramic Components Engine Testing - Builds Nos. 12-14 involve testing of second generation ceramic hardware fabricated under subtask 9.3. The actual ceramic components to be evaluated will depend on the design modifications, and final materials supplier selection to be conducted at a later stage in Phase II. If multiple suppliers for a specific component design remain the engine testing would most likely invclve a rainbow of materials/suppliers for each part. The objective of the second generation engine testing is to assess the hardware in design configurations that are intended for the 4000 hour field test in Phase III. The final build (No. 14) will include all three components at the design TRIT of 1121°C (2050°F). The duration of this test is scheduled to be 50 hours. Performance (thermal efficiency, output power, emissions) should be optimal at this point. The final Phase II engine test will provide the performance baseline for the Phase III field testing.

4.5.3 Engine Rig System Configuration

A trade-off study was conducted to determine the most cost effective means of mechanically loading the engine. As mentioned earlier, the standard approach would have been to purchase a complete generator package so that the engine would be loaded in exactly the same manner as the 4000 hour field test engine. However, when the trade-off study was completed, it became apparent that other loading devices had advantages that outweighed the generator option. The load device options were: 1) generator, 2) cold end drive dynamometer, 3) hot end dynamometer, and, 4) no power turbine.

The various cost trade-offs involved the required support systems for each load device but did not define a comparison in the engine loading performance limitations of each device. The generator option clearly provides the best duplication of field test engine loading but is the most expensive option. The cold end dynamometer, a much less expensive option, could duplicate the critical steady state engine performance requirements but could not accurately duplicate the start and shutdown transient conditions. A favorable trade-off in the evaluation of this load device option however was the availability of a functional 7000 HP water-brake dynamometer making this a more attractive option. The hot end dynamometer would have required a 2 shaft engine configuration which is not the configuration that is to be used in the 4000 hour field test and which has some fundamental hardware differences with the single shaft engine configuration. The final option of "no" power turbine simply uses exhaust back pressure as the means of controlling engine firing temperature at the design point and is therefore not as reliable or as repeatable as the other three options even though this option is the least expensive.

The conclusion to this trade-off study was the selection of the cold end drive dynamometer in which a 7000 HP Hoffman water-brake dynamometer is to be used to load the engine rig to the design conditions.

The engine rig is limited to a rotational speed of 14,950 RPM and a TRIT of 1121°C (2050°F) with all three ceramic component systems installed. The engine can be loaded continuously to over 7000 HP using the Hoffman water-brake dynamometer at an output shaft speed of 1800 RPM. Standard Centaur 50 vibration monitors have been installed with setpoint limits consistent with production units. The engine will be fueled by natural gas (standard) and the lube oil systems are all standard for the Centaur 50. Non-standard modifications to the production engine/generator package (package includes the engine, generator, mounting skid, and electronic controller) are: 1) modifications to the mounting skid to accommodate the dynamometer (versus generator) base mounting configuration and 2) software modifications to the engine controls for water brake loading.

4.5.4 Facility Location and Test Engine

Facility Location - Locating a facility for the gasifier test rig installation followed the engine test philosophy which required engine testing uninterrupted by other Solar programs. Additionally, the facility needed to be close to the engine assembly and engineering facilities for two reasons: 1) quick access to the engine by engineering personnel, and 2) keeping engine transportation, and the possibility of ceramic component damage, to a minimum. The facility also had to have the appropriate emissions permits in place since the lead time for acquiring new permits in the state of California is usually prohibitive.

A selection was made for the use of Building 16 at Solar Turbine's Kearny Mesa Plant for the following reasons:

- An existing structure
- Permitted for emissions for a Mars class engine (14000 HP)
- Existing electrical, water, high pressure air, and natural gas wiring/plumbing
- Existing cooling tower for water from dynamometer
- Existing "hot-well" reservoir for dynamometer discharge water
- Existing 10 ton overhead bridge crane for engine installation/removal
- Close to engineering and engine assembly facilities
- Dedicated facility for CSGT gasifier rig only

As a result of this selection the test cell construction in Building 16 was initiated.

Test Engine - The engine selected to be the test bed for the CSGT program is the Centaur 50 single shaft engine with a low emissions SoLoNOx combustion system (Centaur 50S). The engine was ordered in June, 1993 and was delivered to the designated test cell in July of 1994 following the "green run" acceptance test. The engine (S/N 442H) is a new sales order engine with all new hardware dedicated to the CSGT program. The engine was assembled in the Solar Turbines Kearny Mesa Plant and was acceptance tested at the Harbor Drive facility in the cold end drive test cell. The acceptance test was performed to production test standards for the Centaur 50 engine and the engine was accepted after having achieved the required performance within the vibration limitations specified in the standard test specification.

The engine and dynamometer are mounted on a standard production slave skid designed for a Centaur 50 single shaft engine with a standard combustor assembly (Figure 4-9). A minor modification to the location of the engine fuel control assembly had to be made to accommodate the

larger diameter of the SoLoNOx combustor housing. A second modification to the skid was required to enable mounting of the dynamometer since the skid was designed to utilize a generator. Both modifications are reversible to the original standard production configuration. The skid incorporates an engine oil cooler of the shell/tube type which has been mounted behind the dynamometer for greater accessibility.

Figure 4-10 shows the CSGT engine rig control room and Figure 4-11 the rig operator panel.

Controls - The Centaur 50 test bed engine rig is electronically controlled by a standard production model Allen Bradley Turbotronics II digital control. The Turbotronics II controller is a Programmable Logic Controller (PLC) that can be reprogrammed in real time as required during an engine test. The start transient controller setpoints for lightoff RPM, temperature ramp rate, and setpoint temperature are all programmable so that the test engineer can modify the start transient parameters as required to obtain a repeatable "soft" lightoff condition and highly controlled engine acceleration. The Turbotronics II control also includes fault interlock circuits with critical dynamometer, functions such as: 1) oil pressure to the trunion bearings, 2) discharge water temperature, 3) RPM, etc. These fault circuits are designed to provide a warning to the operator as well as automatically shut down the engine should any of these critical parameters reach predetermined unsafe levels. This is a feature typical in digital electronic engine controllers which has successfully eliminated and/or reduced catastrophic engine system failures.

Load Device - The load device being used on the CSGT gasifier rig installation is a 7000 HP Hoffman water-brake dynamometer. The steady state drive speed for this load device is 1800 RPM and the dynamometer is driven through a jack shaft connected to a low speed gearbox attached to the cold end of the gasifier engine. The low speed gearbox is a standard product for 60 Hz generator drive applications.

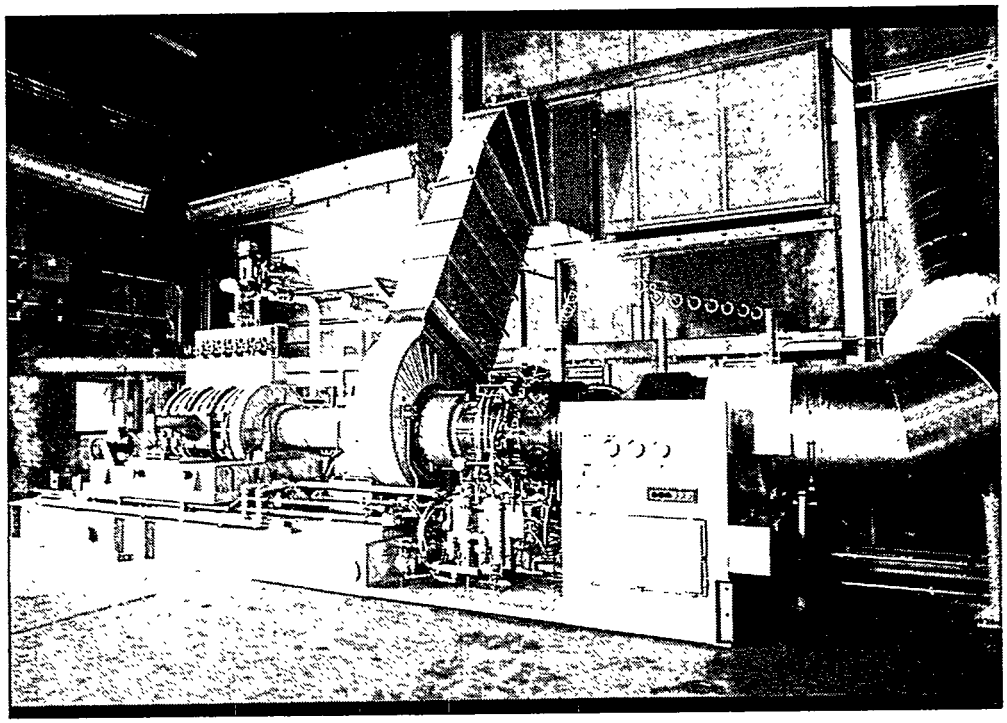

Figure 4-9. CSGT Centaur 50 Engine Rig

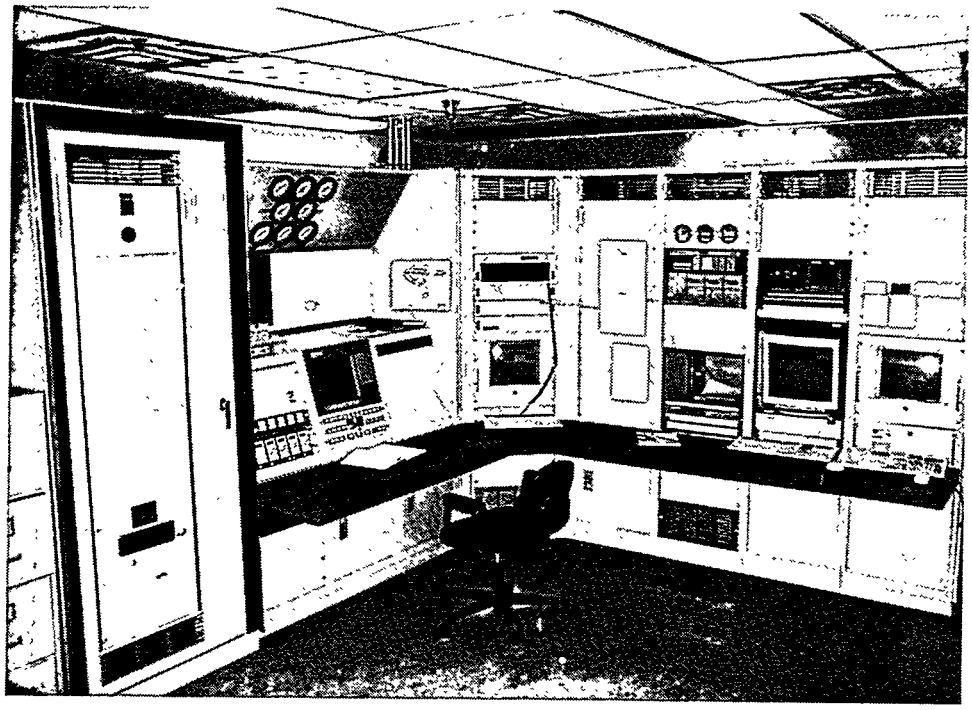

Figure 4-10. CSGT Engine Rig Control Room

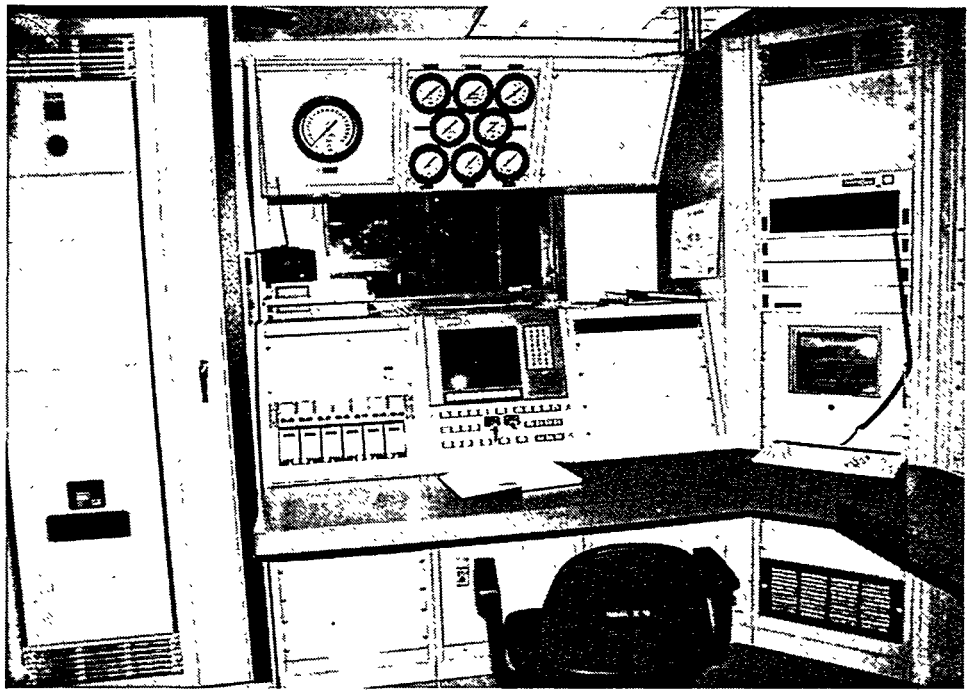

Figure 4-11. CSGT Engine Rig Operator Panel

Other considerations in the selection of the Hoffman dynamometer include: 1) availability, 2) ability to provide adequate load, 3) ability to closely simulate the 4000 hour field test site engine load requirements, 4) facility requirements to support the dynamometer, 5) overall cost as compared to other load device choices.

It was determined that since the dynamometer had been unused for the previous eight years, and since it was a "one of a kind" load device, it would be prudent to completely disassemble, inspect, and refurbish the unit as needed before mounting the device on the engine rig slave skid. The ability of the dynamometer to exactly duplicate the operating cycle of the field test engine is slightly compromised by the inability of a water-brake load device to duplicate transient engine step-load conditions. The dynamometer rotor however has approximately the same inertia weight of a generator armature and should provide a reasonable engine start transient simulation. The rational on the CSGT program to "dump" approximately 80% of the compressor discharge flow directly into the exhaust stack and bypass the engine hot section on a trip shutdown simulation greatly reduces the effect of a trip shutdown on the ceramic component stresses. Since these stresses are considered to be relatively benign due to this operational philosophy, it is less important that the load device have a capability to exactly duplicate this step - unloading function. It can be rationalized therefore that the ability of the load device to impose "step" loads on the engine is not a critical test condition. Again, the PLC allows the test engineer to reprogram the Turbotronics II engine control logic to slow the engine start transient such that relatively benign thermal stresses are imposed on the ceramic components also easing the effect of rapid transient conditions.

A critical factor in the selection of the load device was the cost of the load system. The use of the water-brake dynamometer provides a significant cost reduction over a generator system. The use of a generator requires a load bank of resistors to dissipate electrical power produced by the generator as load is applied to the engine. This load bank includes transformers, switch gear, and wiring, along with the added cost of the generator.

5.0

TASK 9.0 - MATERIALS SELECTION AND COMPONENT DEVELOPMENT

This task involves procurement, fabrication, and testing of ceramic test specimens and components. The results of the testing will be incorporated in design iterations for Task 7. Subscale and full scale combustor liner testing is described separately in Section 6.0 (Task 10 - Low Emission Combustor). The work is performed in three subtasks:

Subtask 9.1 - Component Design and Material Selection (WBS 2.9.1) - This subtask mostly involves the procurement of test specimens and simulated or subscale component hardware from the ceramic suppliers. Test specimens include flexure bars and tensile bars for component testing to be performed under subtask 9.2. Simulated hardware pertains mostly to blade attachment specimens and cold spin test specimens for simulated blade testing. Subscale hardware includes first generation can type combustor liners and assemblies for testing under Task 10.

Subtask 9.2 - Component Fabrication Development and Testing (WBS 2.9.2) - This subtask is quite varied and includes the procurement and testing of first generation blades and nozzles, and second generation subscale combustor liners. The testing involves laboratory testing of test specimens and simulated components, and proof testing and engine rig testing of first generation blades and nozzles. Included in subtask 9.2 are long term testing of ceramics and the development and application of nondestructive evaluation (NDE) methods for ceramic components and associated test specimens.

Subtask 9.3 - Component Manufacture and Testing (WBS 2.9.3) - Ceramic components for installation into the ceramic stationary gas turbine for the 4000 hour field test in Phase III will be procured and proof tested under this subtask. These are second generation ceramic components incorporating design modifications resulting from testing under Subtasks 9.1 and 9.2.

Progress during the reporting period is summarized in this section and includes excerpts from direct inputs from the suppliers as progress summaries, updates on Solar specifications including material specifications and receiving inspection procedures, a status report on NDE procedure development, a review of mechanical property testing and data base development, and results of blade attachment testing.

Although most of the fabrication work was performed under subtask 9.1 and most of the test development and testing was carried out under subtask 9.2 the write up does not rigorously distinguish between these subtasks. No subtask 9.3 work has been performed to-date.

5.1 TASK 9.0 - SUMMARY

A great deal of activity under this subtask was represented by the activities of the suppliers on the CSGT team. Table 5-1 summarizes the fabrication and deliverable efforts of the suppliers.

Materials specifications are part of the material supplier deliverables and are required to ensure approved fixed processes are used to produce reproducible material. Material specifications are referenced on the engineering design drawings.

Receiving/Inspection procedures have been defined and documented in ISO 9000 format and include procedures for storing and tracking government material and Materials Review Board (MRB) action for discrepant parts.

Table 5-1. Suppliers and Deliverables

Supplier	Deliverables
AlliedSignal Ceramic Components (CC)	GN-10 flexure bars, attachment specimens, prototype blades
Kyocera Industrial Ceramic Corporation (KICC)	SN-253 flexure bars, tensile bars, attachment specimens, prototype blades and nozzles
Norton Advanced Ceramics (NAC)	NT164 flexure bars, tensile bars, attachment specimens, prototype blades NT230 flexure bars, combustor rings
Carborundum	Hexoloy® SA flexure bars, tensile bars, combustor tiles
NGK Insulators, Ltd. (NGK)	SN-88 flexure bars, tensile bars, prototype nozzles
Babcock & Wilcox (B&W)	Al_2O_3/Al_2O_3 CFFC flat coupons, ring burst specimens, combustor liners
DuPont Lanxide Composites (DLC)	SiC/SiC CFCC flat tensile bars, flexure specimens, ring burst specimens, combustor liners
BF Goodrich	SiC/SiC CFCC coprocessed rings, combustor liners

The Phase II work at Argonne National Laboratory (ANL) and the Caterpillar Technical Center focussed on the development of NDE methods which included radiography, laser scattering, selected area X-ray Computed Tomography (X-ray CT), fluorescent penetrant inspection (FPI), and specific damping capacity. Most work was performed to obtain defect/property correlations on test specimens, and on combustor liners, with a limited amount of work on attachment specimens.

Mechanical property tests are being performed at temperatures representative of component design temperatures, i.e. 1093°C (2000°F) for the blade airfoil, 760°C (1400°F) for the blade root attachment, 1288°C (2350°F) for the nozzle, and 1149-1204°C (2100-2200°F) for the combustor. Standard flexure and tensile tests are being performed to provide data on fast fracture, static fatigue, dynamic fatigue and stress relaxation. The data base is then being used in conjunction with finite element stress/temperature analyses to perform component life prediction using SPSLIFE and NASA CARES/LIFE codes as discussed in Sections 3.0 and 6.0. The test data are being generated at Solar, UDRI, and the suppliers. Additional information is being made available from experimental work at ORNL performed under separate contracts.

Blade root attachment testing has so far focussed on the dovetail and early pin designs. The ceramic materials tested were GN-10 (CC), SN-253 (KICC), and NT164 (NAC). Under the static load tests the dovetail designs have survived up to ~400% of design stress and pinned designs up to ~200% of design stress.

Progress in all of these areas is discussed in more detail in the following sections.

5.2 SUPPLIER PROGRESS SUMMARIES

Inputs from the suppliers pertaining to the deliverables listed in Table 6-1 are summarized below.

5.2.1 AlliedSignal Ceramic Components (CC)

CC is supplying GN-10 silicon nitride blades for the Phase II CSGT effort. CC has made recommendations using an interactive engineering approach with Solar to improve the quality and reduce the cost of fabricating the dovetail and pinned root attachment specimens. CC has supplied

flexure bars for oxidation, slow crack growth and sticking studies. Five dovetail attachment specimens, five pinned root attachment specimens, and 15 pins were also delivered. The test bars, attachment specimens and pins were fabricated from pressure slip cast plate stock. The plates were HIP'ed and sectioned in preparation for final machining. Density determination was completed before the parts were sent out for machining. Finished parts were then post heat treated, dimensionally and visually inspected, and penetrant inspected. Fluorescent penetrant and X-ray inspection were performed on all flexure bars. Any test bars, attachment specimens or pins which were rejected by CC due to surface imperfections or nonconformity were sent to Solar for NDE analysis.

CC also reviewed Solar's first generation blade designs and made comments regarding tolerancing, datum structures and component design. CC is currently in the process of fabricating 100 GN-10 dovetail blades and 150 co-processed flexure bars. These blades and flexure bars will be made using the same fabrication process which was used for the attachment specimens. Slip casting of stock material has been completed as well as evaluation of the pre-sinter machining process. Dimensional analysis of the airfoil and refinement of the pre-sinter machining is ongoing. Statistical process control of in-process material characteristics has contributed to high yields during casting, drying and pre-sintering. An inspection plan has been formulated to ensure that deliverable hardware meets Solar's requirements for NDE, mechanical properties, part handling and marking. First blade and test specimen delivery is due in the spring of 1995.

5.2.2 Kyocera Industrial Ceramic Corporation (KICC)

KICC is supplying SN-253 silicon nitride blades for the Phase II CSGT effort. KICC has reviewed Solar's designs and made recommendations to improve the fabricability and reduce the cost of making the dovetail and pinned root attachment specimens. KICC has fabricated flexure bars for oxidation, slow crack growth and sticking studies and tensile bars with co-processed flexure bars. Five dovetail attachment specimens, five pinned root attachment specimens, and 15 pins were also delivered. KICC also provided five modified two-tanged pinned root SN-253 attachment specimens and 15 oblong pins. To accomplish the fabrication, billets, cylinders and plates of SN-253 were obtained from Kyocera in Japan. The plates and cylinders were fabricated using Kyocera's hybrid molding process so that the test material duplicated that of the future blades to be fabricated. Billets for the attachment specimens, however, were fabricated by cold isostatic pressing. KICC performed the final grinding of all of the items, except the tensile specimens, which were ground for KICC by Chand Kare. KICC also inspected their deliverables dimensionally, visually, with fluorescent penetrant inspection (FPI), and radiographically. Any test bars, attachment specimens or pins which were rejected by KICC due to surface imperfections or nonconformity were sent to Solar for NDE analysis.

KICC also reviewed Solar's first generation blade designs and made comments regarding tolerancing, fabricability and component design. KICC is currently in the process of fabricating 100 SN-253 two-tanged pinned root blades, 120 pins and 150 co-processed flexure bars. Raw materials for fabrication have been ordered and tool design has been completed. Tooling has been ordered from a proven supplier in Japan. Tooling is scheduled to be completed by November, 1994. KICC provided sketches of the proposed dimensional inspection fixtures. Also, a summary of the NDE FPI and radiographic specifications suitable for use on the print were provided. First blade, pin and test specimen delivery is due late spring 1995.

KICC was provided with preliminary prints and a stereolithography model for the nozzle design for fabricability review. A quotation for cost and delivery was also supplied. Through iterative discussion between KICC and Solar's design team, the nozzle design was modified to improve the

fabricability and lower the cost of fabrication by KICC. KICC has been selected to fabricate the first generation SN-253 nozzles based on the material properties and component life prediction. Solar will release the nozzle drawing in November 1994 for KICC to begin fabrication.

5.2.3 Norton Advanced Ceramics (NAC)

NT164 silicon nitride and NT230 reaction bonded silicon carbide are candidate materials for hot section components. The NT164 was considered for the blade and the nozzle and the NT230 for combustor rings. NAC delivered all the flexure bars (50 as-fired and 210 machined) as well as 50 buttonhead tensile rods on schedule. They also successfully completed delivery of 6 pinned and 6 dovetail attachment specimens made of NT164 and supplied a specially fabricated tapered specimen with different machining finishes for NDE. NAC experienced problems with the fabrication of the NT230 combustor rings. The primary issue has been the formation of defects in the interior of the component due to differential cooling across the cross section. Also, pools of free silicon contributed to the formation of small cracks.

NAC has reviewed the drawing for the dovetail blade and are confident they can fabricate the component. NAC is currently in the process of producing a first article component for evaluation. NAC has had initial success with an alternate glass encapsulant for the blade and will supply Solar flexure bars to evaluate relevant properties. NAC will deliver a total of 100 first generation NT164 rotor blades and 150 co-processed flexure bars.

NAC also reviewed the nozzle drawings. The NT164 candidate material did not meet the life prediction criteria established by Solar for the nozzle. Consequently, NT164 was not selected for this component.

5.2.4 NGK

NGK's SN-88 silicon nitride was one of the four candidate materials for the nozzle. As part of this task NGK supplied Solar with ORNL buttonhead tensile rods (50) for dynamic fatigue and stress rupture testing as well as machined (210) and as-fired flexure bars (50) for slow crack growth and oxidation testing. NGK has a well established NDE inspection sequence for their test specimens as well as their components. NGK met the delivery schedules required of the Statement of Work (SOW) on most of their deliverables. NGK had to extend delivery of the buttonhead tensile specimens because the Solar Material Review Board (MRB) team requested rework on a batch that did not meet dimensional requirements. As part of this task NGK visited Solar twice.

NGK also played a key role in detailing dimensional tolerances on the nozzle drawing. A video conference call between NGK (Japan) and Solar design personnel was crucial in defining fabrication limitations. NGK has now received the finalized version of the first generation nozzle as well as the computer data in ANSYS compatible format. NGK has proposed making prototype quantities using an alternate process that would reduce processing time to 5 months for the first set of 12 nozzles. NGK is currently providing Solar with as-fired flexure bars made by the alternate process for evaluation.

5.2.5 Carborundum

Carborundum's Hexoloy® SA was a candidate material for the combustor and the nozzle. Carborundum successfully delivered flexure bars (210 machined and 50 as-fired) as well as 50 ORNL buttonhead tensile rods. The dimensional tolerance of the Carborundum tensile specimens were well within the requirements of the drawing. Carborundum has also delivered to Solar three versions of the tile configurations for subscale testing. Carborundum had a few dimensional

problems with forming these tiles individually. A warpage problem has been solved by modifying the heat treatment process.

The Hexoloy® SA material marginally did not meet the life prediction criteria for the nozzle and was not selected as a primary candidate. However, it will remain under consideration as a nozzle backup material.

5.2.6 DuPont Lanxide Composites (DLC)

Solar has received all of DLC's deliverables for subtask 9.1. All of the parts supplied by DLC were fabricated from their Nicalon SiC fiber-reinforced enhanced SiC matrix composite material. Included are three 20 cm (8 in.) diameter by 20 cm (8") long subscale combustor liners, six ring burst specimens, 129 flexure specimens, 16 tensile specimens, and 15 interlaminar shear stress specimens. The fibrous preforms were infiltrated using the chemical vapor infiltration (CVI) technique. The subscale combustor liners were nondestructively evaluated at Argonne National Laboratory using infrared- based thermal diffusivity mapping and X-ray computed tomography. Both methods showed anomalies in the cans, especially in one of the three liners. This liner will undergo air-coupled ultrasound nondestructive inspection before it is tested in the rig.

DLC design engineers developed preliminary thermal and stress analysis models for the full scale inner combustor liner and subscale combustor liner. Input was obtained from Solar design engineers on stress and temperature boundary conditions for both models.

DLC supplied a rough draft of the enhanced SiC/SiC composite material specification.

5.2.7 Babcock & Wilcox (B&W)

Under subtask 9.1 Solar has received one 20 cm (8 in.) diameter by 40 cm (16 in.) long 2-D filament wound subscale combustor liner, two 20 cm (8 in.) diameter by 20 cm (8 in.) long 3-D woven subscale combustor liners, two ring burst specimens, 60 transverse and 60 axial flexure specimens, 10 transverse and 10 axial tensile specimens, 15 transverse and 15 axial interlaminar shear stress specimens, and one NDE standard. All of the parts supplied by B&W, except the first (40 cm long can) were fabricated from Nextel 610 alumina fiber-reinforced alumina composite material. The fibrous preform was infiltrated using a sol-gel process. A third 3-D can woven from amorphous Nextel 610 and then fired in the preform state will be delivered in December, 1994. The remaining four ring burst specimens will also be delivered toward the middle of December.

B&W supplied a rough draft of the alumina/alumina composite material specification.

5.2.8 BF Goodrich Supertemp

BF Goodrich Supertemp is a part supplier for full scale SiC/SiC CFCC combustor liners under the program. These liners will be used in early engine rig testing to approximate as closely as possible the conditions expected in the combustor with ceramic liner substrates. Unlike the other combustor liner materials suppliers, BF Goodrich is not involved in development work for their parts. Rather they are using their existing process to fabricate full scale parts under a subtask of Task 7.0.

Fabrication of the preforms for the combustor inner and outer liners was subcontracted to Drexel University. Delivery of the full scale Nicalon fiber-reinforced SiC composite combustor liner under Task 7.0 was delayed from early September to early December, 1994, because of an equipment

failure at Drexel University. Both inner and outer liners will undergo CVI processing in the same furnace run.

5.3 MATERIALS SPECIFICATIONS AND RECEIVING INSPECTION

5.3.1 Material Specifications

Material specifications are required for pre-production and production hardware. The specifications serve as a quality control tool and ensure that specimens and components are fabricated using the same raw materials and approved fixed processes and that established minimum property requirements are met.

Material specifications have been developed and issued as internal Solar "Controlled Engineering Specifications" (CES9-XXX) for several of the suppliers and others are currently in process. Only one supplier, NGK, has indicated that they would prefer not to produce a material specification for their SN-88 silicon nitride following the outline suggested by Solar. They will provide material controlled by their own internal specification which does not have elevated temperature property requirements. At some future time, should NGK's material be selected for production engines there would be a governing requirement for a Solar approved specification. It is also recognized that some materials have reached a greater degree of maturity and that processes and resulting properties for newer materials will likely be revised over time. Table 5-2 summarizes status of Engineering Specifications for the program materials.

Table 5-2. Material Specification Status

Supplier	Material	Engineering Specification Status
CC	GN-10	CES9-381 In Final Draft
KICC	SN-253	CES9-383 In Final Draft
NAC	NT164	CES9-378 Released
CARBORUNDUM	HEXALOY® SA	CES9-379 Released
DLC	SiC/SiC	Rough Draft Prepared
B&W	Al_2O_3/Al_2O_3	Rough Draft Prepared
SOLAR	Material Handling	ES 2110 Released
SOLAR	Laser Marking	ES 2120 Released
SOLAR	Ceramic Rec./Inspect.	Operation Practice T.EFO3-3-1 Released

5.3.2 Receiving Inspection

A detailed procedure has been implemented to control receipt and inspection of all CSGT ceramic parts. Solar has designated a locked area at its Harbor Drive facility as the Ceramics Government Stores. A Government Stores Custodian was appointed to control the issue of government property to Solar employees and suppliers. A Material Review Board (MRB) was created for each component (combustor, nozzle, and blade) to review Supplier Disposition Requests (SDRs) as needed.

Solar Operation Practice No. T.EF03-3-1 establishes the general practices for receiving and inspecting ceramic specimens and components. Guidelines for visual inspection, part identification, and dimensional inspection are outlined in Operations Practice T.EF03-3-1 as well. If discrepancies are found at any point, a W/N (Withholding Notice) is issued on the part and a MRB meeting is held

to determine the course of action. If a part is in conformance, the Principal Investigator (PI) will define the course that the part will take, which may include additional dimensional inspection, nondestructive characterization, additional visual inspection, physical and/or mechanical testing, or other specified inspection or testing. The PI also establishes a schedule for routing of parts after the receiving/inspection procedures are complete.

Figure 5-1 shows the flowchart of the general tasks outlined in the Operations Practice. The PI's and the Government Stores Custodian play key roles in the timely implementation of the receiving/inspection practice. Parts are received by one of these individuals and logged into the Government Stores record within 24 hours of receipt. At the time of log-in, the condition, quantity, and description of the parts are verified. Also, the shipping documentation is checked for completeness, and government property number(s) are assigned to the parts received. If information is missing and the responsible PI cannot resolve the issue with the supplier, a Report of Discrepancy(ROD) will be issued. If parts are discrepant, a W/N will be issued and a MRB meeting is called.

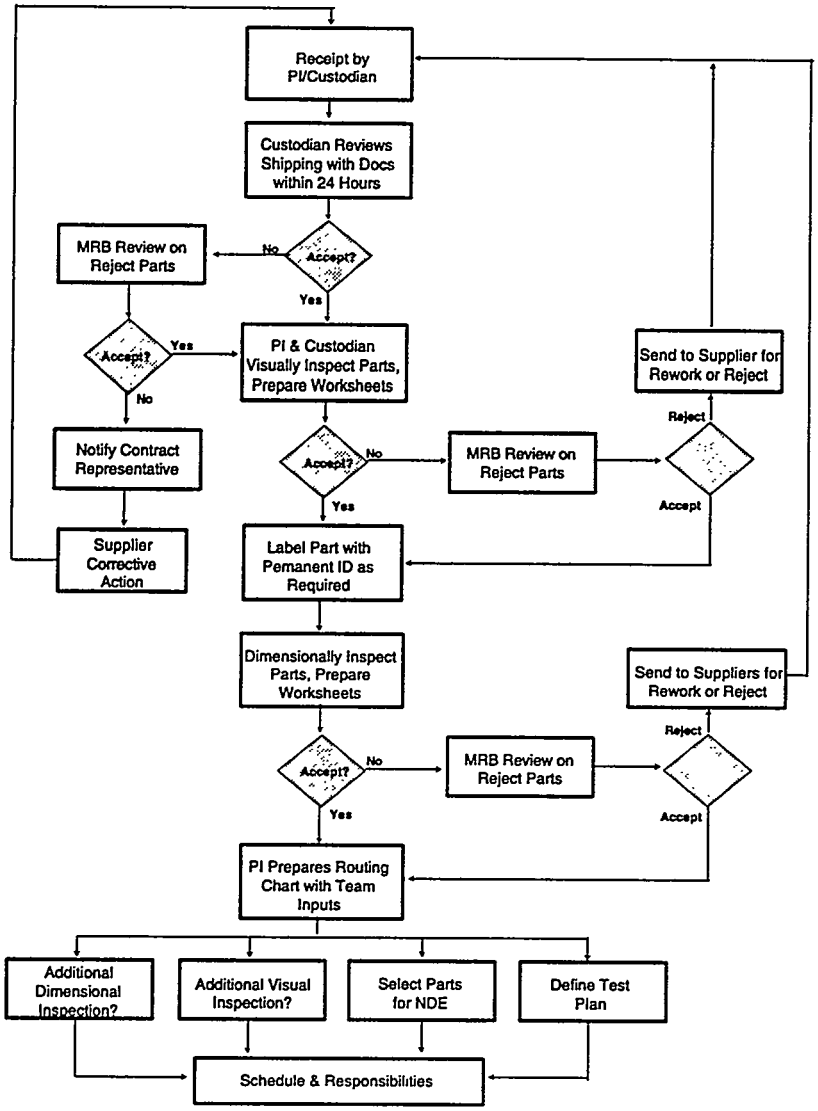

Figure 5-1. Schematic of Solar's Receiving/Inspection Procedure for Ceramics

5.4 NON-SUPPLIER SUBCONTRACTS

5.4.1 Sundstrand Power Systems (SPS)

SPS has provided support in several areas during the reporting period. SPS participated in the evaluation of ceramic material information with special emphasis on component life-limiting material characteristics. As part of this activity SPS completed life assessment for fast fracture and slow crack growth for the Phase I designs using SPSLIFE and NASA CARES/LIFE computer routines. The data of this study have been reported (1). The conclusions pertaining to the design of the primary ceramic components have been referenced and/or discussed in some detail in Sections 3.0 (Task 7.0 - Engine Design) and Section 6.0 (Task 10.0 - Low Emission Combustor). SPS has also taken part in discussions with visiting suppliers and has been part of Solar's materials team.

SPS has also supported prototype manufacturing, testing and evaluation with particular emphasis on long term material performance. Structural input files on the most recent blade and nozzle designs have been analyzed by SPS and component life has been assessed using properties of some of the candidate materials. SPS is currently working on the creep behavior of the candidate nozzle materials. The status of the work to date on the nozzle designs is reported in Section 3.0.

5.4.2 University of Dayton Research Institute (UDRI)

The objective of the UDRI subcontract has been to determine long term mechanical properties for the candidate nozzle and blade materials under conditions similar to those in the CSGT program. UDRI has completed the dynamic fatigue tensile testing of four nozzle materials (NT164, SN-253, SN-88 and Hexoloy® SA) on schedule. Ten specimens each were tested at two different crosshead speeds (four decades different) at 1288°C (2350°F), the approximate temperature of the nozzle airfoil hot spot area. The results of these tests were instrumental in the selection process of the nozzle candidate materials and suppliers (see Section 3.0). Static stress rupture tests for 1000 hours are currently in progress on three candidate nozzle materials. UDRI has also just completed evaluation of tensile rods of NT164, machined from cylinders rather than near net shape castings which were used for a previous lot of specimens. The UDRI data will be discussed in detail in Section 5.5 (Materials Property Testing).

5.4.3 NDE at Argonne National Laboratory (ANL) & the Caterpillar Technical Center (CAT TC)

ANL and CAT TC are jointly responsible for the development of methodologies for nondestructive evaluation (NDE) of test specimens, simulated and subscale components and full size components under the program. ANL's role involves primary responsibility for NDE methodology development and application of the methodologies to screening and "finger printing" of CSGT specimens and parts. CAT TC provides the industrial interface and its responsibility is to ensure that the methodologies once developed and demonstrated are transferred to Solar for implementation in its ceramic materials and component evaluation. Staff of CAT TC has been working on site at ANL to facilitate the technology transfer.

5.4.3.1 NDE Work Plan

ANL's Phase II work focused on the development of several nondestructive evaluation methods for the candidate monolithic and CFCC materials. The plans for monolithic test coupon and component NDE are summarized in Tables 5-3 and 5-4. The plan for CFCC test specimen and component NDE are given in Tables 5-5 and 5-6.

Table 5-3. Monolithic Test Specimen NDE Plan

Test Specimen	NDE Methods to Be Employed	Purpose
Flexure Bars	- Radiography - FPI - Laser Scatter - Specific Damping Capacity	- Determine spatial resolution limit - Obtain property /microstructure correlation - Obtain baseline signatures
Tensile Bars	- Radiography - FPI - Laser Scatter - Selected Area X-ray CT	- Obtain data through NDE methods before and after long term creep/stress rupture/ oxidation exposure
Attachment Specimens Dovetail and Pinned Root	- Radiography - Laser Scatter - FPI	- Correlation of NDE data with proof testing - Correlation of NDE data with fracture behavior

Table 5-4. Monolithic Component NDE Plan

Component	NDE Methods to Be Employed	Purpose
Blades	- Radiography - FPI - Laser Scatter (Dovetail only) - Specific Damping Capacity	- Accept/reject component - Establish pre-engine test baseline signature
Nozzles	- Radiography - FPI - Laser Scatter (Airfoil only)	- Accept/reject component - Establish pre-engine test baseline signature
Segmented Combustor Liners Rings and Tiles	- Radiography - FPI - Specific Damping Capacity	- Accept/reject component - Establish pre-engine test baseline signature

Table 5-5. CFCC Test Specimens NDE Plan

Component	NDE Methods to Be Employed	Purpose
Subscale Combustor Liners	- X-ray CT - X-ray Single Wall Through Transmission - Infrared Imaging - Air-Coupled Ultrasonics	- Delamination Detection - Full Wall Density Uniformity - Full Field RT Thermal Property - Delamination/Density
Flat Tensile Bars	- X-ray CT - X-ray Through Transmission - Infrared Imaging	- Delamination Detection - Through Thickness Uniformity - Correlate with X-ray data; study thermal properties

Table 5-6. CFCC Component NDE Plan

Component	NDE Methods to Be Employed	Purpose
Full Scale Combustor Liners	- X-ray CT - X-ray Single Wall Through Transmission - Infrared Imaging - Air-Coupled Ultrasonics	- Delamination Detection - Full Wall Density Uniformity - Full Field RT Thermal Property - Delamination/Density

To date development efforts have been carried out primarily on mechanical test specimens and subscale combustor liners. Some work has also been done on reject specimens and specimens with intentionally placed defects. For the monolithic materials, correlations between the 40x visual inspection and NDE methods have been established. The most prominent defects have been seen in the NAC NT164 material. Iron inclusions have been detected using laser scatter and radiography, and have been correlated with visual and metallographic observations. Glassy pools in the NT164 material were found visually and with laser scatter, but not with radiography. Another example of correlation between methods is the detection of a "mottled" appearance in CC's GN-10 material. The mottling was detected visually, using laser scatter, and using radiography. It appears that the mottling is a variation in local density of the material.

Correlations have also been established for the CFCC materials. Indications of lower density and possibly delamination in the same areas of the same DLC SiC/SiC liner have been detected with X-ray CT and infrared imaging based thermal diffusivity mapping (see Figure 5-2). Single wall through transmission X-ray at ANL has shown major fiber misalignment and after exposure delamination in B&W alumina/alumina liners. These data correlate with ultrasonic inspection data generated by B&W.

The work done on the test specimens is intended to establish readiness of the selected NDE methods for first generation components. The current status of the selected methods for each component is detailed below.

5.4.3.2 Status of Readiness for First Generation Components

Blades - Radiography, Fluorescent Penetrant Inspection (FPI), and laser scatter (machined dovetail root only) will be used on the blade components. Protocol for the digital radiography method is defined, but the actual defect size detection limit has not been established. Also, the best detector has not been selected. The laser scatter method is ready for the dovetail root, but like the digital radiography method, the actual defect size detection limit has not been defined. Protocol for FPI is still under development. Issues to be resolved include the effects of surface roughness and microstructure on results. A method for high resolution direct digital imaging has been established for FPI. For the pinned root configuration, ANL has suggested that a high magnification optical boroscope be used with FPI to inspect the internal bore in the root section.

In an effort separate from CSGT, specific damping capacity is being developed by CAT-TC in conjunction with ANL. Sensitivity to known defects is being established with this method. Data will be gathered on CSGT first generation blades using specific damping capacity. It is anticipated that this method will give a quick way of distinguishing acceptable parts from reject parts.

Nozzles - Radiography, FPI, and laser scatter (airfoil only) will be used for the first generation nozzles. The state of readiness is the same as that for the blades, except that laser scatter for the airfoil region needs a motion control stage for automatic data acquisition.

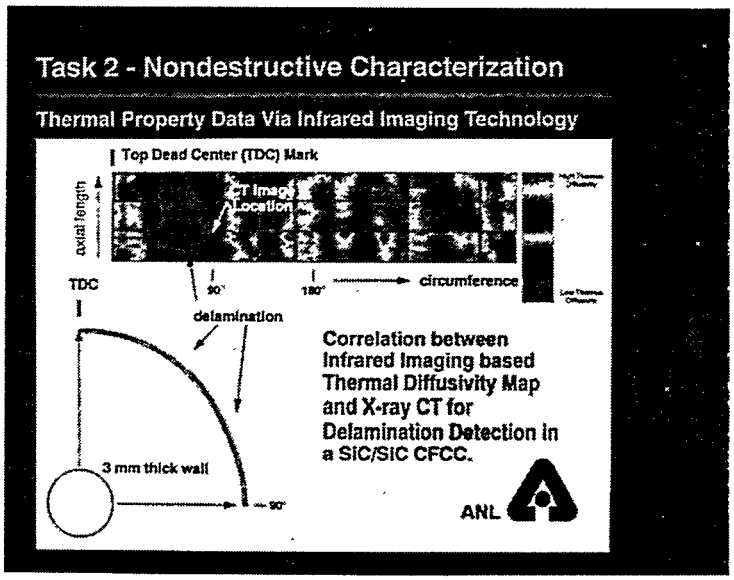

Figure 5-2. Infrared and X-Ray CT Scans of SiC/SiC CFCC Subscale Combustor Liner

Segmented Monolithic Combustor Liners - Radiography, FPI, laser scatter, and specific damping capacity (under CAT-TC's program) will be used on the monolithic tiles and rings. The status is the same as for the blades.

CFCC Liners - X-ray computed tomography, through-wall X-ray film radiography, and infrared full field room temperature thermal diffusivity mapping have been under development for the CFCC liner materials. The protocol for all three methods is established for the subscale liners and first generation components.

5.4.3.3 Near-Term NDE Work

Test specimens are being nondestructively characterized at ANL. The results of the mechanical tests will be correlated to the NDE data on each bar. Solar, ANL and CAT TC will review this information to establish the viability of the NDE methods under development. A similar approach will be taken for NDE data and mechanical testing/rig data on tensile bars, attachment specimens, and subscale combustor liners.

5.5 MATERIALS PROPERTY TESTING

5.5.1 Testing Requirements

Blade - Since the maximum temperatures of the blade airfoil and the blade root are below 1121°C (2050°F) the failure modes of principal concern for the blade are fast fracture and slow crack growth. The following material tests were planned for the blade:

1. Dynamic fatigue testing (2 decades difference in crosshead speed) of machined flexure bars at 760°C (1400°F) (attachment peak temperature).

2. Dynamic fatigue testing (2 decades difference in crosshead speed) of as-fired flexure bars at 1093°C (2000°F), simulating a temperature close to the maximum airfoil temperature.

3. Fast fracture testing at relevant temperatures, to complete the database.

4. Static flexure fatigue testing at 760°C (1400°F) for up to 4000 hours.

Nozzle - Failure modes for the nozzle may fall into the regime of fast fracture, slow crack growth, creep, or a combination of these effects because the peak temperature could be as high as 1288°C (2350°F). The peak stress occurs at the peak temperature. Therefore the test plan will include investigation of all three modes.

1. As-fired flexure bar testing at two different crosshead speeds (2 decades different) at a test temperature of 1288°C (2350°F).

2. Dynamic fatigue testing of tensile rods at two different crosshead speeds (4 decades different) at a test temperature of 1288°C (2350°F).

3. Stress relaxation tests at 1288°C (2350°F).

4. Stress rupture testing of tensile rods for up to 10,000 hours.

Combustor - The peak temperature of the combustor rings and tiles is in the 1149-1204°C (2100-2200°F) range. Since it has been established that silicon carbides show very little time dependent degradation at this temperature, the primary failure mode of concern is fast fracture. Sticking between adjacent tiles and rings in the engine is possible and tests to evaluate this problem are underway.

5.5.2 Testing Conditions

The above mentioned tests are being carried out at three locations: Solar, University of Dayton Research Institute (UDRI),and Oak Ridge National Laboratory (ORNL) under a separate DOE contract. To enable completion of the data gathering efforts tensile creep frames, purchased from Advanced Test Systems (ATS), were installed at the testing facilities. The test facilities and the experimental procedure at each of the facilities is given below.

Figure 5-3 is a schematic representation of the creep/stress rupture test machine that will be used by ORNL. The test frames at Solar and UDRI are very similar to this machine. The primary difference is that ORNL uses a contact extensometer, Solar uses laser extensometers, and UDRI uses a customized laser speckle interferometer system to measure strain in their machines. Solar also uses an MTS hydraulic system for flexural and cyclic fatigue testing.

The buttonhead tensile specimens having a nominal gage length of 35 mm (1.38 in) and a diameter of 6.35 mm (.25 in.) are used. The final grinding direction in the gage and transition section is longitudinal, to minimize failure from the surface.

The flexure specimens were supplied both in the machined and the as-fired condition. The machining direction is typically parallel to the longest side of the bar. The dimensions of the flexure bars were 3x4x50 mm (.12 x .16 x 1.97 in.). Specimens are tested according to MIL-STD-1942(A) (specimen size B) with the outer span being 40 mm (1.57 in.) and the inner span being 20 mm (.79 in.). The machined flexure bars were ground to a 0.4 micrometer (16 microinch) finish. The as-fired surface acted as the tensile face in the tests.

Flexural strength at Solar was measured in four point bending following MIL-STD-1942. The tests specimens were loaded at crosshead speed rates of 0.004 cm/s (0.095 in/min) and 0.00004 cm/s (0.00095 in/min). Elevated temperature flexural tests were conducted in high temperature furnaces attached to the test machine.

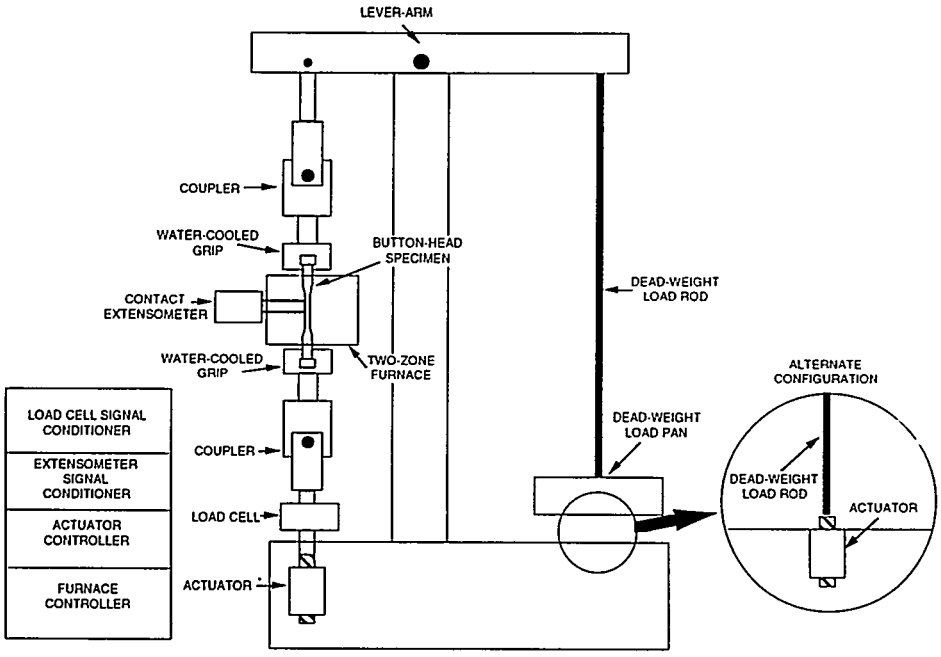

Figure 5-3. Schematic Representation of the Stress Rupture Machine at ORNL

Stress rupture tests were conducted by first heating the tensile specimen in a high temperature furnace to 1288 °C (2350°F) and then applying the required load on the specimen. The ATS stress rupture machines have a 20:1 lever arm and use free weights. The stress rupture machines at UDRI and ORNL have the added feature of being able to load the specimen to failure after the stress rupture test.

Fracture origins were determined by light microscopy and scanning electron microscopy (SEM). The microstructures of the candidate materials were also studied using light microscopy and SEM on polished specimens and fractured specimens. Electron Dispersive X-ray (EDX) analysis was used for composition determination.

5.5.3 Dynamic Fatigue Testing for Blades

5.5.3.1 Dynamic Fatigue Testing at Room Temperature

Room temperature strength degradation of silicon nitrides has been reported in the literature. The available database was reviewed for the three candidate blade materials: NT164, GN-10 and SN-253. Dynamic fatigue strength deterioration as a function of crosshead speed data was found in literature for NT164 and SN-253. Solar conducted dynamic fatigue strength tests for GN-10 on machined flexure bars. Table 5-7 gives the results of this test. The mean strength showed a deterioration from 796 MPa (117 ksi) to 659 MPa (97 ksi). The slow crack growth exponent of approximately 24 is the lowest among the candidate materials.

The slow crack growth exponent for the other two materials NT164 and SN-253 are 26 and 100, respectively, as determined from literature data.

Table 5-7. Room Temperature Dynamic Fatigue Flexure Testing Results of GN-10

Crosshead Speed cm/s (in/min)	No. of Specimens Tested	Average Strength MPa (ksi)	Weibull Modulus m	Standard Deviation MPa (ksi)	Slow Crack Growth Exponent n
0.004 (0.095)	10	796 (117)	10	81 (12)	24
0.00004 (0.00095)	10	659 (97)	9	78 (11)	

5.5.3.2 Dynamic Fatigue Testing at 760°C (1400°F)

Literature data in this temperature range is not available for all the candidate materials. Table 5-8 summarizes the results of data obtained from Solar's machined flexure bar testing at the two crosshead speeds for three candidate materials.

SN-253 shows the greatest resistance to slow crack growth among the candidate materials. It is the only blade material that does not have a HIP-densification step after sintering. Unlike the NT164 and GN-10 materials, where even for a machined surface remnants of HIP encapsulants weaken the parent material, SN-253 exhibits better strength retention.

One of the NT164 flexure specimens fractured at an unusually low stress of 565 MPa (82 ksi) at the faster crosshead speed. A microstructural analysis of the specimen (Figure 5-4) indicated the source of failure to be a 38 micrometer (0.0015 inch) inclusion just below the surface. EDX analysis of the defect shows iron present in the inclusion. The presence of glassy pools with dendrites on the surface is the other major type of defect noticed (Figure 5-5). The SN-253 fracture surface did not have any major defects that acted as the source of failure. It was more difficult to identify the starting point of failure for this material. The major feature of SN-253, noticed under the scanning electron microscope is the presence of small protrusions distributed evenly on the surface (Figure 5-6). A clear correlation between the origin of failure and these protrusions was not established.

Table 5-8. Dynamic Fatigue Flexure Testing Results at 760°C (1400°F) for Three Silicon Nitrides

Material Crosshead Speed cm/s (in/min)	No. of specimens tested	Average Strength MPa (ksi)	Weibull Modulus m	Standard Deviation MPa (ksi)	Slow Crack Growth Exponent n
GN-10 0.004 (0.095)	20	674 98	14	43 6	28
GN-10 0.00004 (0.00095)	20	575 83	15	42 6	
SN-253 0.004 (0.095)	20	790 115	10	82 12	112
SN-253 0.00004 (0.00095)	20	758 110	13	59 9	
NT164 0.004 (0.095)	20	900 131	10	92 13	38
NT164 0.00004 (0.00095)	20	800 116	9	83 12	

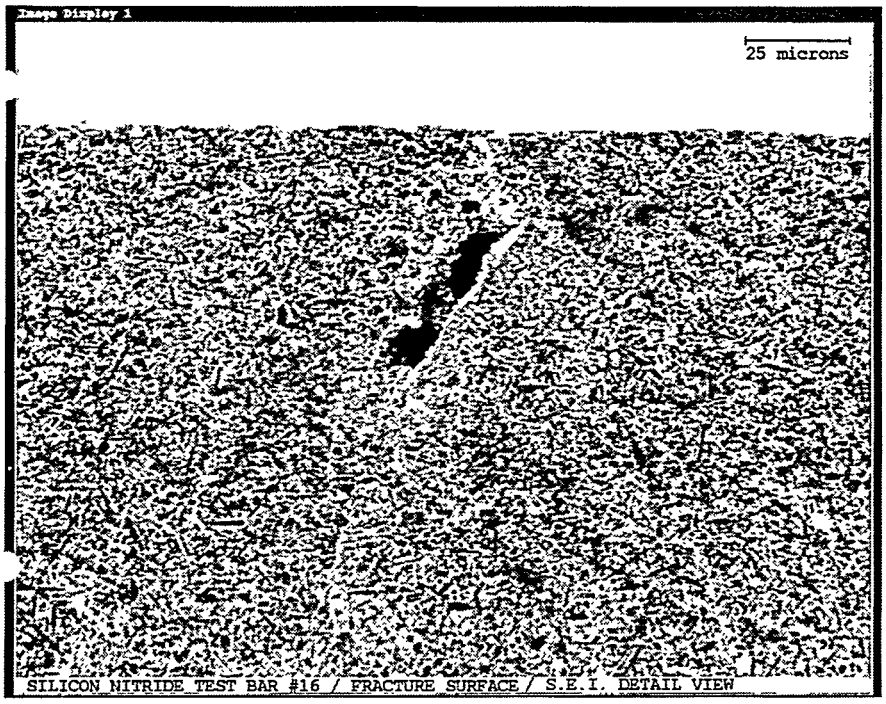

Figure 5-4. Scanning Electron Micrograph of Fracture Initiation Site for NT164. Mag: 500x

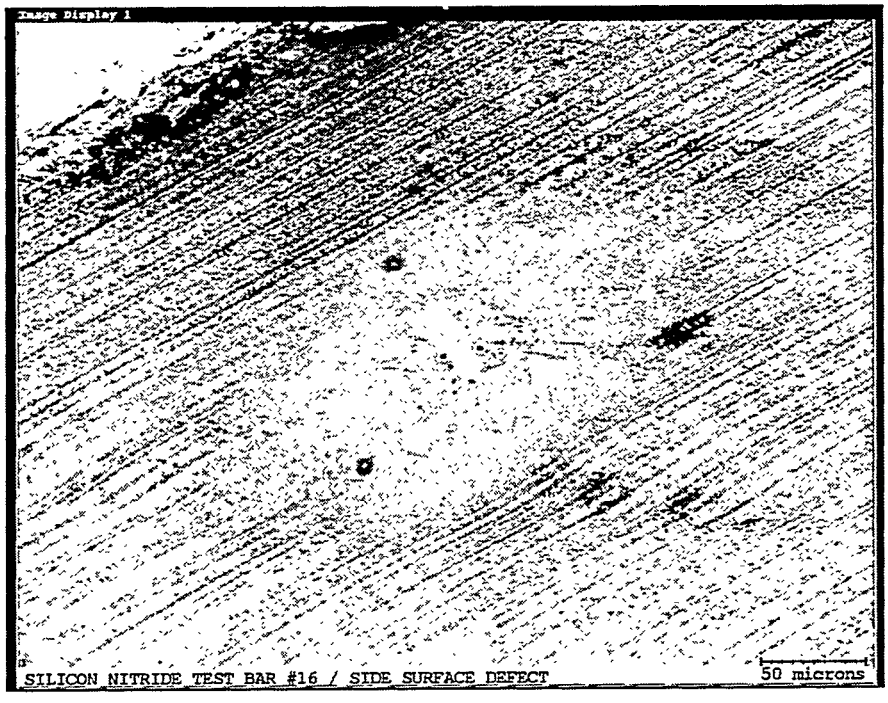

Figure 5-5. Glassy Pools on NT 164 Machined Surface. Mag: 250x

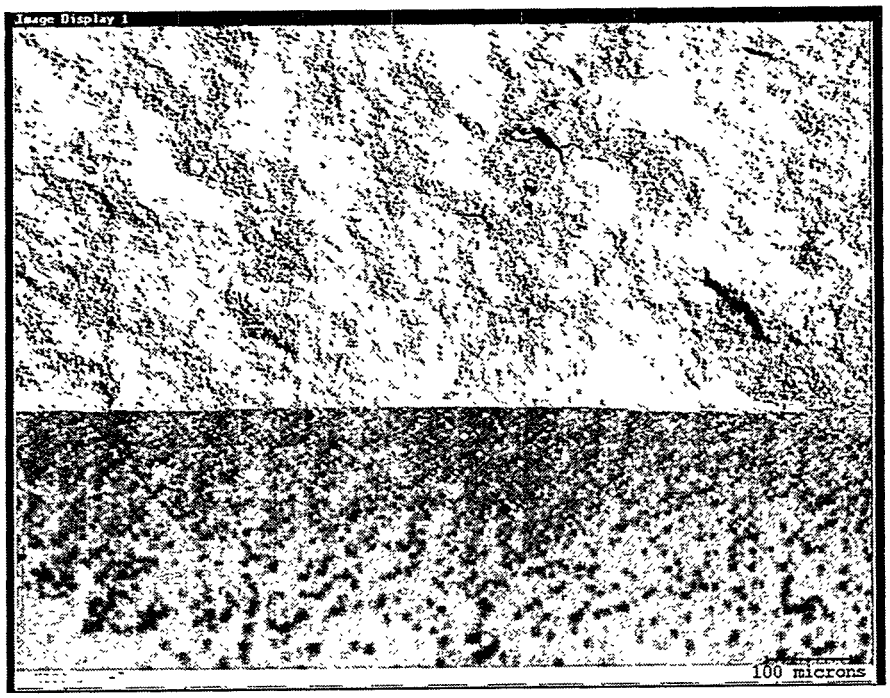

Figure 5-6. SN-253 Surface Showing Regular Protrusions. Mag: 88x

5.5.3.3 Dynamic Fatigue Testing at 1093°C (2000°F)

Since the airfoil of the blade may experience a peak temperature close to 1093°C (2000°F) and the airfoil is in the as-fired condition, as-fired flexure bars of one of the candidate materials, NT164, were tested in dynamic fatigue at 1093°C (2000°F). Table 5-9 gives the test results.

Table 5-9. Dynamic Fatigue Testing of As-Fired Flexure Bars at 1093°C (2000°F) for NT164

Crosshead Speed cm/s (in/min)	No. of Specimens Tested	Average Strength MPa (ksi)	Weibull Modulus m	Standard Deviation MPa (ksi)	Slow Crack Growth Exponent n
NT164 0.004 (0.095)	10	634 (93)	7	101 (15)	44
NT164 0.00004 (0.00095)	10	574 (85)	9	78 (11)	

The strength degrades at a similar rate in going from the 0.004 cm/s (0.095 in/min) to 0.00004 cm/s (0.00095 in/min) crosshead speed as compared to the 760 °C (1400°F) degradation for the machined NT164 flexure bars. However, a negative feature of the as-fired surface is the greater variability in the data set compared to test data for the machined surface. Failures originated at iron inclusions as well as at pores on the surface.

Using the machined flexure data at 760°C (1400°F) and Wiederhorn-Evans slow crack growth equations to estimate the 99.9% probability of survival (POS) flexure strength the time to failure is well in excess of 10,000 hours for the SN-253 as well as for the NT164 material, assuming the design stress for the flexure bar is 255 MPa (37 ksi).

5.5.4 Dynamic Fatigue Testing for Nozzles

5.5.4.1 As-Fired Dynamic Fatigue Testing

The airfoil of the nozzle will be in the as-fired condition. Therefore dynamic fatigue testing of as-fired flexure bars at the nozzle airfoil peak temperature has been conducted on the candidate nozzle materials. Table 5-10 gives the results of this testing.

Table 5-10. Dynamic Fatigue Testing of As-Fired Flexure Bars at 1288°C (2350°F)

Material Crosshead Speed cm/s (in/min)	No. of Specimens Tested	Average Strength MPa (ksi)	Weibull Modulus m	Standard Deviation MPa (ksi)	Slow Crack Growth Exponent n
NT164 0.004 (0.095)	7	561 (81)	4*	119 (17)	50
NT164 0.00004 (0.00095)	7	514 (75)	22*	20 (2.9)	
SN-88 0.004 (0.095)	15	645 (95)	18	39 (5.8)	96
SN-88 0.00004 (0.00095)	15	595 (86)	31	24 (3.6)	
Hexoloy® SA 0.004 (0.095)	4	537 (78)	--	--	22
Hexoloy® SA 0.00004 (0.00095)	12	441 (64)	4	84 (12)	

* The Weibull modulus was computed and is given here for comparison purposes only. The number of test specimens was to small to establish a true m value.

The SN-88 silicon nitride shows excellent dynamic fatigue behavior. Hexoloy® SA is expected to have a very high slow crack growth resistance as well. However, the strength of the silicon carbide is at least 138 MPa (20 ksi) lower than that of the SN-88 material. The very low values of m (Weibull modulus) for Hexoloy® SA and NT164 make them less attractive candidates for the nozzle. It should be noted that the number of NT164 specimens tested is not sufficient to obtain an accurate determination of the Weibull modulus.

5.5.4.2 Tensile Dynamic Fatigue Testing

Tensile dynamic fatigue testing of the four candidate nozzle materials was carried out at the University of Dayton Research Institute (UDRI). Twenty tensile specimens of each material were tested at crosshead speeds of 0.04 cm/s (0.95 in/min) and 0.000004 cm/s (0.000095 in/min.). These tests were run on an Instron 1361 Universal testing machine using the Instron "Super Grip" and Instron short furnace. The results of all the tests to date, are given in Table 5-11.

The failures were typically more surface dominated at the slower crosshead speed. Failure origins for NT164 were all volume initiated at the faster crosshead speed, but ten out of eight failures at the slower crosshead speed were surface initiated. For SN-253 four out of ten failures at the faster crosshead speed were volume initiated. All failures at the slower crosshead speed were surface initiated. For SN-88 at the faster crosshead speed all failures were volume initiated. Six out of ten failures were surface initiated at the slower crosshead speed. This transition to more surface related failures is in agreement with the theory that the environment is inducing the surface cracks to grow at a faster rate, causing them to predominate over the volume defects as testing time increases. Analysis of defects on the surface at the two crosshead speeds did not give a value of n that differed significantly from data that had both surface and volume defects.

The NT164 strength was considerably lower (range: 103-138 MPa or 15-20 ksi) than was evident from data obtained for a similar NT164 under the Ceramic Technology for Advanced Heat Engines (CTAHE) program in the same temperature range. Following testing at 1288°C (2350°F) the NT164 specimens showed a typical spotted surface (Figure 5-7). Light element energy dispersive X-ray spectroscopy (EDS) analysis using an Auger spectroscopy system revealed a relative high concentration of sodium in this region (Figure 5-8). Figure 5-9 shows a volume fracture origin. EDS of this surface revealed a Fe inclusion. These inclusions seem to be a major source of low strength fractures. Therefore the low strength failures appear to be either caused by migration of sodium from the encapsulant glass (used in the HIP process) to the dark areas or due to the frequent presence of Fe inclusions.

The SN-253 material exhibited the highest Weibull modulus of any of the candidate materials. As a result the ratio of tensile strength to flexure strength of this material can be expected to be very high. Figure 5-6 shows protrusions on the surface . Their origin is unclear. The degradation in average strength in going to the slower crosshead speed is almost 207 MPa (30 ksi) and all the failures were surface related.

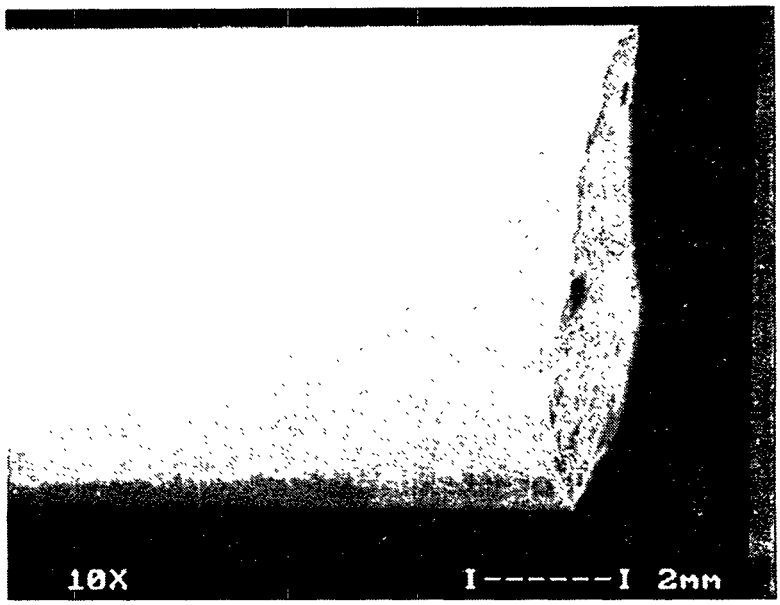

Figure 5-7. Spotted Surface on Tensile Specimen Tested at Slower Crosshead Speed (1288°C - 2350°F)

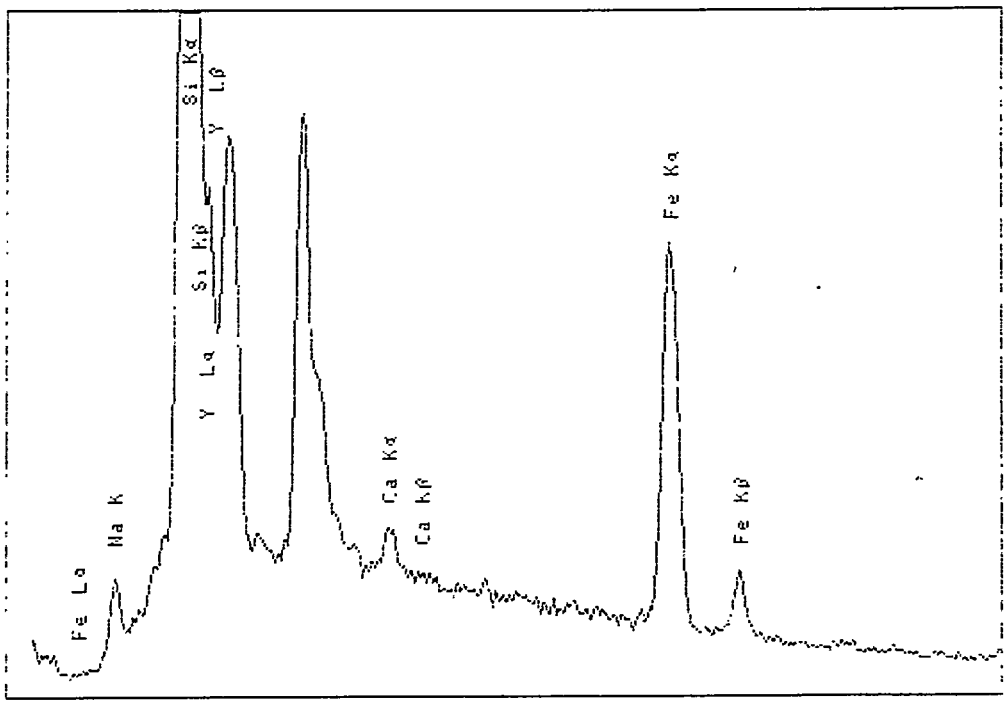

Figure 5-8. EDS of Spots Showing High Concentration of Na

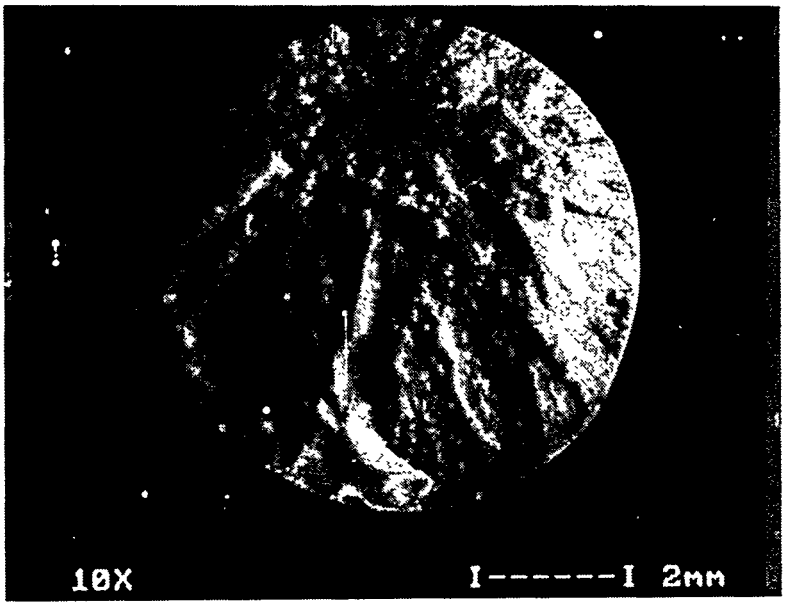

NT-164 SMG-94-1-42 H4-158 UDRI#940292

Figure 5-9. Typical Volume Inclusion Initiated Failure. Inclusion Usually has High Fe Concentration.

Table 5-11. Tensile Dynamic Fatigue at 1288°C (2350°F)

Material Crosshead Speed cm/s (in/min)	No. of Specimens Tested	Average Strength MPa (ksi)	Standard Deviation MPa (ksi)	Slow Crack Growth Exponent n
NT164 0.04 (0.95)	10	442 (64)	22 (3.2)	19
NT164 0.000004 (0.000095)	10	276 (40)	39 (5.6)	
SN-253 (0.04) (0.95)	10	590 (86)	27 (3.9)	21
SN-253 (0.000004) (0.000095)	10	385 (56)	14 (2.0)	
SN-88 0.04 (0.95)	10	461 (67)	55 (8)	182
SN-88 0.000004 (0.000095)	10	438 (64)	17 (2.4)	
Hexoloy® SA 0.04 (0.95)	10	453 (66)	56 (8.1)	65
Hexoloy® SA 0.000004 (0.000095)	10	393 (57)	85 (12)	

SN-88 has a lower fast fracture strength level compared to SN-253 but it retains almost all the strength at the slower crosshead speed (even better than the silicon carbide). The extent of strain before failure is unusually high as compared to the other silicon nitrides. The Hexoloy® SA shows minimal degradation at the slower crosshead speed. The tensile strength of the material however is lower than that of SN-88 and SN-253, but higher than that of NT164.

5.5.4.3 Static Fatigue Testing for Nozzle Materials

One each of SN-88 and NT164 (CTAHE vintage) buttonhead tensile specimen are currently being tested in static fatigue at Solar. The test is being conducted at 1288°C (2350°F) and the specimens are subjected to a tensile stress of 241 MPa (35 ksi). Both the specimens have survived in excess of 1500 hours. Alignment was assured by attaching strain gages (12) to the specimens at room temperature and burning of the adhesive at a higher temperature. Thermocouples very close to the specimen monitor temperature accurately. Temperature control is crucial at this temperature, because SN-88 undergoes a noticeable transition in a 68°C (122°F) range above the test temperature.

5.5.4.4 Stress Relaxation Tests

Tests are being performed to generate data that can be used to predict stress relaxation in industrial gas turbine components such as the nozzle that are subject to constant thermal strains under service conditions. Stress decay due to creep can have a significant effect on component life. The data discussed below was generated at ORNL.

Figure 5-10 compares the results at 1300°C (2372°F) of applying an initial stress of 276 MPa (40 ksi) on tensile specimens of SN-253, SN-88 and NCX 5102 (a research variant of NAC's NT154/NT164 silicon nitrides) and then switching to strain control. All the silicon nitrides exhibit varying degrees of stress relaxation. This behavior is beneficial in redistributing the peak stress in the nozzle. The SN-88 tensile specimen showed the greatest relaxation (from 276 MPa to 34 MPa or 40 ksi to 5 ksi), which is in agreement with the known ability of this material to creep readily.

5.5.5 Future Materials Property Testing

Testing of as-fired flexure bars under blade and nozzle airfoil conditions will be completed. More recently developed materials such as AS-800 from CC will be included in the testing matrix if preliminary results are encouraging. Oxidation testing of the two nozzle candidate materials is in progress. Other testing includes long term (> 5000 hrs) stress rupture tests at Solar, UDRI and ORNL.

5.6 BLADE ATTACHMENT TESTING

Blade attachment testing involves the evaluation of various ceramic blade root configurations under static and cyclic loading. Because ceramic blade to metallic disk attachments typically degrade due to the combination of centrifugal (CF) blade loads on a ceramic to metallic interface and relative motion (tangential sliding) at the loaded interface due to differential thermal expansion of the ceramic blade and metallic disk, the CSGT attachment testing focuses on these two primary conditions.

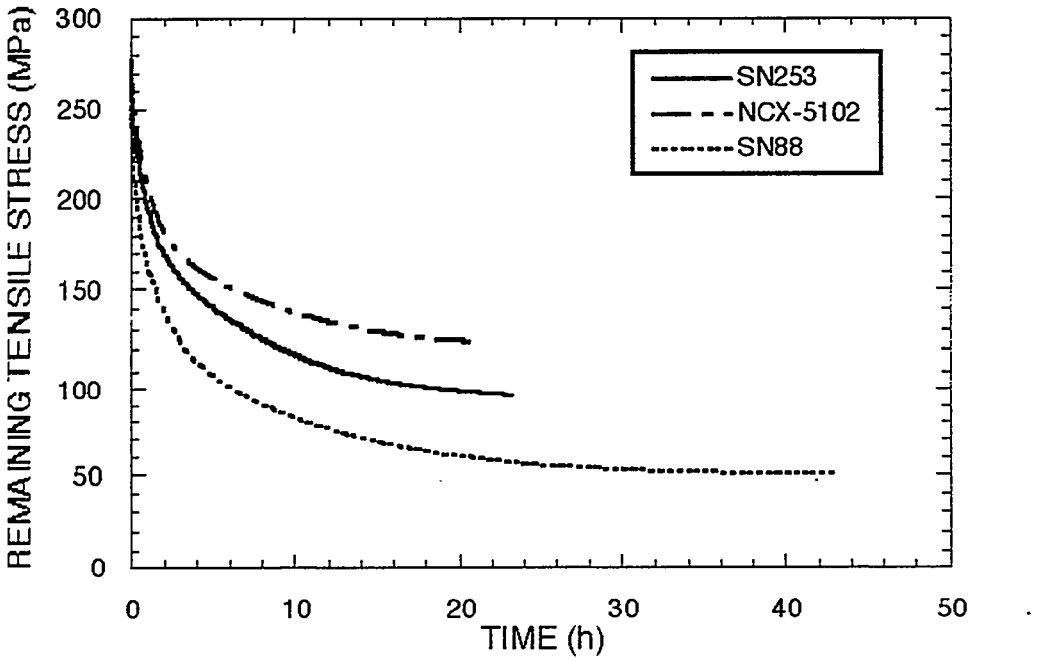

Figure 5-10. Stress Relaxation Data at 276 MPa (40 ksi) for SN-253, SN-88 and NCX 5102

Figure 5-11 shows the dovetail root and pinned root attachment specimens which were supplied by AlliedSignal Ceramic Components (GN-10), Kyocera Industrial Ceramics Corporation (SN-253) and Norton Advanced Ceramics (NT164) for testing in a tensile testing apparatus. The grips for the attachment specimen testing were constructed from Waspalloy, which is the disk material that will be used for actual engine testing. Figure 5-12 shows a pinned root attachment specimen test in progress. The attachment testing is being conducted at loads representing full CF load conditions, cyclic temperature and CF load conditions, and room and elevated temperature failure loads. The behavior of various compliant layer configurations for the dovetail blade attachment specimens at these conditions is also being evaluated. Prior to each test, the specimens are inspected dimensionally and visually at 40X magnification. Following each test the specimens are carefully examined both visually and microscopically to determine the failure origin and mechanism for failure.

Table 5-12 summarizes the results of attachment testing for the dovetail root design to-date. At room temperature the dovetail specimens failed at stresses 3-4 times the design stress. Figure 5-13 shows a failed dovetail attachment specimen with its failure origin depicted in Figure 5-14. A thin (0.13 mm/0.005 in.) nickel compliant layer material was used for room temperature testing in order to simulate the behavior of the actual compliant layer material (nickel based alloy) at the elevated blade root temperature in actual service. The nickel compliant layer provided any deformations during loading which would identify uneven loading of the specimen during testing. The nickel based alloy is used for testing at 760°C (1400°F) which is the approximate steady state temperature of the blade root in service. Testing to date has shown that the selected compliant layer material has performed well under the blade root conditions.

A single test was performed at the steady state blade root temperature (Table 5-12). The failure load in this test was markedly lower than in the room temperature test, but was over 2 times the design stress at actual engine operating conditions. Some sticking of the blade attachment specimen and compliant layer material in the metallic grip was observed in the test. This was partly due to opening of the dovetail grip (0.16 mm or~0.006 in.) at the high load and elevated temperature. Evidence of contact stress damage was seen in the failed specimen and compliant layer material. Mechanical spreading of the metallic grip should not occur in actual service since adjoining blades in the disk will counteract the opening of the dovetail attachment in the disk. However, the dimensions will still open or "spread" due to the high thermal expansion of the metal compared to the low expansion of the ceramic. Also the loads in the disk during actual service will be much lower. Analysis of this test is continuing. Modification of the compliant layer is currently being examined to eliminate any sticking, to provide more compliance at initial engine start-up, and to provide improved damping of the ceramic blade.

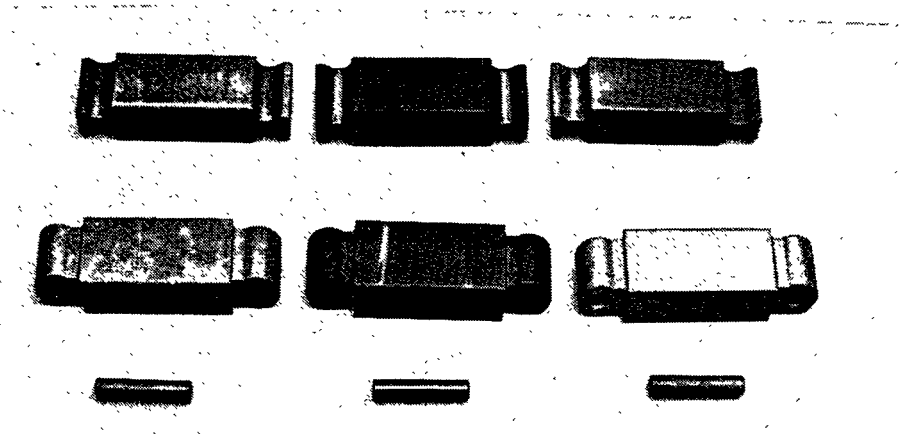

Figure 5-11. Blade Attachment Specimens for Tensile Testing

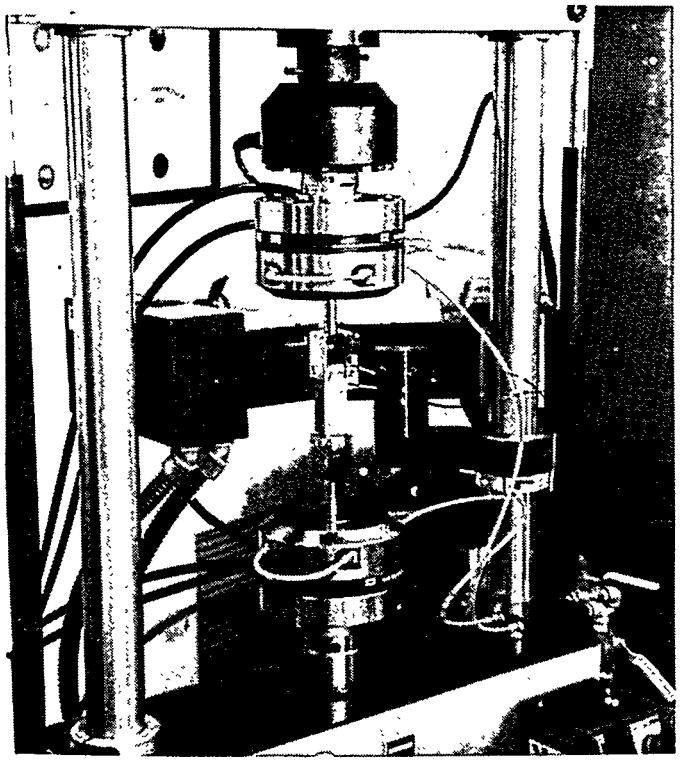

Figure 5-12. Pinned Root Attachment Test in Progress

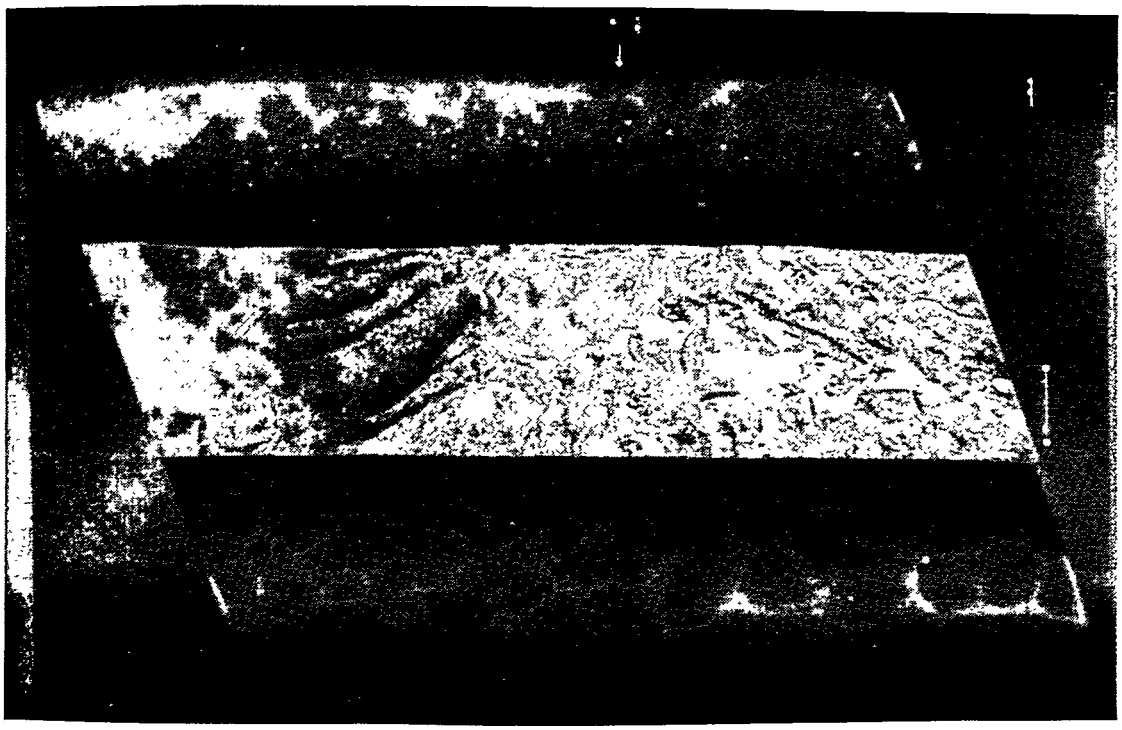

Figure 5-13. Fracture Surface for GN-10 Dovetail Attachment Specimen Failure

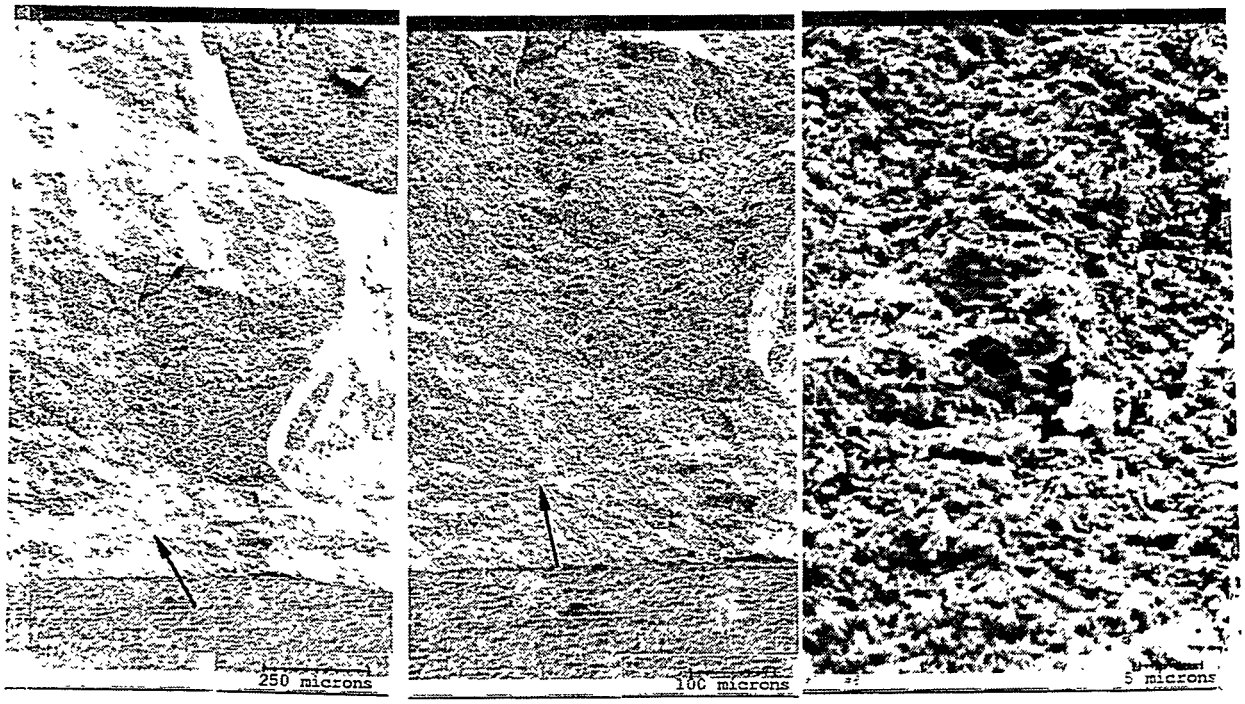

Figure 5-14. Failure Origin of GN-10 Dovetail Attachment Specimen at Three Magnifications

Table 5-12. Results of Dovetail Root Attachment Testing

Material	Test Temperature	Failure Stress	Comments
GN-10 Si_3N_4	Room Temperature	No Failure	Test performed in duplicate stopped at 100% design load (221 Mpa, 32 ksi).
GN-10 Si_3N_4	Room Temperature	924 MPa (134 ksi)	Failure in dovetail neck section
NT164 Si_3N_4	Room Temperature	855 MPa (124 ksi)	Failure in dovetail neck section
SN-253 Si_3N_4	Room Temperature	745 MPa (108 ksi)	Failure in dovetail neck section
SN-253 Si_3N_4	760°C (1400°F)	579 MPa (84 ksi)	Failure in dovetail neck section

The results for the pinned root attachment specimen testing are given in Table 5-13. The pinned root attachment specimens failed at stresses between 540 and 620 MPa (78 and 90 ksi), close to the steady state stress level predicted for the design of this pinned blade design. To evaluate the effect of surface finish, various combinations of attachment specimens and pins with different surface finishes (between 0.20 and 0.81 microns or 8 and 32 microinch.) were evaluated. Pins with a surface finish of .81 microns (32 microinches) exhibited failure in the pin as is shown in Figure 5-15. Through microscopic evaluation the failure was determined to have occurred at a radial machining mark (see Figure 5-16). The pins with a surface finish of 0.2 microns (8 microinches) exhibited failure in the attachment specimen as is shown in Figure 5-17.

Table 5-13. Results of Pinned Blade Attachment Testing

Attachment Specimen Material	Pin Material	Test Temperature	Failure Stress	Comments
GN-10 Si_3N_4	GN-10 Si_3N_4	Room Temperature	550 MPa (80 ksi)	Pin failure, internally initiated
GN-10 Si_3N_4	SN-253 Si_3N_4	Room Temperature	587 MPa (85 ksi)	Fracture in attachment
NT164 Si_3N_4	NT164 Si_3N_4	Room Temperature	540 MPa (78 ksi)	Pin failure in radial machining groove
SN-253 Si_3N_4	SN-253 Si_3N_4	Room Temperature	620 MPa (90 ksi)	Fracture in attachment
SN-253 Si_3N_4	SN-253 Si_3N_4	Room Temperature	540 MPa (78 ksi)	Fracture in attachment

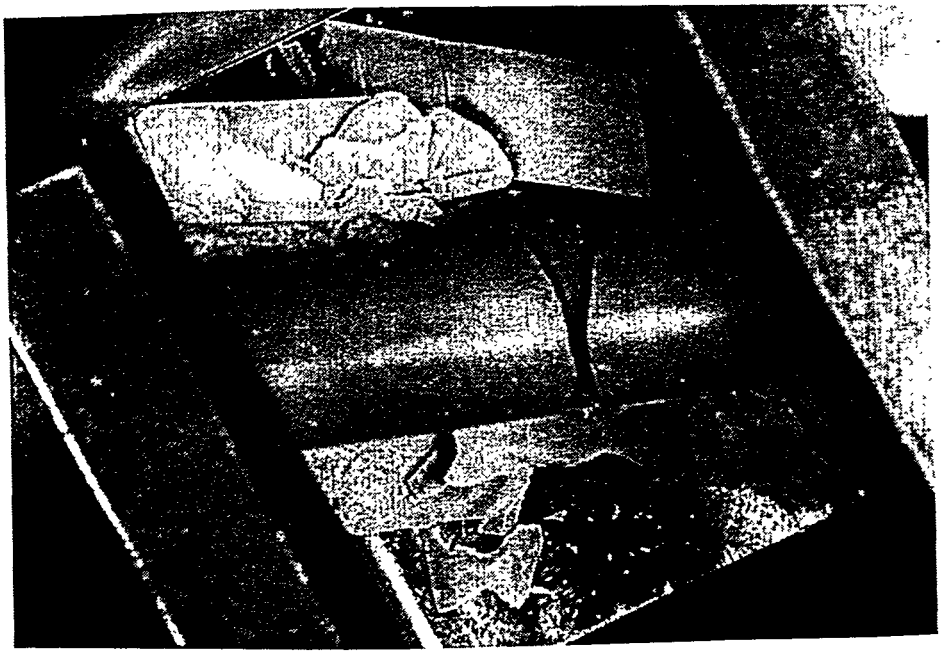

Figure 5-15. Pinned Root Attachment Failure in Pin

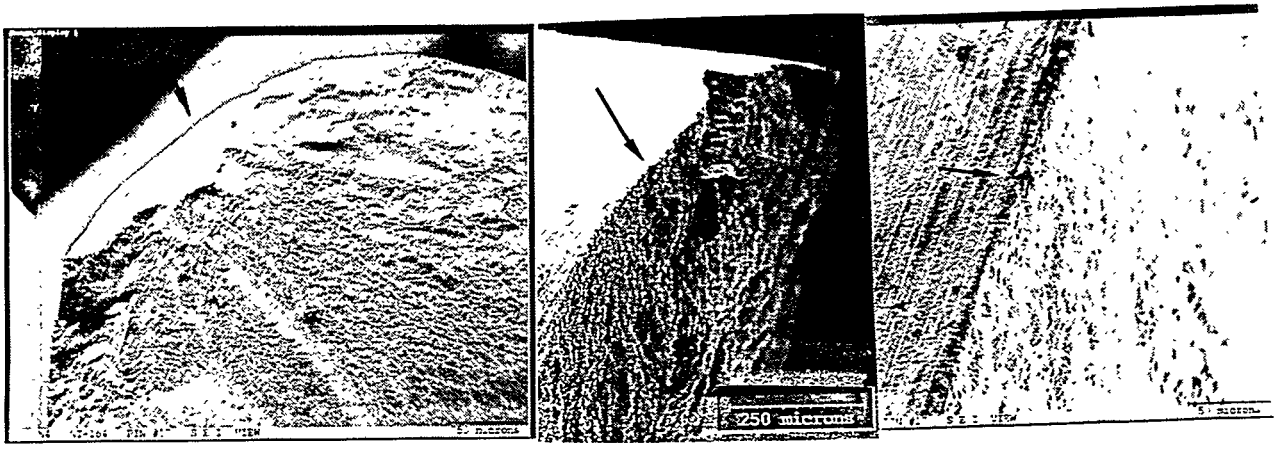

Figure 5-16. Failure Origin of Pin in Machining Groove

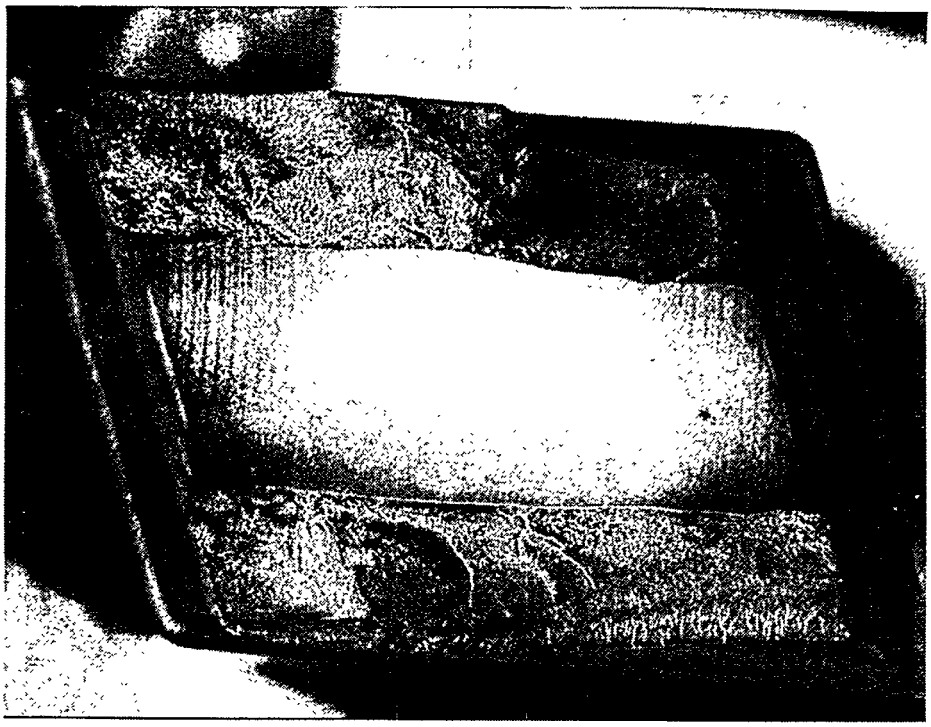

Figure 5-17. Failure of Pinned Root Attachment Specimen

Figure 5-18 microscopically shows the failure origin of an attachment specimen. Although the surface finish of the pin impacted the failure location and mechanism, the surface finish did not appear to have a significant effect on the failure load of the specimens. A comparison of the dovetail and pinned root attachment specimen testing at room temperature from each of the three suppliers is shown graphically in Figure 5-19. The room temperature failure stress of the dovetail root attachment specimens was considerably higher than that of the pinned root attachment specimens.

The pinned root blade design has been modified to reduce design stress levels to ~255 MPa (37 ksi) from the original levels of 586 MPa (85 ksi). It is expected that the design change will provide a margin of safety by a factor of about 2. Attachment specimens of the modified pinned root blade design have been fabricated of SN-253 (KICC) and will be tested under conditions similar to those for the dovetail design. KICC was selected to fabricate these specimens, since they were selected to fabricate the actual pinned ceramic blades. These specimens are currently undergoing dimensional and 40X visual inspection prior to testing.

Cold spin testing will be conducted on simulated or dummy mass blades machined from attachment specimens (Figure 5-20). Spin testing to rotational speeds that simulate engine CF blade loads on the simulated blades will be conducted at ambient conditions. Because elevated temperature data can be obtained from attachment testing under conditions approximating the blade root in service, hot spin testing in not considered at this point in the program. Cold spin testing will also be performed on first and second generation blades as a proof test. The blades will be tested at speeds resulting in stresses corresponding to 120% of the design stress. Blades that pass the proof test will be used in the engine rig test.

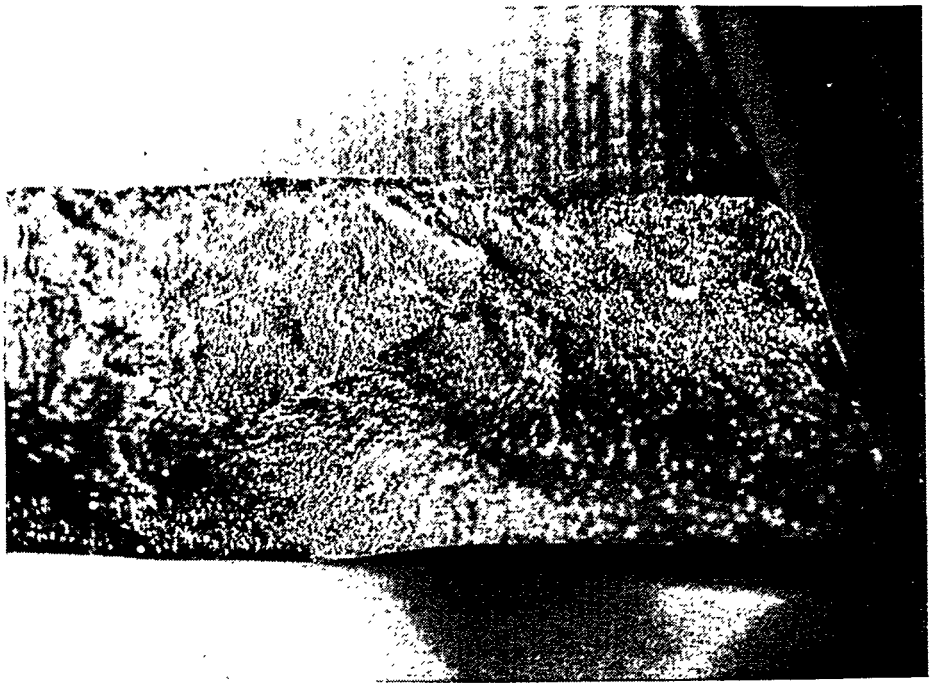

Figure 5-18. Failure Origin of Pinned Root Attachment Specimen

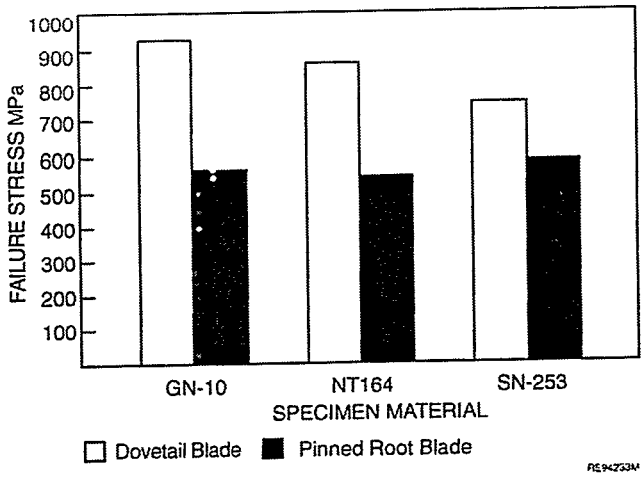

Figure 5-19. Comparison of Dovetail and Pinned Attachment Specimen Test Results

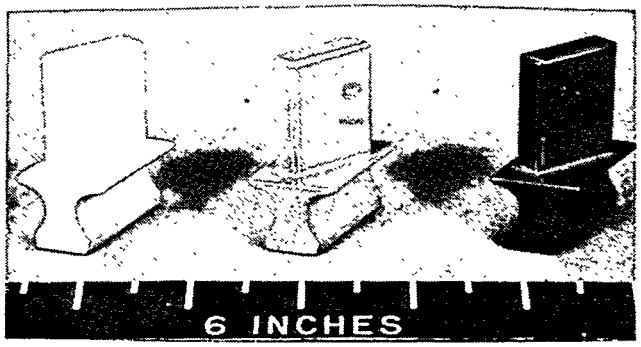

Figure 5-20. Simulated Blade Spin Specimen

5.7 COMPONENT FABRICATION

Slip cast and bisque machined airfoil GN-10 blades, and pressure slipcast airfoil NT164 blades are presently being manufactured. Both have fully densified machined roots. Production quantity quotes have been received from several suppliers. Quotes received show significant cost savings over single crystal cooled/coated metallic blades. Figures 5-21 and 5-22 show pre-sintered and fully sintered castings of GN-10 and NT164 first generation blades, respectively.

Twin-lug pinned blades are being manufactured with hybrid molded cast airfoils and fully densified machined roots of SN-253 material. They are somewhat more expensive than dovetail blades, but are still cost-competitive with state-of-the-art single crystal metallic blades.

Nozzles are being fabricated from SN-253 and SN-88 silicon nitride materials. Delivery is scheduled for the summer and fall of 1995.

Subscale combustor hardware, including monolithic tiles and rings and CFCC liners were delivered and testing is in progress. Details of the subscale combustor hardware can be found in Section 6.0.

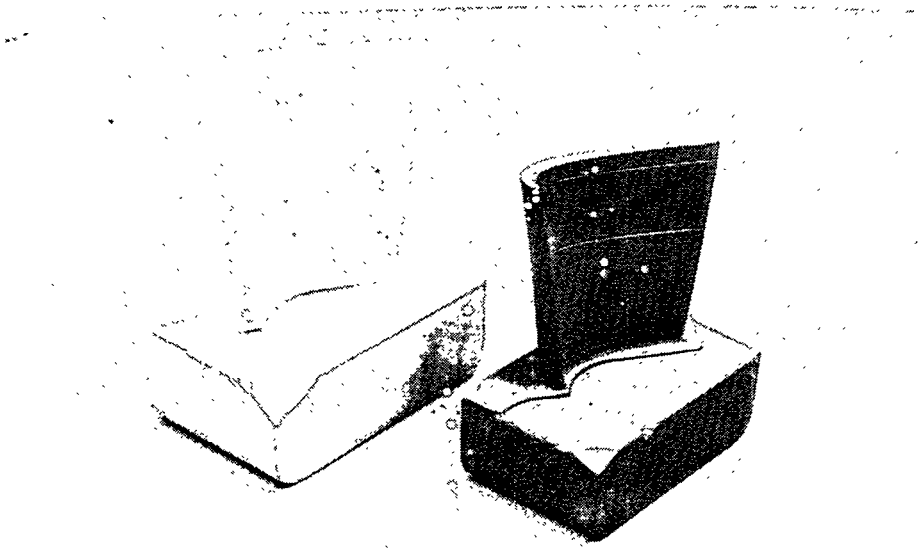

Figure 3-21. GN-10 Pre-sintered (Left) and Fully Dense (Right) Blade Castings

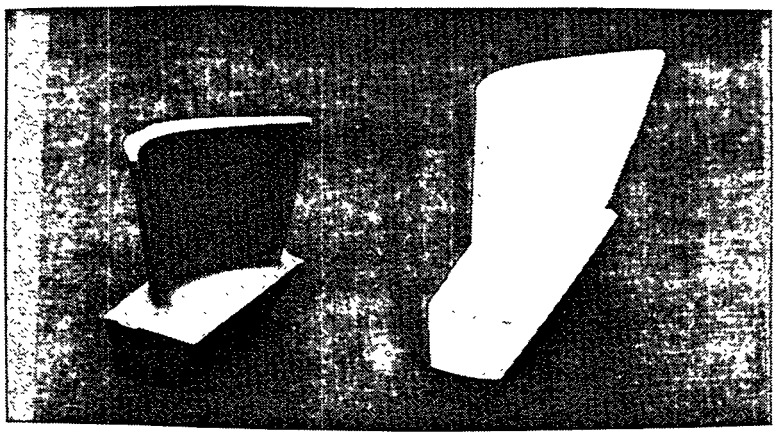

Figure 3-22. NT164 Fully Dense (Left) and Pre-Sintered (Right) Blade Castings

REFERENCES

1. "Application of SPSLIFE to Preliminary Design Evaluation and Life Assessment of CSGT Components", A. Saith, P.F. Norton, and V.M. Parthasarathy. ASME paper 94-GT-420, presented at the International Gas Turbine and Aeroengine Congress and Exposition, The Hague, The Netherlands, June 13-16, 1994.

6.0

TASK 10.0 - LOW EMISSION COMBUSTOR

Described here is the design and fabrication and development of a hot-wall low emission combustor. The goals of the combustor development is is to achieve less than 25 ppmv of NOx in engine testing. As an additional task, a second combustor design of an ultra-low emission combustor is also being developed. The Solar CSGT program has set a target of demonstrating 10 ppmv NOx or better for the combustor to be developed under this task. Three preliminary ceramic combustor designs conceived in Phase I were detailed, monolithic tiles, monolithic rings, and integral CFCC liners. These prototype components are to be evaluated in can (subscale) and annular (full scale) combustor rig testing and in the CSGT engine rig.

Combustion activities for the CSGT fall into two broad areas:

- Demonstration of a ceramic gas turbine combustor using Solar's Centaur 50S (Solar Centaur 50 engine with SoLoNOx combustor) gas turbine as the development engine. This represents the major combustor-related program activity. The SoLoNOx combustor configuration is annular, similar to the metallic SoLoNOx combustor.

- An investigation into the role that ceramics can play in reducing gas turbine combustor NOx emissions to ultra-low levels (10 ppmv or less). These levels may not be achieved with an annular configuration. Therefore, the development for ultra-low emission levels will also consider can type combustors. The eventual combustor configuration will be either an off-line can type or an annular configuration.

6.1 Annlar Centaur 50S Combustion System

The Centaur 50S is one element of Solar's new SoLoNOx line of low emissions gas turbines. SoLoNOx emissions are currently guaranteed at 42 ppmv NOx and 50 ppmv CO on natural gas. NOx guarantees at 25 ppmv will be offered starting in 1995. Operating parameters of the Centaur 50S relevant to the combustion system are shown in Table 6-1.

The goal of the combustion system development work is to incorporate ceramics into the Centaur 50S to enhance component durability and reduce emissions. Durability gains are expected through the higher temperature capabilities of ceramics relative to metals. Emissions benefits are expected in the area of reduced CO emissions since ceramic combustors can tolerate higher wall temperatures than metal combustors. The higher wall temperatures will reduce flame quenching along the wall which can be a significant source of CO in lean premixed flames.

Table 6-1. Combustion Parameters for Centaur 50S*

Parameter	Value
Combustor Air Flow	15.7 kg/s (34.5 lb/s)
Compressor Discharge Temperature	318°C (605°F)
Pressure Ratio	9.4
Turbine Rotor Inlet Temperature	1010°C (1850°F)

* Under nominal Centaur 50S full load operating conditions

To date, the full scale ceramic combustor development effort has involved work in three areas:

- The design of a full scale annular combustor for the Centaur 50S that utilizes ceramics for the highest temperature regions of the combustor liner. Designs for both composite and monolithic ceramic materials are being developed. As a retrofit combustion system, the ceramic combustor NOx and CO emissions goals are 25 and 50 ppmv, respectively. While the 25 pmmv NOx goal is to be achieved to meet the statement-of-work objectives Solar has set a stretch goal of 10 ppmv for the CSGT engine.

- The design and fabrication of subscale cylindrical ceramic combustors. Rig testing of these subscale combustors will allow materials evaluations, assessments of various ceramic component configurations (rings, tiles and cylinders), and the evaluation of metal/ceramic interface geometries. The subscale testing will support the development of the full scale Centaur 50S annular combustor.

- Finite element modelling of the full scale and subscale ceramic combustors to ensure that material temperature and stress limits are not exceeded. In addition, the stress calculations are being used to define subscale test conditions to ensure that the subscale and full scale ceramic combustor components are subjected to similar stress levels.

6.2 Ultra-Low Emissions Combustor

The goal of the annular combustion development work is to document and exploit the NOx reduction benefits associated with ceramic gas turbine combustors in a can type off-line configuration. Specifically, the work is focussed on reducing NOx emissions from 25 ppmv to 10 ppmv or less through the use of ceramics.

A key characteristic of lean premixed combustion is that as flame temperature and, consequently, NOx emissions are lowered, CO emissions tend to increase. As a result, NOx reductions are limited by the formation of unacceptably high CO levels. The role of ceramics in reducing NOx emissions is related to the ability of a hot ceramic wall combustor to limit CO emissions. If CO emissions can be kept low through use of a ceramic liner, then the flame temperature can be lowered to levels consistent with ultra-low NOx emissions.

As a first activity in this task, three different subscale, lean-premixed combustors will be evaluated in a rig environment to assess the relationship between combustor liner cooling and CO formation. Subscale rig testing will be conducted at Centaur 50S conditions using a ceramic combustor liner, an advanced effusion-cooled metal liner, and a conventional film-cooled metal liner. Comparisons of the CO emissions from these burners will allow an assessment of the emissions benefits associated with advanced cooling methods and ceramics. A key element common to all the testing will be the use of a prototype, premixing fuel injector that achieves an extremely high level of fuel/air premixing.

Beyond this initial testing, the application of ceramics to the Centaur 50S to achieve ultra-low NOx levels will be addressed.

6.3 Annular Scale Combustor Development

6.3.1 Full Scale Combustor

The production Centaur 50S combustor design has been modified to incorporate three different configurations using ceramic components. In all three cases, ceramics are limited to the hottest

areas of the liner which are the inner and outer cylindrical segments of the annular combustor configuration (Figure 6-1). The upstream dome and downstream inner and outer conical sections remain metallic, although modified to accommodate the ceramic components.

Figure 6-2 is a cross-section of the first combustor configuration which employs one-piece CFCC inner and outer cylinders contained between the metallic dome and downstream combustor cones. The assembly is held together by bolting the metallic dome to the inner and outer convectors which are integral with the downstream cones. Compliance in the axial direction is provided using metallic bellows at the aft ends of the ceramic cylinders.

The CFCC combustor configuration illustrates a design feature common to all three ceramic combustor designs. A "rolling element" interface system is used at both ends of the cylindrical sections to mate with the metallic dome and cones.

Fig. 6-3 is a cross-section of the attachment region for the outer CFCC cylinder and the combustor dome structure of the combustor. The ceramic cylinder is covered with a layer of insulation that reduces the liner radial temperature gradient and the corresponding thermal stress. Though insulated, the liner will operate below its 1204°C (~2200°F) maximum temperature limit.

The liner and insulation are contained within a metallic "girdle" structure which applies a radially inward force to retain the CFCC liner in position. The girdle structure is a cylinder that is partially slit in the axial direction at a number of circumferential locations. The slitting reduces the stiffness of the structure and allows the girdle to act as a radial spring. The compliance of the girdle allows it to remain in contact with the insulation and the ceramic cylinder despite different thermal expansion characteristics.

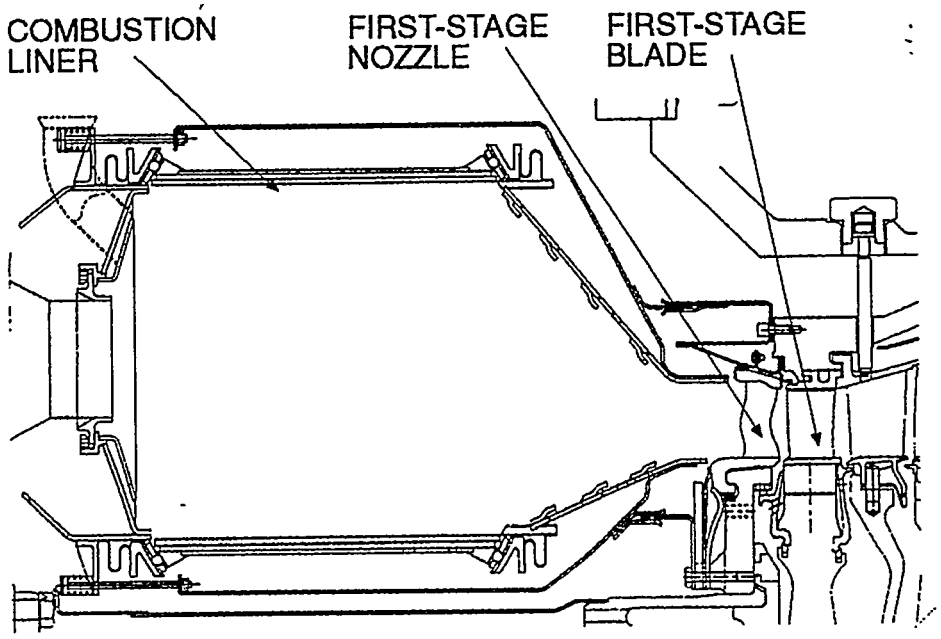

Figure 6-1. Cross Section of Centaur 50S Annular Combustor Liner

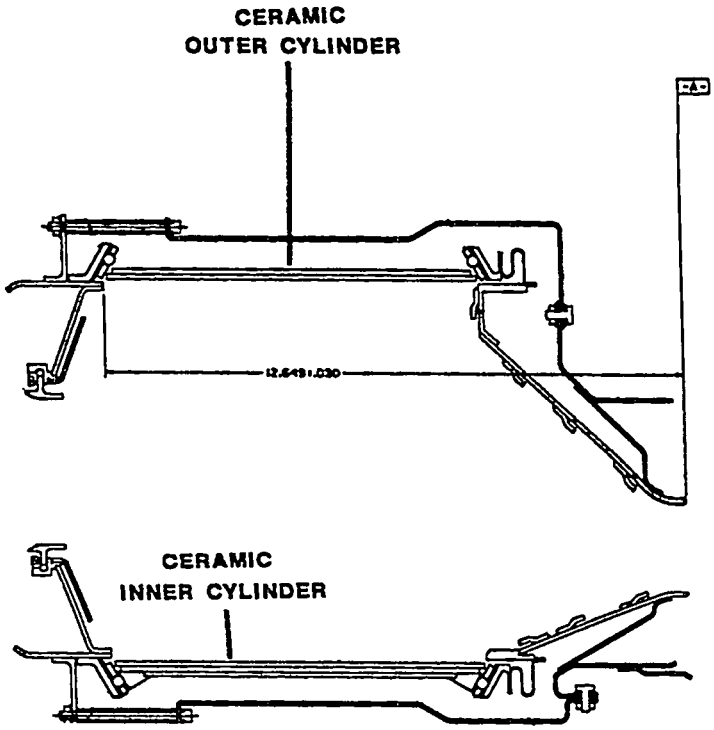

Figure 6-2. Cross Section of Annular Combustor Employing CFCC Cylinders

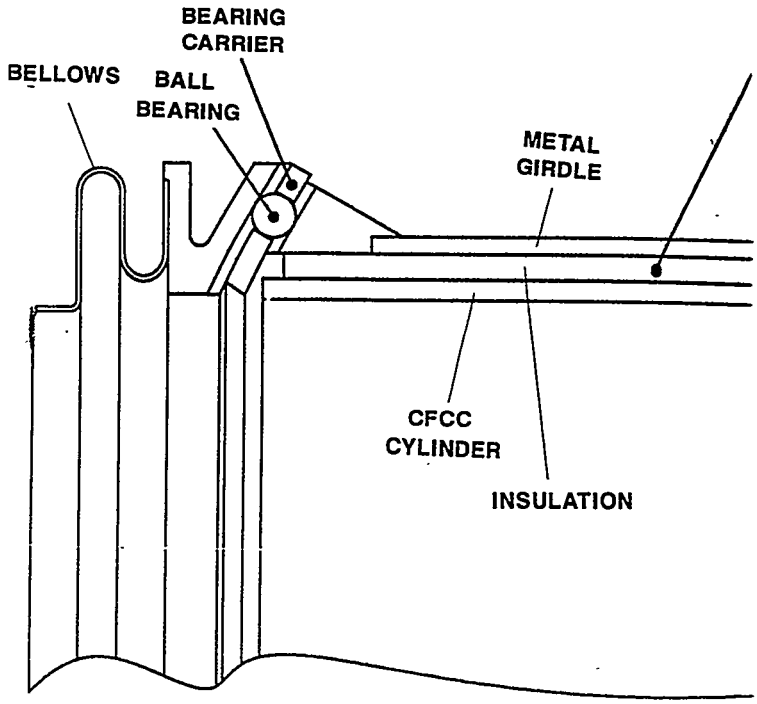

Figure 6-3. Cross Section of the Attachment Region for the Outer CFCC Liner

For the CFCC combustor, the axial compressive force used to hold the combustor assembly together is transmitted through the girdle structure.

Each end of the girdle has a conical flange with slots machined into the flange. Opposing flanges are positioned on the dome and cone sections of the combustor. Ball bearings are positioned in the machined slots and are retained by a conical "carrier" between the flanges. The ball bearings maintain a gap of a few mils between the flanges and allow thermal expansion differences between parts to be accommodated through a rolling contact.

The compressive force holding the combustor assembly together reacts through the inclined faces of the girdle flanges to push the girdle against the insulation and CFCC liner. The compliant nature of the girdle keeps the girdle, insulation and CFCC liner in contact at all times.

The bellows structure in the assembly is used to accommodate axial expansion, distribute loading circumferentially and dampen mechanical vibrations.

The second and third combustor designs use monolithic combustor components rather than CFCC materials. In these designs, the combustor cylinder is segmented into either "rings" or "tiles" to reduce thermal stresses. Figures 6-4 and 6-5 show subscale monolithic ring and tile designs, respectively. In the ring design, a series of four 5.0 cm (~2-inch) long rings comprise the cylindrical sections of the combustor. The rings have a shiplap edge design for piloting of adjacent ring elements. The end rings are configured to accept the ball bearings for the rolling element interface. Unlike the CFCC design, the compressive load used for combustor assembly is transmitted through the ceramic components.

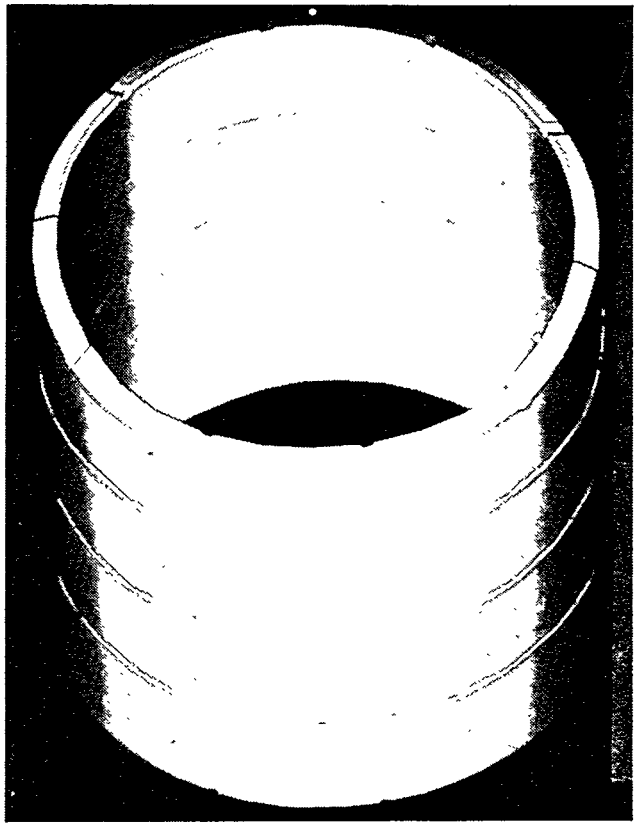

Figure 6-4. Subscale Monolithic Ring Design for the Combustor Liner

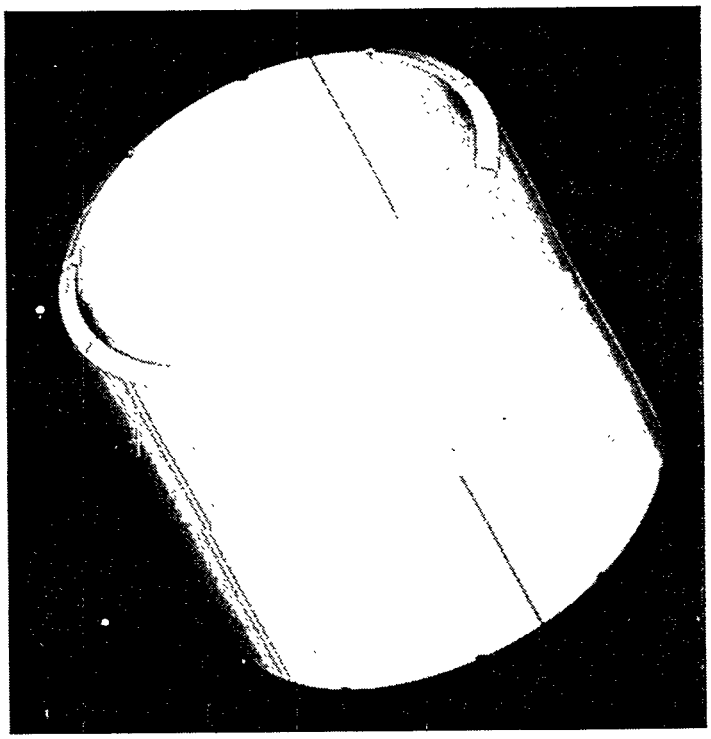

Figure 6-5. Subscale Monolithic Tile Design for the Combustor Liner

The ring design also incorporates a girdle and insulation layer, although the girdle design lacks the flanges of the CFCC girdle. The balance of the attachment hardware is similar to that of the CFCC design.

A third combustor concept is similar to the ring approach although the ceramic rings are replaced by ceramic tiles or staves. In concept, the tiles are formed by slicing the combustor cylinders axially into a number of uniform components. Each tile segment extends over the entire length of the combustor cylindrical section as shown in Figure 6-1. Twenty four tiles are used to form the outer liner. The tiles are interlocked along their edges with their neighboring tiles. Interlock geometries involving shiplap and beveled edge geometries will be assessed experimentally. Assessments of the tile design have indicated that the tile configuration is inappropriate for the inner combustor cylinder since the combustor pressure drop will tend to disengage the tiles. At the present time, tiles are only being considered as an option for the outer liner with rings being used for the inner cylinder. A ring design is also considered as an alternate design for the outer liner provided life assessment data is favorable.

6.3.1.1 Stress Analyses and Life Assessment

CFCC Liners - Stress analyses of the full scale designs are in progress to quantify thermally-induced stresses in the ceramic parts. The models used reflect the non-uniform (non-axisymmetric) wall temperature distribution resulting from the use of multiple fuel injectors in the annular combustor. The individual injectors create intermittent hot spots on the liner wall.

Figure 6-6 shows a finite element analysis (FEA) temperature map for the CFCC designs. FEA stress maps for the SiC/SiC and Al_2O_3/Al_2O_3 CFCC's are shown in Figures 6-7 and 6-8, respectively.

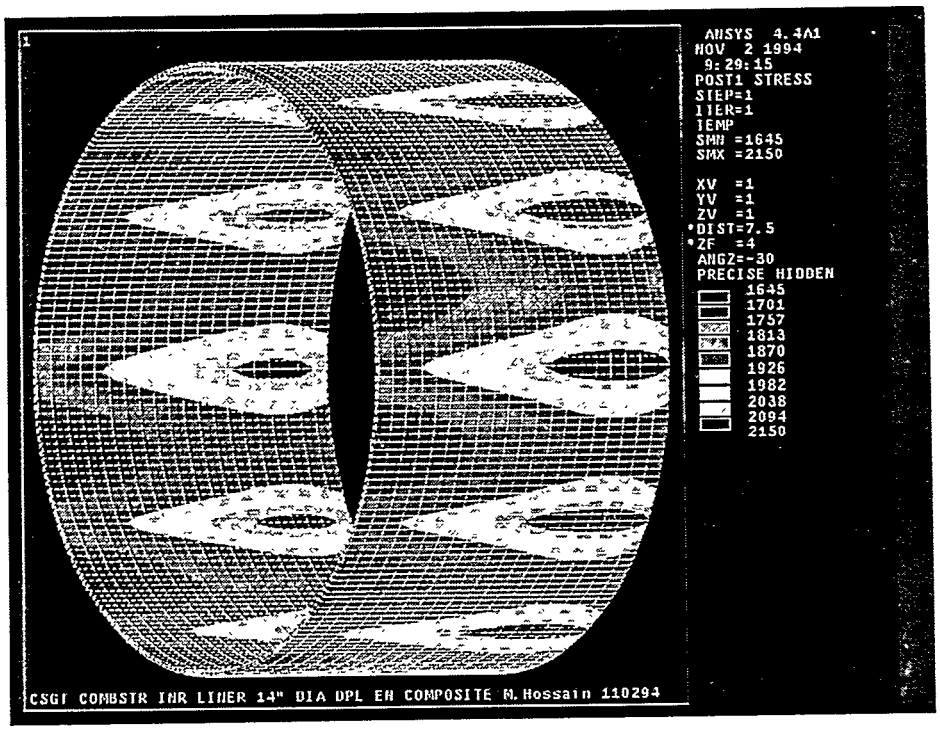

Figure 6-6. FEA Temperature Map for CFCC Inner Combustor Liner

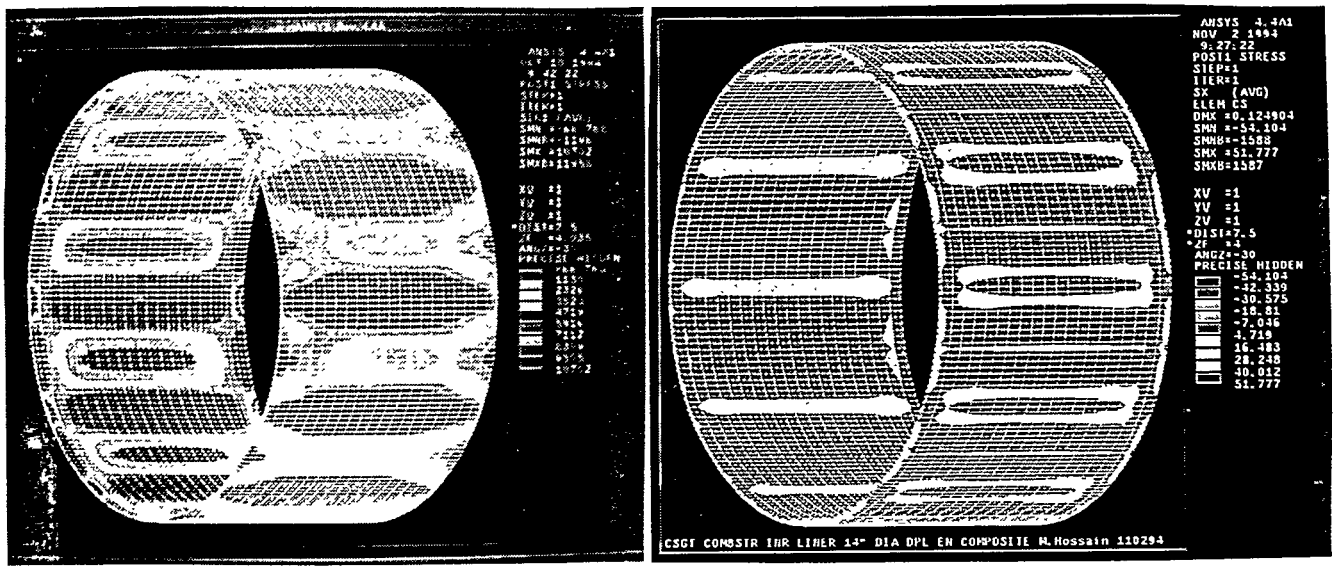

(A) Maximum Principal Stress Map **(B) Through-the-Thickness Stress Map**

Figure 6-7. FEA Stress Map for SiC/SiC CFCC Inner Combustor Liner

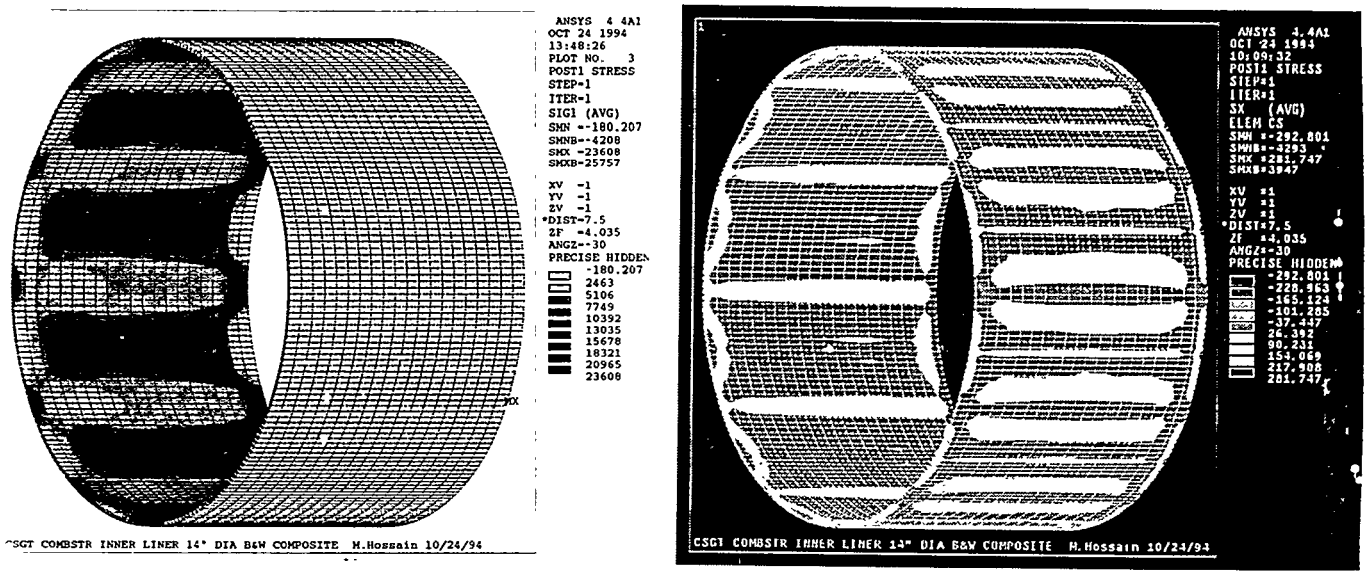

(A) Maximum Principal Stress Map **(B) Through-the-Thickness Stress Map**

Figure 6-8. FEA Stress Map for Al_2O_3/Al_2O_3 CFCC Inner Combustor Liner

For the SiC/SiC CFCC liners, maximum principal stresses (MPS) on the order of 78 MPa (11 ksi) are predicted. This MPS is near the limit defined by CFCC manufacturers at which first microcracking can begin. For liners the MPS is about 163 MPa (~24 ksi). No failure limit is known for this oxide/oxide CFCC material.

Monolithic Tiles - The results of the stress/temperature analyses performed to-date on monolithic ceramics have been summarized in Table 6-2. The analyses were conducted on Phase I designs at operating temperatures as high as 1365°C (2490°F).

Table 6-2. Stress Analysis Summary for Inner Monolithic Combustor Liners

Component	Material	Temperature Range °C (°F)	Surface Stress MPa (ksi)	Internal Stress MPa (ksi)
Integral Inner Liner	Hexoloy® SA	1010°C-1365°C (1850°F-2490°F)	198 (29)	197 (29)
Integral Inner Liner	Hexoloy® SA	927°C-1204°C (1700°F-2200°F)	182 (26)	182 (26)
Axial Tile	Hexoloy® SA	1010°C-1365°C (1850°F-2490°F)	189 (27)	191 (28)
4-Ring Inner Liner	Hexoloy® SA	1010°C-1365°C (1850°F-2490°F)	75 (11)	78 (11)

Life assessment studies for various monolithic combustor designs have been conducted by Sundstrand Power Systems (SPS) under subcontract to the CSGT program using the SPSLIFE computer program (2). The procedure for life assessment with SPSLIFE has been explained elsewhere (1,3).

Figure 6-9 shows FEA temperature and stress maps for a ceramic axial combustor tile operating at temperature conditions outlined in Table 6-2. An MPS value of 191 MPa (~28 ksi) was established using Hexoloy® SA as tile material.

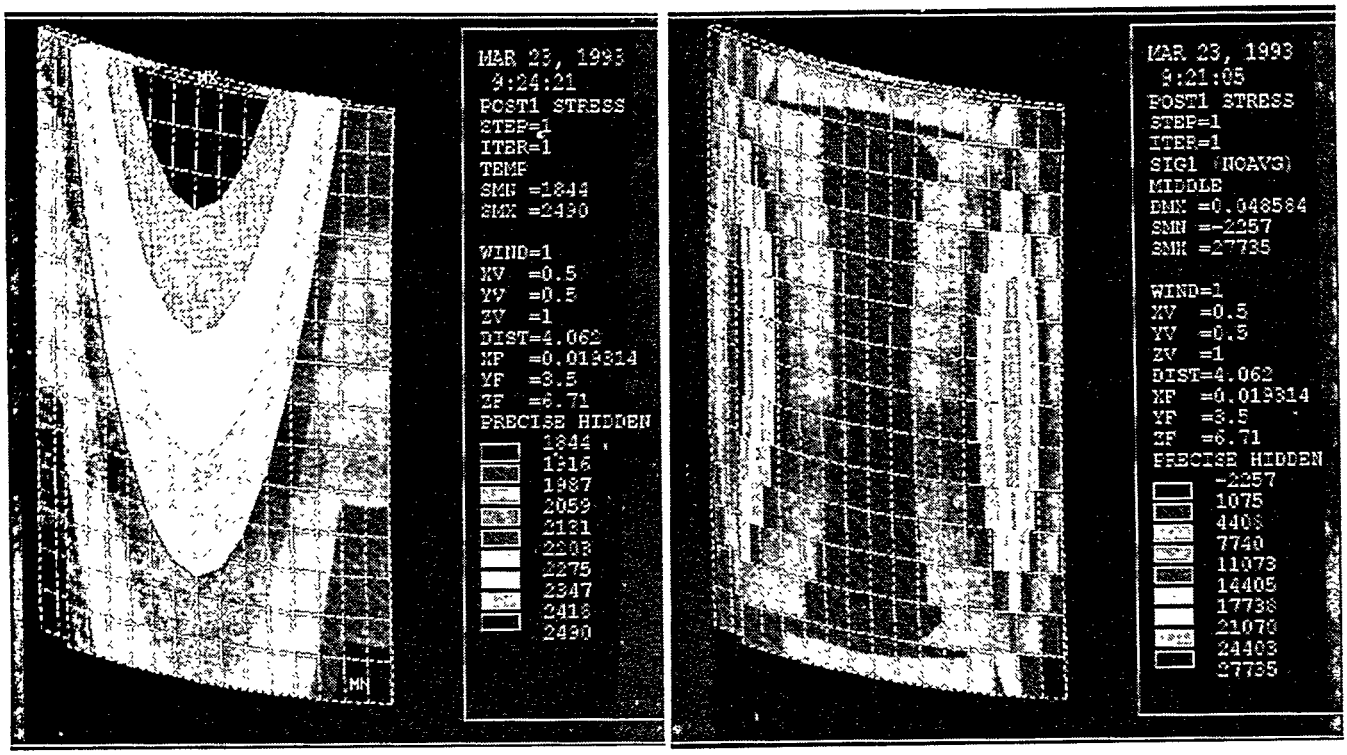

(A) Temperature Map **(B) Stress Map**

Figure 6-9. FEA Maps of a Hexoloy® SA Combustor Tile

The design assessment map for this scenario is shown in Figure 6-10. The map is plotted for a design life of 30,000 hrs. The two large surfaces of the tile were assumed to be in the as-fired condition; the four sides and mating surfaces were assumed to be in the machined condition. The component is safe in the creep mode with creep life in excess of 1.8 M hrs being assessed. An oxidation analysis could not be performed because of lack of data. The solid lines show that the tile has a fast fracture probability of survival (POS) of approximately 99% as predicted by SPSLIFE. NASA CARES/LIFE gives a fast fracture POS for each tile of 99.13%. The dashed lines show approximately 96% POS in slow crack growth predicted by SPSLIFE. CARES/LIFE analysis predicts a POS for each tile of 97.59%. This data indicate that slow crack growth is the life limiting failure mode for the axial tiles.

Since the size of the outer and inner tiles is approximately the same the POS can be expected to be similar as well assuming a similar temperature and stress distribution. The combined POS for an entire inner liner made up of 10 axial tiles is estimated at 78.4% ($0.9759^{10} = 0.784$) and for the outer liner made up of 24 individual outer liner tile 55.6% ($0.9759^{24} = 0.556$). The data suggests that the POS values are unsatisfactory for a 30,000 hr service life at maximum wall temperatures of 1365°C (2490°F).

Monolithic Rings - Figure 6-11 shows a stress map for a 4-ring inner combustor liner of Hexoloy® SA. The MPS is 75 MPa (~11 ksi) for the rings, The temperature distribution (see Table 6-2) is assumed to be similar to that of the axial tiles extrapolated over a 10 tile inner liner segment. The two large surfaces of the liner ring were assumed to be in the as-fired condition while the two ends

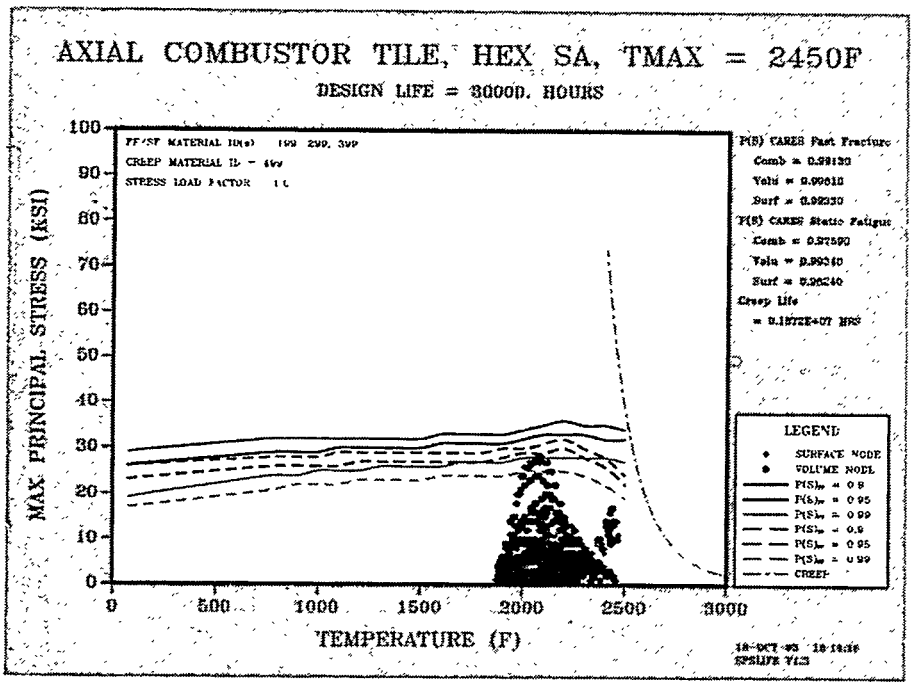

Figure 13

Design Assessment Map for Axial Combustor Tile, Hexoloy SA, Tmax = 2450F (Scenario 9)

Figure 6-10. Life Assessment Map for a Hexoloy® SA Combustor Tile

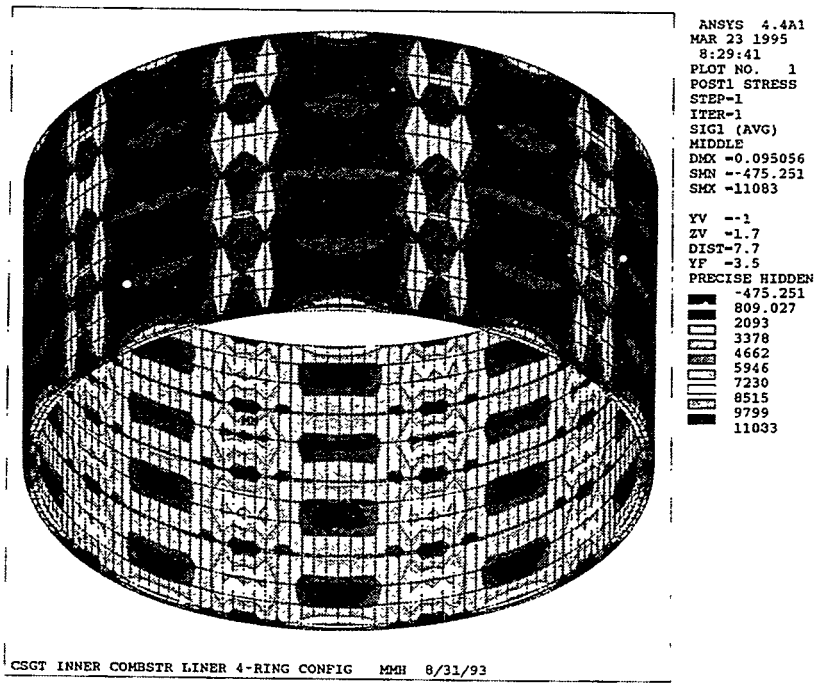

Figure 6-11. FEA Stress Map of a Hexoloy® SA Combustor Ring Assembly

were assumed to be in the machined condition. Figure 6-12 shows the SPSLIFE design assessment map based on a 30,000 hour service life. Creep life was assessed to be 11.2 M hours. Oxidation life was not assessed. The component is safe in fast fracture with POS predicted at 100%. The CARES/LIFE module in SPSLIFE predicted a slow crack growth life of 100% as well. The monolithic ring design for the inner liner rings is thus very attractive based on life assessment data. Stress analysis and life assessment for the outer liner has not been performed as of yet. Since the outer liner rings will be larger life assessment for the inner liner rings will present the most favorable scenario. Most likely, POS will be less favorable for the outer liner rings.

Monolithic Integral Combustor Liner - Although POS values are expected to be less than for monolithic rings and tiles stress analysis and life assessment was also conducted for an integral inner combustor liner of Hexoloy®SA. The FEA temperature profile is similar to that for the tile and monolithic ring scenarios (see Table 6-2). The FEA stress map is shown in Figure 6-13. MPS values are about 198 MPa (29 ksi). The SPSLIFE design assessment map is shown in Figure 6-14. Service life is assumed to be 30,000 hrs. Creep life is adequate at 315,000 hrs. Oxidation life was not assessed. Fast fracture POS predicted by the NASA CARES module of SPSLIFE is inadequate at 46.85% and slow crack growth life from NASA CARES/LIFE data is unacceptable at 7.19%.

Since the stress state is largely determined by the temperature gradient on the part the effect of lowering the maximum liner wall temperature to 1204°C (2200°F) was evaluated for the integral liner design. POS values increased to 60.69% in fast fracture and to 15.36% in slow crack growth for 30,000 hrs of operating life. These values are still inadequate for an integral liner design of Hexoloy® SA.

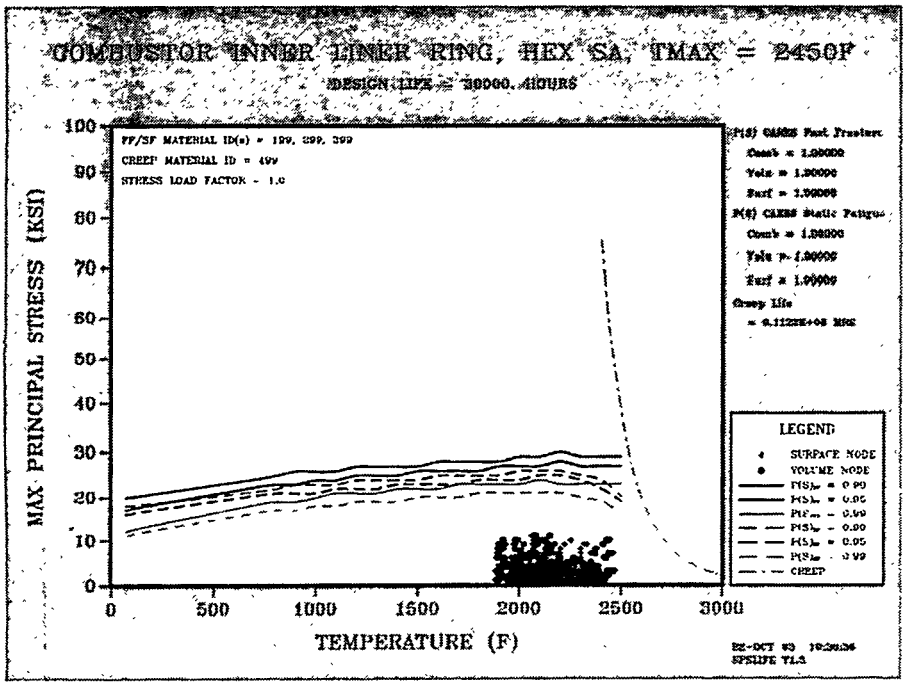

Figure 16
Design Assessment Map for Combustor Inner Liner Ring, Hexoloy SA, Tmax = 2450F (Scenario 11.

Figure 6-12. Life Assessment Map for a Hexoloy® SA Combustor Ring

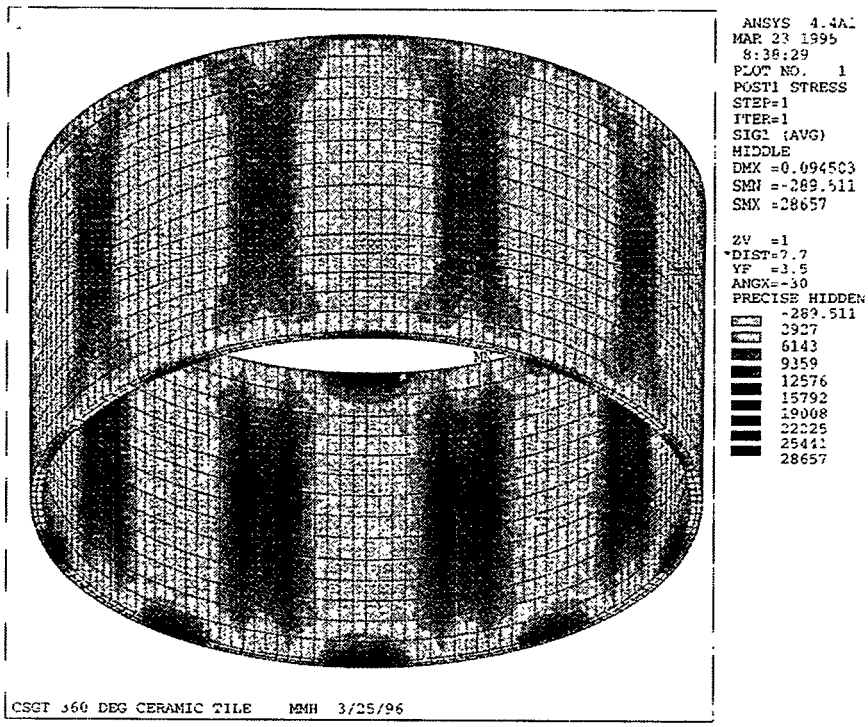

Figure 6-13. FEA Stress Map of a Hexoloy® SA Integral Combustor Liner

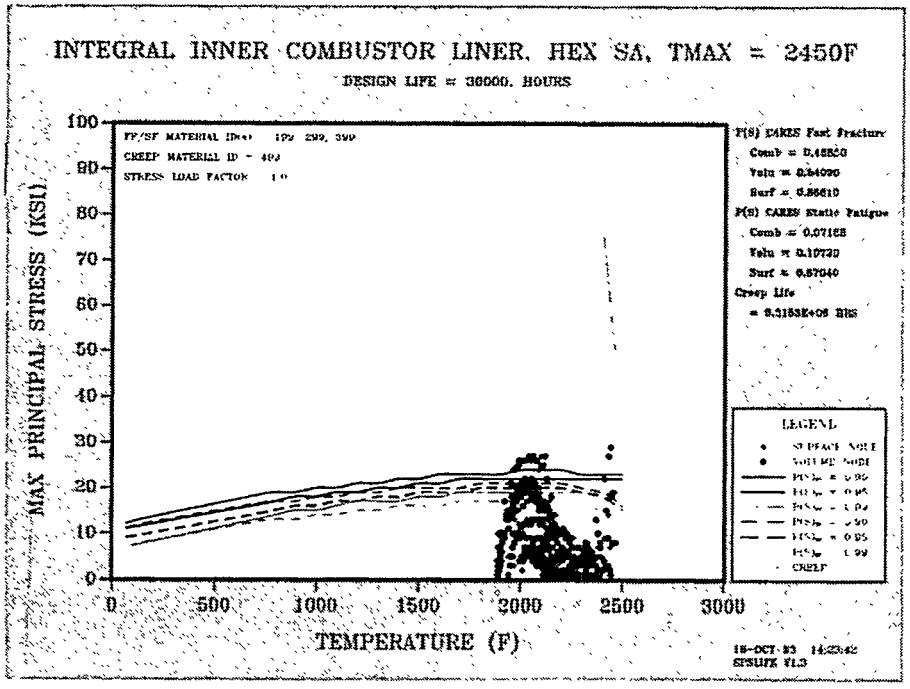

Figure 15

Design Assessment Map for Integral Inner Combustor Liner, Hexoloy SA, Tmax = 2450F (Scenario 10)

Figure 6-14. Life Assessment Map for a Hexoloy® SA Integral Combustor Liner

Combustor Life Assessment Summary - A review of the life assessment data for the various combustor liner configurations indicate that only the combustor ring design provides adequate life at the design wall temperature of 1365°C (2490°F). Both an integral line design and a tile design were felt to be inadequate on the basis of overall POS values for an entire combustor liner. A decision was made at that point to lower the maximum liner temperature for all designs to 1204°C (2200°F). No effect on the POS for the ring design is anticipated since the POS values were already at maximum. The tile design was not evaluated at the lower liner wall temperature either. POS values are expected to improve, but it is questionable whether acceptable predicted service life will be acceptable. Future life assessment studies will include life assessment for the monolithic ring and tile designs using different materials. The ultimate decisions in the design, materials, and supplier selection for the components to be used for the field test will largely depend on the life assessment data.

6.3.2 Subscale Combustor Designs and Testing

Subscale ceramic combustor testing is being carried out to support the development of the full scale annular combustor for the Centaur 50S. Key aspects of the subscale work will be:

- An early assessment of the ceramic/metal interface configurations adopted for the full scale combustor
- An assessment of the durability of various CFCC materials in the form of 20 cm (~8 inch) diameter cylinders at typical gas turbine combustor operating conditions
- An evaluation of 20 cm (~8 inch) ceramic cylinders formed from monolithic ceramic rings and tiles at combustor operating conditions. One-piece monolithic cylinders are not being evaluated because of projected high thermal stresses and low POS for a one-piece cylinder.

All the subscale hardware will be tested in an existing combustion rig using a production SoLoNOx fuel injector. The subscale can combustor rig is shown in Figure 6-15. Figure 6-16 shows the rig layout with the can combustor in position. The ceramic-to-metal attachment concepts are representative of the full scale hardware designs described above. Of greatest interest will be the performance of the girdle and rolling element interface aspects of the full scale design. Experience gained with the subscale systems will be reflected in the full scale design.

Preliminary stress results from finite element models of the SiC/SiC CFCC subscale configuration show ceramic stress levels near 14 MPa (2 ksi). To increase material stresses to levels expected in the full scale ceramic parts 75 MPa (11 ksi), variations in insulation thickness or selective cooling of the subscale liner will be employed.

All of the subscale work will be carried out in an existing combustor test rig . Test conditions for the subscale testing are:

- Inlet pressure: 620 kPa (90 psig)
- Inlet temperature: 321°C (610° F)
- Air flow rate: 0.57 kg/s (1.25 lb/s)

Materials and configurations to be evaluated are presented below:

Configuration	Material
Composite cylinder	DLC SiC/SiC CFCC
	B&W Al_2O_3/Al_2O_3 CFCC
	BFG SiC/SiC CFCC
Rings	NAC NT230
Tiles (2 geometries)	Carborundum Hexoloy® SA

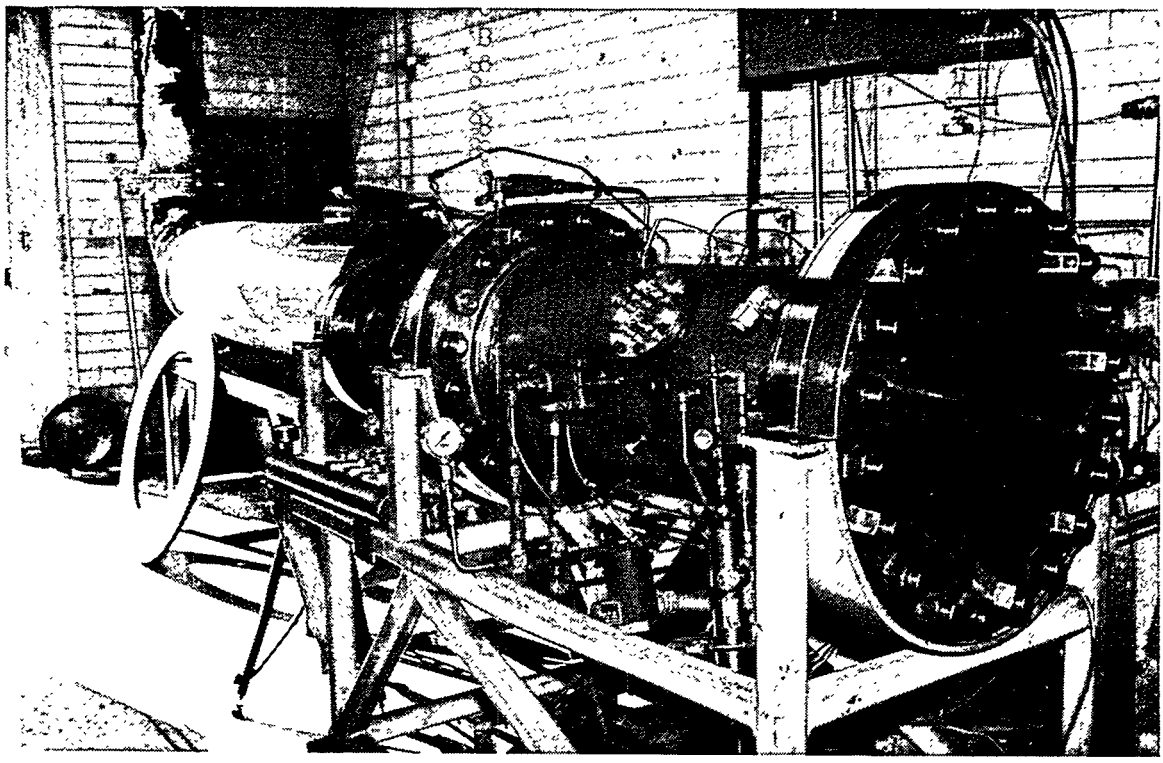

Figure 6-15. Subscale Can Combustor Rig

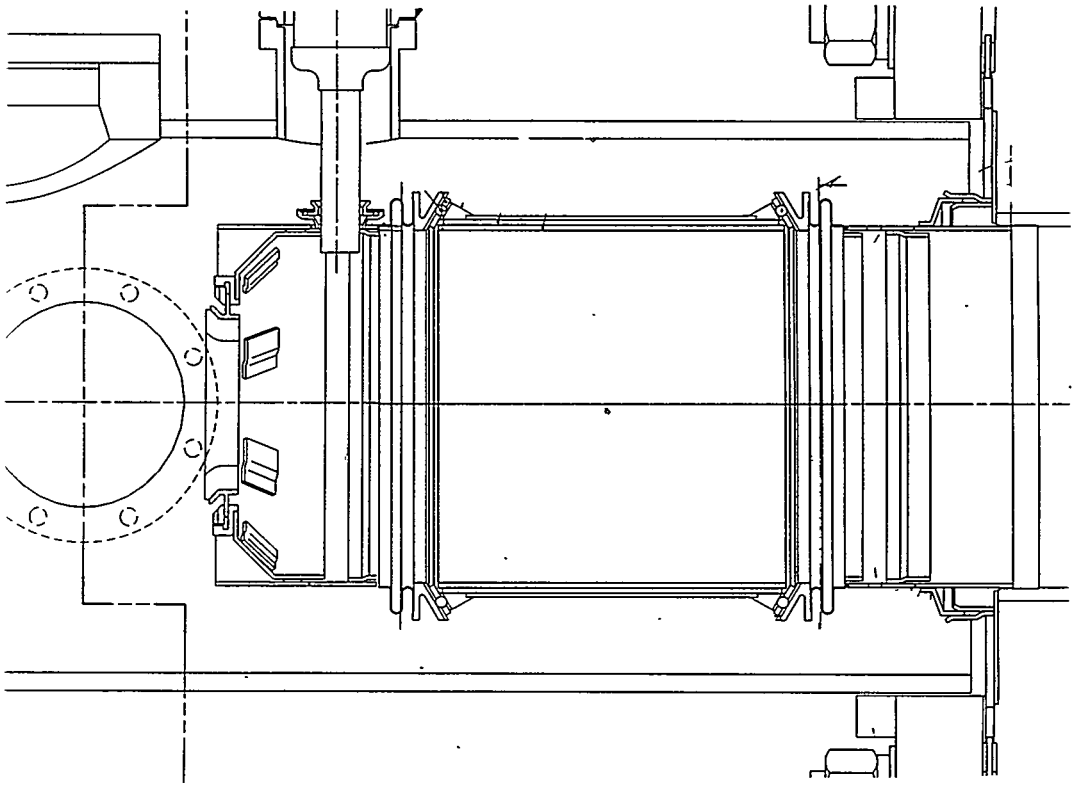

Figure 6-16. Subscale Can Combustor Layout with Can in Position

Figure 6-17 shows subscale combustor hardware fabricated by the suppliers. The can configurations are approximately 20 cm (8 inch) long x 20 cm (8 inch) diameter. Wall thicknesses vary from 3.2 mm (0.12 inch) for CFCC materials to about 9.5 mm (0.38 inch) for the monolithics.

Testing of each material and configuration will involve a series of tests of increasingly longer duration. All the candidates will be subjected to 1 and 10 hour tests. Selected candidates will be further tested for periods of approximately 100 hours. If appropriate, 1000 hours tests may be conducted to support the final down-selection of candidates for the full scale combustor design.

During the longer tests, material durability will be assessed by allowing the wall temperatures to cycle between specified maximum and minimum levels. Natural gas flows will be varied cyclically every two minutes to simulate gas turbine load variations. The temperature gradients set up in the combustor materials will provide a meaningful test of material durability.

Combustor wall temperatures will be monitored with a series of 15 thermocouples attached to the outside surface of the liners. The type K, 1.0 mm (0.040 inch), thermocouples will be located in three axial rows (0, 120 and 240 degrees) with five thermocouples per row (1 inch axial spacing). The maximum subscale ceramic wall temperature limit has been set at 1204°C (2200°F) for the monolithic liners and at 1177°C (2150°F) for the CFCC liners which matches the full scale limit. A fuel shut-off will activate if local wall temperature exceeds these limits. The wall temperature data will be used to verify boundary conditions used for material stress computations.

Before and after each test run the combustor liners will be inspected both visually and by NDE (at Argonne National Laboratory).

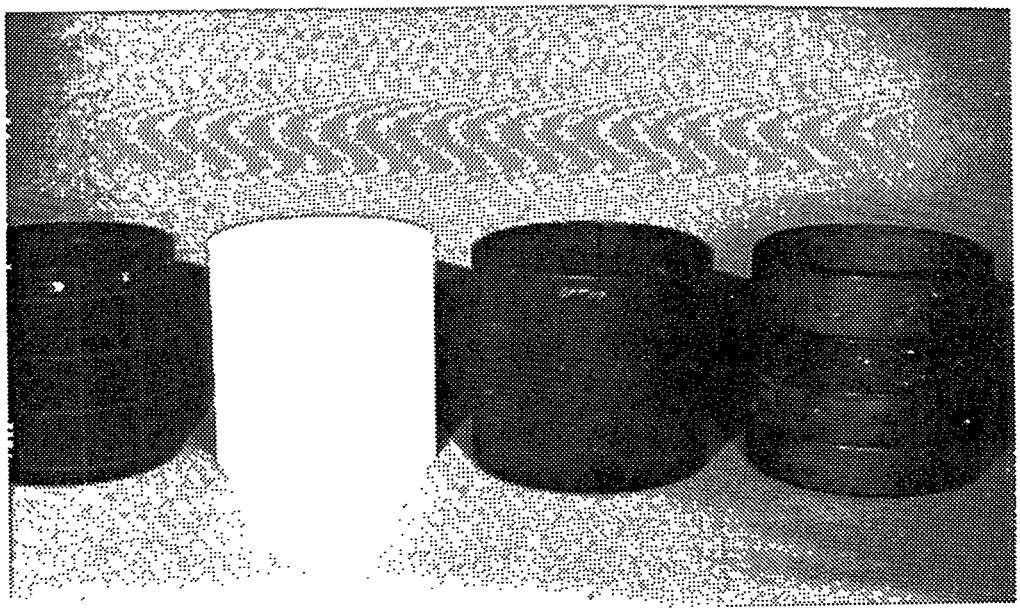

Figure 6-17. Subscale Combustor Hardware. From left to right: DLC SiC/SiC CFCC liner, B&W Alumina/Alumina CFCC Liner, Carborundum Hexoloy® SA tiles, NAC NT230 rings

Solar has evaluated a number of CFCC and monolithic materials in subscale testing under an in-house R&D program. Can geometries were 40 cm (16 inch) long x 20 cm (8 inch) diameter. Tests have been run typically for 1-2 hrs at design wall temperatures of about 1204°C (2200°F). Most of these cans survived the test but occasional delaminations in CFCC liners have been observed. One Nicalon/SiC CFCC can was tested and survived for 100 hours in a cyclic test (1500 cycles) between 704°C and 1204°C (1300°F and 2200°F). A Al_2O_3/Al_2O_3 CFCC subscale liner supplied to Solar by B&W was tested early in Phase II of CSGT program for 2 hours at a maximum wall temperature of 1038°C (1900°F). This can survived the test. Post-testing NDE evaluation by ANL showed some delamination in this can which had a filament wound fiber preform structure. Since delamination was found to be a persistent problem with the filament wound Al_2O_3/Al_2O_3 CFCC a processing change was recommended to B&W. The change involves replacing the filament wound preform with a woven 3-D preform and subsequent subscale liners supplied under the CSGT program, an example of which has been shown in Figure 6-17, were fabricated with the new structure.

More recently, preliminary subscale testing has been completed as part of the test rig and combustor assembly commissioning activities. This initial testing was conducted using a production Centaur 50 SoLoNOx fuel injector and a CFCC cylindrical combustor procured as part of an inhouse study of ceramic combustors.

The primary focus of the test was to check out all facility systems prior to testing with CSGT materials. In addition, preliminary combustor performance in terms of emissions, ceramic liner temperatures and ceramic/metal interfaces was assessed. Figure 6-18 shows the variation of combustor emissions at fixed air flow but increasing fuel flow. Typical lean premixed emissions characteristics are observed with increasing fuel/air ratio: NOx emissions increase and CO emissions decrease.

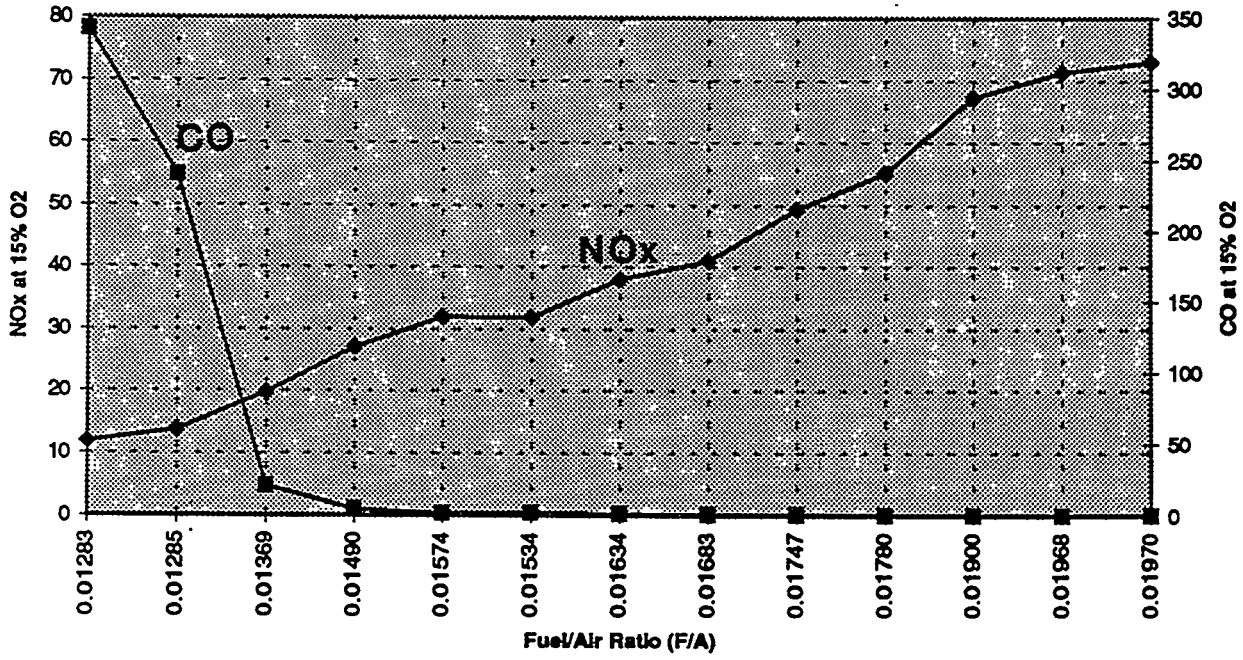

Figure 6-18. Variation of Combustor Emissions

At the nominal Centuar full load design point (f/a = 0.016), emissions on the order of 35 ppm NOx and 2 ppmv CO are observed. The data in Figure 6-18 indicate that a rematching of the air flow split of the combustor could reduce NOx emissions to below 20 ppmv with CO remaining below 50 ppmv. These emissions levels are within the Centaur 50S emissions limits. The emissions data also show a NOx potential down to the 10 ppmv level, although with high CO. Ultra-low emissions testing will be focussing on the achievement of these NOx levels in conjunction with low CO through the minimization and control of combustor liner cooling air.

Figure 6-19 presents ceramic liner wall temperature data from the checkout test. Presented are maximum, minimum, and average temepratures from 15 thermcouples mounted on the liner outer maximum wall temperature is well within the temperature capability of the CFCC materials being assessed in this program.

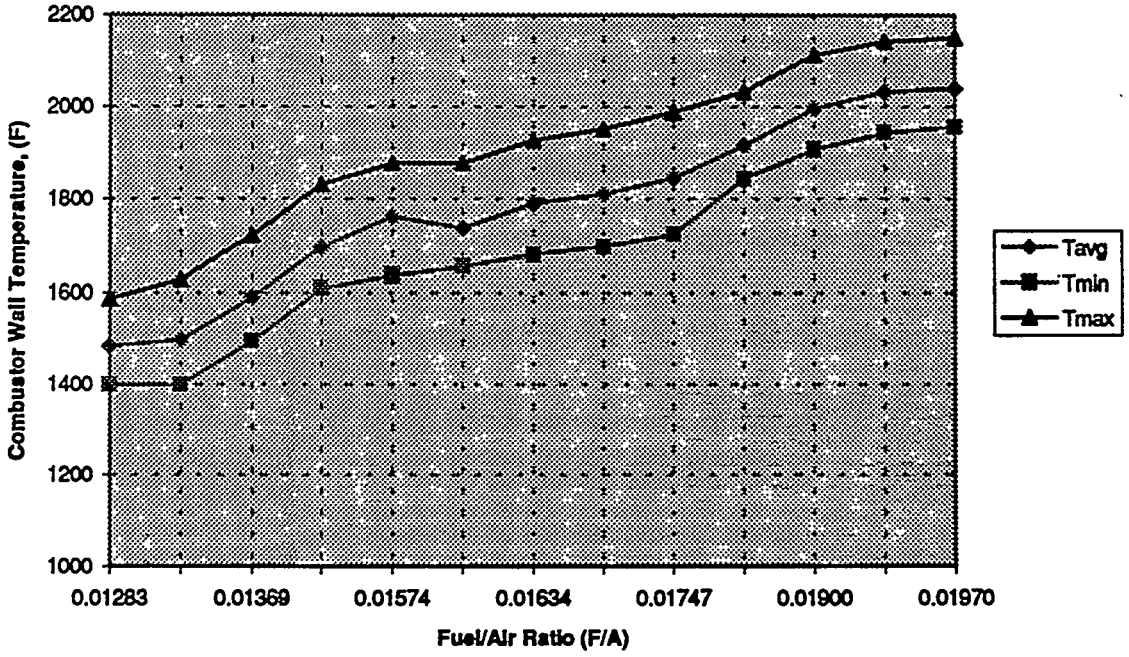

Figure 6-19. Ceramic Liner Wall Temperature Data

6.4 Ultra-Low Emissions Combustor Design

The near-term goal of this task is to document the emissions advantages of a can type ceramic gas turbine combustor liner. The potential application is for an off-line can type or can-annular combustor configuration. As mentioned above, the key characteristic of a ceramic combustor liner in terms of emissions will be its ability to operate at higher temperatures than a conventional metal liner. This will result in lower CO formation in the vicinity of the combustor wall which, in turn, will allow reductions in the combustor flame temperature. The ultimate result will be lower NOx emissions.

The rig testing to be conducted under this task will extend the subscale testing carried out in support of the full scale combustor development. Testing will be carried out at Centaur 50S conditions using 20 cm (8 inch) diameter cylindrical combustors, similar to those for the subscale testing for the annular combustor development.

In the initial evaluation both lean-premixed and rich-lean systems were considered but the latter was not selected for initial evaluation because it was considered that:

- Silicon-based ceramics may degrade under the reducing conditions of a rich-lean environment.

- Single can combustor designs are simpler than two-chamber rich-lean designs. Based on Solar's experience with the fabrication of simple combustor tiles and rings it was felt that significant fabrication difficulties could slow down the delivery of test combustors of the rich-lean type seriously impeding the progress of the work scheduled.

Because of Solar's extensive experience with the lean-premix system and the good test results with the cylindrical subscale liners it was decided to concentrate on the lean-premix system at this time and revisit the rich-lean system if the lean-premix strategy proved unpromising. Liners fabricated for the subscale testing for the annular combustor design can be used for the ultra-low emissions combustor testing. If promising the subscale can design can be scaled up to a full scale off-line can or can-annular combustor configuration.

Three different lean-premixed systems will be evaluated:

- A CFCC cylindrical liner (Figure 6-20)

- An effusion-cooled metal liner (Figure 6-21)

- A louvered, film-cooled metal liner (Figure 6-22)

The CFCC combustor is unique in that only backside convective cooling of the liner is employed to maintain acceptable ceramic liner temperature of 1177°C (2150°F). Unlike the two metal combustors, air injection through the combustor liner is not employed. Thus, flame quenching and CO formation will be minimized. The metal, effusion-cooled liner uses air injection to maintain liner temperatures below about 816°C (1500°F). However, the use of a multitude of small holes in the liner results in the use of much less cooling air than with a louvered liner. The louvered liner is representative of conventional film-cooling techniques employed for industrial gas turbines and uses the most air to maintain acceptable metal temperatures.

Each of the three combustors will be evaluated using a standard SoLoNOx injector and a prototype ultra-low NOx injector. The ultra-low NOx injector is designed to provide enhanced fuel/air premixing and has been shown in earlier, Solar-funded rig tests to provide reduced NOx emissions.

In the CFCC liner testing the test hardware is constrained between a metallic dome on the upstream end and a metallic "dilution zone" at the aft end. The liner is convectively cooled on its outside surface by dilution air flowing around the combustor. The test configuration was adopted for ease of testing and does not address the durability requirements that must be met by production gas turbine combustor components.

To reduce air flow requirements, minimal dilution air is employed in the design. Issues relating to pattern factor and exit temperature profile are not part of this particular investigation. The design is flexible enough to accommodate the CFCC component as well as consider various means of insulating the ceramic cylinder to maximize wall temperatures. Emphasis will be placed upon testing a one-piece cylindrical CFCC liner (no rings or tiles) to avoid any possibility of air leakage between ceramic combustor components.

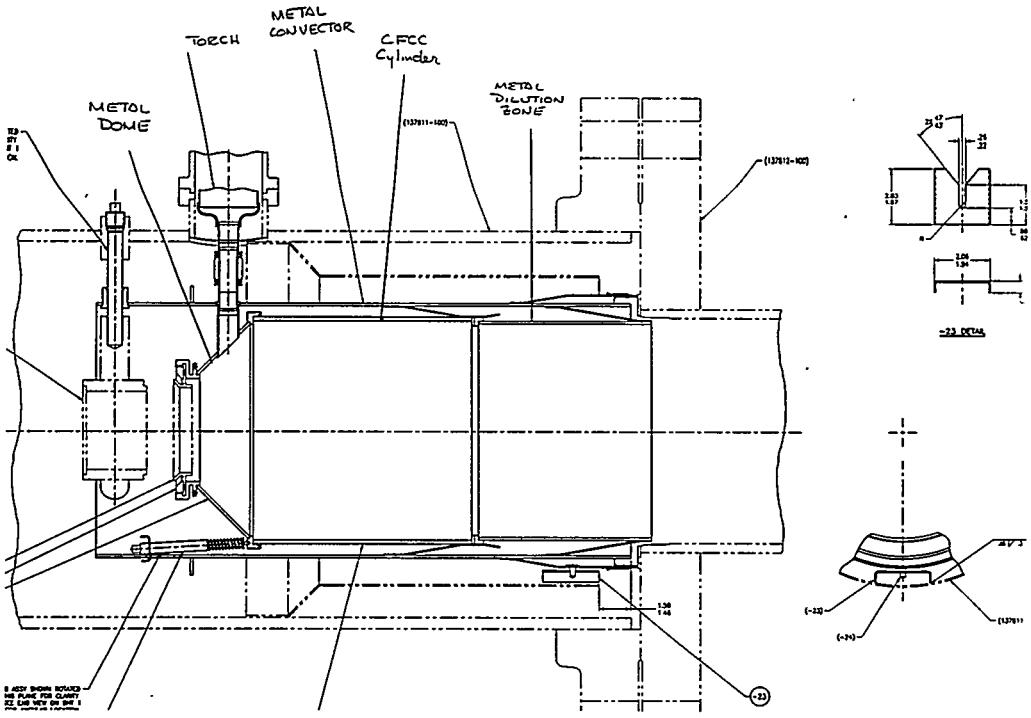

Figure 6-20. CFCC Combustor Liner Configuration

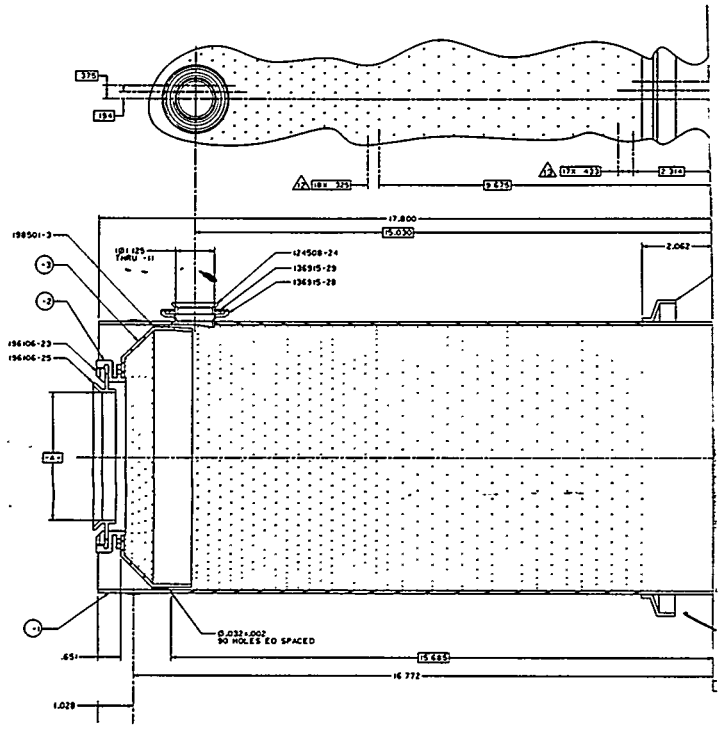

Figure 6-21. Effusion-Cooled Metal Liner Configuration

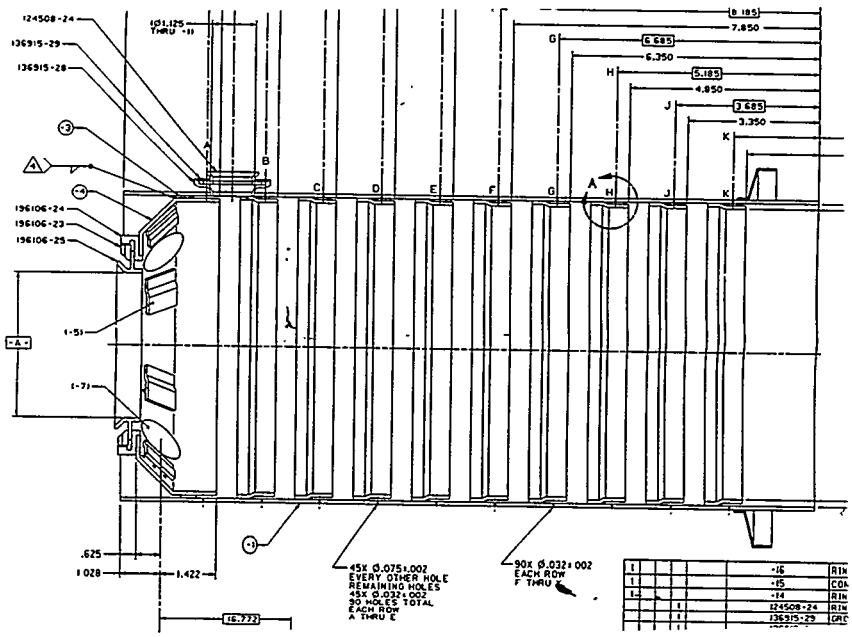

Figure 6-22. Louvered, Film-Cooled Metal Liner Configurations

REFERENCES

1. "Ceramic Stationary Gas Turbine Development Program", 1993, Phase I Final Report, Solar Turbines Incorporated, DOE Contract Number DE-AC02-92CE40960. Under review.

2. "Application of SPSLIFE to Preliminary Design Evaluation and Life Assessment of CSGT Components", A. Saith, P.F. Norton, and V.M. Parthasarathy, ASME paper 94-GT-420, presented at the International Gas Turbine and Aeroengine Congress and Exposition, The Hague, The Netherlands, June 13-16, 1994.

3. "SPSLIFE: A User-friendly Approach to the Structural Design and Life Assessment of Ceramic Components", T. Bornemisza, and A. Saith, ASME paper 94-GT-486 presented at the International Gas Turbine and Aeroengine Congress and Exposition, The Hague, The Netherlands, June 13-16, 1994.

4. M. van Roode, W.D. Brentnall, P.F. Norton, and G.L. Boyd, 1994, "Ceramic Stationary Gas Turbine Development - First Annual Summary", ASME paper 94-GT-313, presented at the International Gas Turbine and Aeroengine Congress and Exposition, The Hague, The Netherlands, June 13-16, 1994.

7.0

TASK 16 - PROGRAM MANAGEMENT AND REPORTING

The project management and reporting functions of Solar and its subcontractors on the program are included in this task, as well as contract and subcontract administration. All project travel for reviews, conferences, and meetings at subcontract facilities is also included. The DOE was regularly informed of all program management activities via Task 16 summaries in the monthly status reports, reviews and this Technical Progress Report.

7.1 PROGRAM STATUS

The summary Phase II Timeline bar chart was presented in Section 2 (Figure 2-1). This Technical Progress Report summarizes the work performed under Phase II for the period April 1, 1993, through October 31, 1994. Table 7-1 summarizes the status of the major milestones for the program.

Table 7-1. CSGT Program Milestone Status

Milestone	Status (Completion Date)
First blade designs	Complete
First nozzle design	Complete
First combustor design	12/94
First engine design	5/95
Engine rig procurement	Complete
Second blade design	8/95
Second nozzle design	7/95
Second combustor design	7/95
Final engine design	6/96
Task 7 design review	7/96
Task 7 topical report	9/96
Engine rig installation	5/95
Task 9.1 design review	1/95
Start task 9.2 engine rig tests	6/95
Complete task 9.2 engine rig tests	3/96
UDRI ceramics screening studies	12/94
UDRI creep studies	5/96
Task 9.2 design review	6/96
Task 9.2 topical report	6/96
Task 9 program review	8/96
Start task 9.3 engine rig tests	5/96
Complete task 9.3 engine rig tests	9/96
Task 10 design review	9/96
Task 10 topical report	9/96
Final materials selection	8/96
Phase II technical progress report	12/94
Phase II final report	9/96

7.2 REPORTS, PAPERS, AND PRESENTATIONS

The following listings contains reports, conference presentations, and papers of work performed under the DOE CSGT program by Solar and its CSGT subcontractors. Included in the list are past presentations and papers submitted for presentation during 1995.

1. "Ceramic Stationary Gas Turbine Development Program", 1993, Phase I Final Report, Solar Turbines Incorporated, DOE Contract Number DE-AC02-92CE40960. Under review.

2. "Ceramic Stationary Gas Turbine Development", M. van Roode, W.D. Brentnall, P.F. Norton, and G.P. Pytanowski. ASME paper 93-GT-309, presented at the International Gas Turbine and Aeroengine Congress and Exposition, Cincinnati, Ohio, U.S.A., May 24-27, 1993.

3. "Ceramic Retrofit Program", M. van Roode. Paper presented at the Joint Contractors Meeting, FE/EE Advanced Turbine Systems Conference, FE Fuel Cells and Coal-Fired Heat Engines Conference, U.S. Department of Energy, Office of Fossil Energy, Morgantown Energy Technology Center, Morgantown, West-Virginia, U.S.A., August 3-5, 1993.

4. "Advanced Small Gas Turbines for Cogeneration", D. Anson, W.P. Parks, Jr., O. Evensen, and M. van Roode. Paper presented at the 7th Congress & Exposition Gas Turbines in Cogeneration & Utility, Industrial and Independent Power Generation, Bournemouth, England, U.K., September 21-23, 1993.

5. "Use of Continuous Fiber Reinforced Composites in Combustor Liner Applications", J.F. Simpson, and L.H. Cowell. Paper presented at the SAE Meeting, April, 1994.

6. "Application of SPSLIFE to Preliminary Design Evaluation and Life Assessment of CSGT Components", A. Saith, P.F. Norton, and V.M. Parthasarathy. ASME paper 94-GT-420, presented at the International Gas Turbine and Aeroengine Congress and Exposition, The Hague, The Netherlands, June 13-16, 1994.

7. "Ceramic Stationary Gas Turbine Development Program - First Annual Summary", M. van Roode, W.D. Brentnall, P.F. Norton, and G.L. Boyd. ASME paper 94-GT-313, presented at the International Gas Turbine and Aeroengine Congress and Exposition, The Hague, The Netherlands, June 13-16, 1994.

8. "Nondestructive Evaluation of CFCC Materials for Combustor Applications," J.F. Simpson and W.A. Ellingson. Paper presented at the American Society Pacific Coast Regional Meeting, Anaheim, CA, October 20, 1994.

9. "Ceramic Retrofit Program", M. van Roode. Paper presented at the Advanced Turbine Systems, Annual Review Meeting, Washington, D.C., November 9-11, 1994.

10. "Nondestructive Characterization of CFCC's Used as Combustor Liners in Advanced Gas Turbines", W.A. Ellingson, and J.F. Simpson. Paper presented at the Fall Materials Research Society Meeting, Boston, MA, November 28 - December, 1994.

11. "Automated Laser Scatter Detection of Surface and Subsurface Defects in Si_3N_4 Components and Comparison with Mechanical Properties," J.S. Steckenrider and V.J. Parthasarathy. Paper presented at the 19th Annual Cocoa Beach Conference, Cocoa Beach, FL, January 8-12, 1995.

12. "Ceramic Stationary Gas Turbine Development: Replacement of Metals with Ceramics", Paper presented at the Turbine Technology Seminar, Solar Turbines Incorporated, Coronado, CA, March 6-10, 1995.

13. "Ceramic Stationary Gas Turbine Development Program - Second Annual Summary", M. van Roode, W.D. Brentnall, P.F. Norton, and B.D. Edwards. ASME paper 95-GT-459, presented at the International Gas Turbine and Aeroengine Congress and Exposition, Houston, TX, U.S.A. June 5-8, 1995.

14. "Ceramic Stationary Gas Turbine Development Program - Design and Life Assessment of Ceramic Components", P.F. Norton, G.A. Frey, H. Bagheri, A. Fierstein, C. Twardochleb, O. Jimenez, and A. Saith. ASME paper 95-GT-383, presented at the International Gas Turbine and Aeroengine Congress and Exposition, Houston, TX, U.S.A. June 5-8, 1995.

15. "Material Characterization of Candidate Silicon Based Ceramics for Stationary Gas Turbine Applications", V.M. Parthasarathy, J.R. Price, W.D. Brentnall, G. Graves, and S. Goodrich. ASME paper 95-GT-249, presented at the International Gas Turbine and Aeroengine Congress and Exposition, Houston, TX, U.S.A. June 5-8, 1995.

16. "Nondestructive Evaluation of Ceramic Composites Used as Combustor Liners in Advanced Gas Turbines", W.A. Ellingson, S.A. Rothermel, and J.F. Simpson. ASME paper 95-GT-404, presented at the International Gas Turbine and Aeroengine Congress and Exposition, Houston, TX, U.S.A. June 5-8, 1995.

17. "Non-destructive Evaluation of Monolithic Ceramics Using Impact-Acoustic Vibration Measurements", R.A. Bemis and W.A. Ellingson. ASME paper 95-GT-403, presented at the International Gas Turbine and Aeroengine Congress and Exposition, Houston, TX, U.S.A. June 5-8, 1995.

18. "Injection Molded and Isopressed α-SiC Components for Stationary Gas Turbine Applications", R.W. Ohnsorg, S.K. Lau, M.O. Ten Eyck, and D.A. White. ASME paper 95-GT-75, presented at the International Gas Turbine and Aeroengine Congress and Exposition, Houston, TX, U.S.A. June 5-8, 1995.

19. "NT164 Silicon Nitride Gas-Turbine Engine Blade Manufacturing Development", E. Bright, R. Burleson, S. Dynan, and W.T. Collins. ASME paper 95-GT-74, presented at the International Gas Turbine and Aeroengine congress and Exposition, Houston, Texas, U.S.A. June 5-8, 1995.

20. Improved Silicon Nitride Materials and Component Fabrication Processes for Aerospace and Industrial Gas Turbine Applications", J. Pollinger. ASME paper 95-GT-159, presented at the International Gas Turbine and Aeroengine congress and Exposition, Houston, Texas, U.S.A. June 5-8, 1995.

21. "Oxide-Oxide Continuous Fiber Ceramic Composites for Gas Turbine Applications," R.W. Goettler, D.L. Hindman, C.L. DeBellis, and J.J. Edwards. ASME paper 95-GT-386, presented at the International Gas Turbine and Aeroengine congress and Exposition, Houston, Texas, U.S.A. June 5-8, 1995.

22. "Ceramic Stationary Gas Turbine Development", M. van Roode, D.A. Rohy, S. Waslo, and W.P. Parks, Jr. Paper to be presented at the International Gas Turbine Congress, Yokohama, Japan, October 23-26, 1995.

7.3 PROGRAM TRAVEL

CSGT team members traveled to conferences and review meetings to present program results. The presentations have been included in the summary in Section 7.2. In addition CSGT staff made two major trips. In early November 1993 a visit was made to Japan to attend the IEA Natural Gas Technologies Conference in Kyoto and to visit major Japanese gas turbine manufacturers, suppliers, and government institutions and laboratories. The itinerary for this visit is shown in Table 7-2. In June, 1994, CSGT staff visited gas turbine and automotive manufacturers, suppliers, and a European Union laboratory during a visit to Germany and The Netherlands. The itinerary for the second trip is given in Table 7-3. Extensive reports of these trips were submitted to the program sponsor.

Table 7-2. Summary of Organizations Visited, Locations, and Dates, During Japan Visit

Organization	City	Date(s)
IEA Natural Gas Technologies Conference	Kyoto	11/1-3/93
NGK Insulators Ltd.	Nagoya	11/4/93
Kawasaki Heavy Industries, Ltd.	Akashi	11/5/93
Osaka Gas Co. Ltd.	Osaka	11/5/93
Fukuyama Paper Co., Ltd.	Osaka	11/5/93
Agency of Industrial Science & Technology (AIST), MITI	Tokyo	11/8/93
Mechanical Engineering Laboratory (MEL), AIST, MITI	Tsukuba	11/8/93
Tokyo Electric Power Company	Tokyo	11/9/93
Ishikawajima-Harima Heavy Industries Co., Ltd.	Tokyo	11/9/93
Central Research Institute of Electric Power Industry (CRIEPI)	Yokosuta	11/10/93
Kyocera Corporation Central Research Laboratory	Kokubu	11/11/93
Hitachi Ltd., Hitachi Works	Hitachi	11/12/93

Table 7-3. Summary of Organizations Visited, Locations, and Dates, During Europe Visit

Organization	City	Date(s)
Bayer	Leverkussen, Germany	6/6/94
Siemens	Munich, Germany	6/7/94
Daimler-Benz	Ulm, Germany	6/8/94
ABB	Heidelberg, Germany	6/9/94
ECN, Joint Research Center	Petten, The Netherlands	6/10/94
ASME TURBO EXPO '94	Den Haag, The Netherlands	6/12-16/94